95,363

MASTER

SECRET

UCRL-5699 (Del.)

UNCLASSIFIED

This document consists of 85 pages.

No. 1 of 1 copies, Series TA.

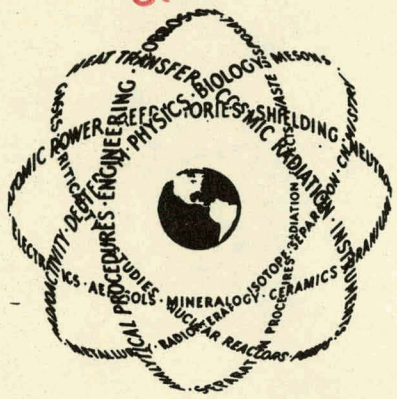

Facsimile Price $ 34.00

Microcard Price $ 2.55
for Access Permittees

Available from the
Division of Technical Information Extension
P. O. Box 1001
Oak Ridge, Tennessee

This document contains Secret-Restricted Data relating to civilian applications of atomic energy.

SPECIAL REREVIEW FINAL DETERMINATION
Class: U
Reviewer KAW Class. U Date 2-6-82

PLUTO QUARTERLY REPORT NO. 1

For July – September 1959

CLASSIFICATION CANCELLED
DATE 11-26-73
For the Atomic Energy Commission
TED REDMON
for the Chief, Declassification Branch

October 8, 1959

Lawrence Radiation Laboratory
University of California
Livermore, California

AEC Research and Development Report

GROUP 1
Excluded from automatic downgrading and declassification

RESTRICTED DATA

This document contains restricted data as defined in the Atomic Energy Act of 1954. Its transmittal or the disclosure of its contents in any manner to an unauthorized person is prohibited.

UNITED STATES ATOMIC ENERGY COMMISSION
Division of Technical Information

SECRET

UNCLASSIFIED

DISCLAIMER

UCRL-5699 (Del.)

UNIVERSITY OF CALIFORNIA
Lawrence Radiation Laboratory
Livermore, California

Contract No. W-7405-eng-48

PLUTO QUARTERLY REPORT NO. 1

(July – September 1959)

By

The Nuclear Propulsion Division Staff

October 8, 1959

THIS PAGE

WAS INTENTIONALLY

LEFT BLANK

PLUTO QUARTERLY REPORT NO. 1

Table of Contents

PLUTO QUARTERLY REPORT NO. 1

(July - September 1959)

Lawrence Radiation Laboratory, University of California
Livermore, California

CHAPTER I. TORY II-A

NEUTRONICS

A comprehensive review is now under way of the neutronic calculations pertinent to Tory II-A criticality. This is felt to be necessary at the present time to facilitate comparisons of several experiments and calculations. Many improvements in the neutronic codes, better techniques, and recently frozen reactor parameters will allow such a survey to be made in a reasonable time.

The basic Spade and Snoopy critical assemblies have been recalculated. In addition, those experiments concerned with molybdenum have also been studied. In the latter group, some hastelloy critical experiments were included. Also, gap effects in assemblies were measured. The Hot Box bare BeO experiment has been completed.

CODES

9-Zoom

The Lawrence Radiation Laboratory IBM 704 code--Short Zoom--(UCRL-5293) a one-dimensional, multigroup, neutron diffusion theory reactor code, has been programmed and debugged for the IBM 709 computer. A number of changes have been made in input format, power convergence, technique of inner iterations, etc. Much of the 709 code is the same as the 704 code. The 709 Zoom is a memory-contained program and is from 5 to 10 times faster than the 704 Zoom. The features of the 709 Zoom include:

(1) Capacity to handle up to 18-energy groups, 15 materials and 40 spatial zones (41 mesh points including both exterior points).

(2) High-order differencing of the differential equations.

(3) Transfer of neutrons permitted between all energy groups.

(4) A power extrapolation technique to speed up the convergence process.

(5) Energy-dependent extrapolation length boundary conditions at the outer boundary in all geometries and at the x = 0 boundary in slab geometry.

(6) Dependence of the fission spectrum upon the energy of the neutron causing fission.

(7) Optional use of a library tape of cross sections for materials, thus a simplified input for production use.

(8) An output (offline) which includes a) listings of all input data, b) effective multiplicative factor, c) spatial and energy distributions of flux, and d) several forms of spatial power distribution.

9-Angie

The LRL IBM 704 code--Angie--(UCRL-5091), a two-dimensional, multigroup, neutron diffusion theory reactor code, has been programmed and debugged for the IBM 709 computer. The input format, power convergence and boundary conditions have been made consistent with its companion code, 709 Short Zoom (UCRL-5682). The 709 Angie is greatly improved in production reliability and is twice as fast as the 704 Angie. Some of the features of the 709 Angie include:

(1) Capacity to handle up to 18-energy groups, 20 materials and a total of 2000 spatial points. The maximum number of spatial points in one space coordinate is 100.

(2) Capacity to handle XY or RZ geometry with up to 99 material regions.

(3) Second-order differencing of the differential equations.

(4) Transfer of neutrons is permitted "up one group" and "down two groups".

(5) A power extrapolation technique to speed up the convergence process.

(6) Energy-dependent extrapolation length boundary conditions (to 2nd order) at all outer boundaries.

(7) Dependence of the fission spectrum upon the energy of the neutron causing fission.

(8) The optional use of "rod regions" with energy-dependent extrapolation length boundary conditions applied at the boundaries of the rod regions.

(9) An output (offline) which includes a) listings of all input data with a region matrix picture, b) effective multiplicative factor, c) spatial and energy distribution of flux, d) and several forms of spatial power distribution.

CALCULATIONS

For the present cycle of calculations, a carefully scrutinized set of cross sections and transfer coefficients are employed. These constants are not viewed as the final, correct set but rather the best available. The transfer coefficients, in particular, are not above criticism since those in the thermal region are based on a Maxwellian spectrum.

It is gratifying to note that the simpler set of transfer coefficients used in Angie (i.e., $\mu^{i+1\leftarrow i}$, $\mu^{i-1\leftarrow i}$, $\mu^{i-2\leftarrow i}$) led to the same k_{eff} over a wide range of core length and reflector thickness as did the more extensive set from Zoom. More specifically, the $|\Delta k_{eff}|$ did not vary by more than 0.05% between corresponding problems. The $\mu^{i-2\leftarrow i}$ (Angie) was taken to be $\sum_{j=i-2}^{j=0}$ $\mu^{j\leftarrow i}$ (Zoom); also $\mu^{i+1\leftarrow i}$ (Angie) $= \sum_{j=i+1}^{j=18} \mu^{j\leftarrow i}$. It was decided therefore to use the simpler Angie coefficients in all Tory II-A problems of the current set.

The present set considers a medium length core (i.e., fueled length of 44.5 inches for cold configuration); fuel elements with a 0.200-inch inner diameter, and 0.295-inch flat-to-flat dimension; and hastelloy R-235 tie rods. The active core is considered to be at 1350°K, although the actual core will have an axial variation of temperature. It is shown that the effect on k_{eff} is very slight. The geometric expansion due to heating is determined radially by the expansion of the front support structure and rear end plate. The axial expansion is determined by expansion of the BeO. The dimensions used in the calculations are in accord with those expected during high temperature operation.

The results of a family of Zoom calculations for a hot Tory II-A are shown in Fig. I-1. The equivalent length ranged from 129 cm to 141 cm, and an equivalent thickness of 10 cm to 40 cm. Appropriate Angie problems which explicitly considered the end reflectors demonstrated that an equivalent length of 130.5 cm should be assigned to the medium length hot core. The

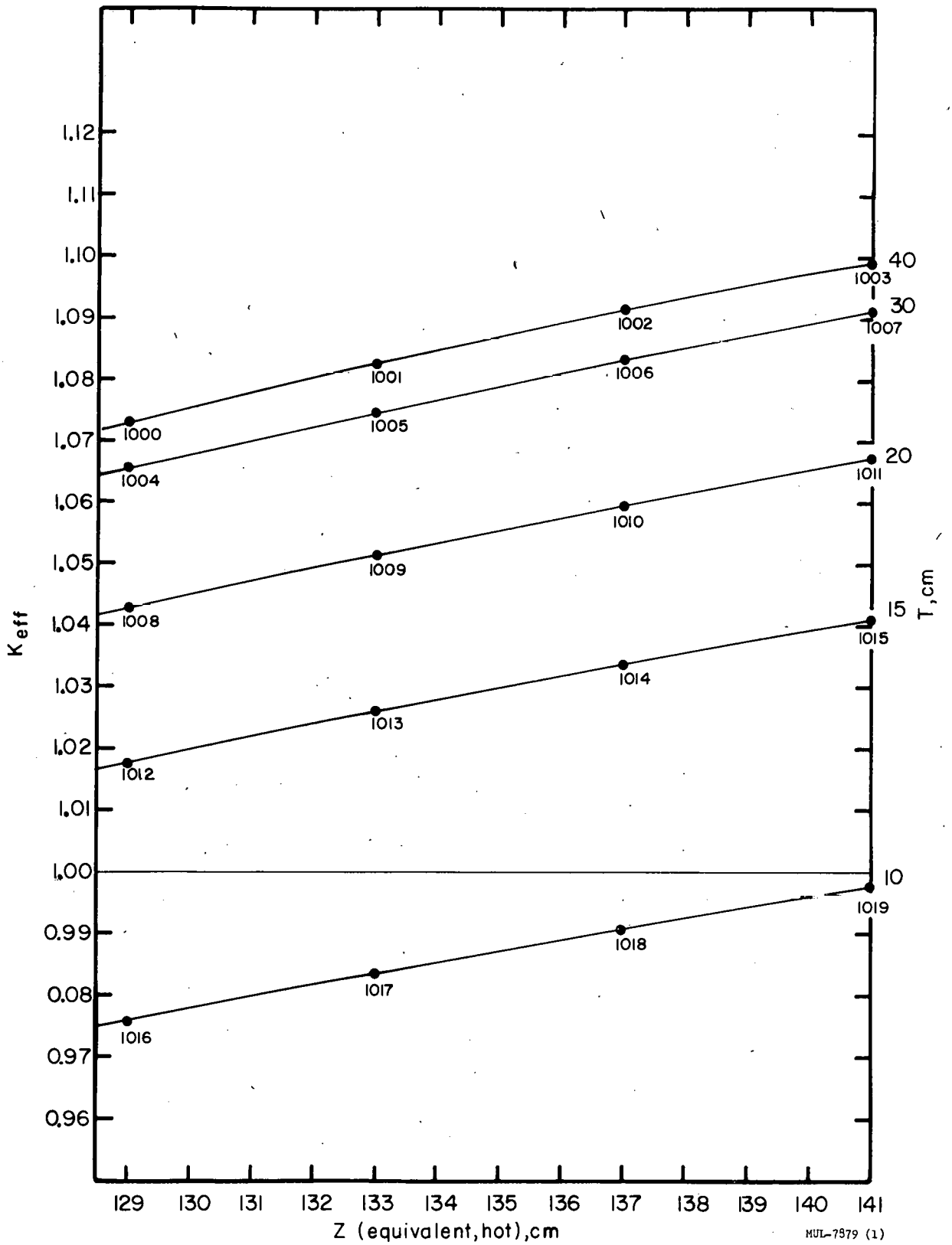

Fig. I-1. K_{eff} as a function of core length Z at constant reflector thickness T.

feul loading was assumed to be uniform and was 8.38% by weight. The fueled BeO was 96% of theoretical density while the unfueled BeO was 94% of theoretical density. Fig. I-2 shows how the power density varies radially for various reflector thicknesses. The effective reflector thickness is expected to be in the range of 15 cm. The core loading will actually vary radially and azimuthally to yield a constant power density in the active core.

Core Tie Rods

It was originally planned that the core tie rods would be coated molybdenum tubes having a 90-mil wall thickness and 7/8-in. diameter. Spade experiments showed this metal to have a much greater deleterious effect than was expected on the basis of published neutronic data. Therefore, hastelloy R-235 of 130-mil wall thickness is called for in the present design. Machine calculations which employ molybdenum cross sections derived from the Spade experiments show that the molybdenum tie rods cost 4.44% more in k_{eff} than hastelloy rods, in spite of the thicker hastelloy walls. The reactivity cost of the hastelloy rods is 3.15%.

Gaps

Several Spade experiments have been performed which provide insight into the effects of gaps in the core and at the core-reflector interface. It is clear at this point that one cannot treat gaps arbitrarily while using a diffusion code. If the gap is sufficiently small, however, smearing of adjoining material to the extent that the density in the gap region is one-half of the adjoining material is seen to be an inoffensive approximation. It is also clear that a very important parameter is the diffusion coefficient of a material. In particular, aluminum must be treated with caution.

Temperature Effects

Preliminary calculations demonstrate that the expansion of the core due to heating has a greater effect on the reactivity than the change in nuclear coefficients.

Angie- R-θ Calculations

The two-dimensional calculations which comprise a part of the current series are partially completed. In Fig. I-3, the configuration corresponding to vane angles of 80° (where θ = 0° when the vanes are completely in) is illustrated. In addition, the effect on power density of the insertion of the vernier rod is shown. Here, a rod is worth $\Delta k_{eff} = 0.0035$. A depression in power

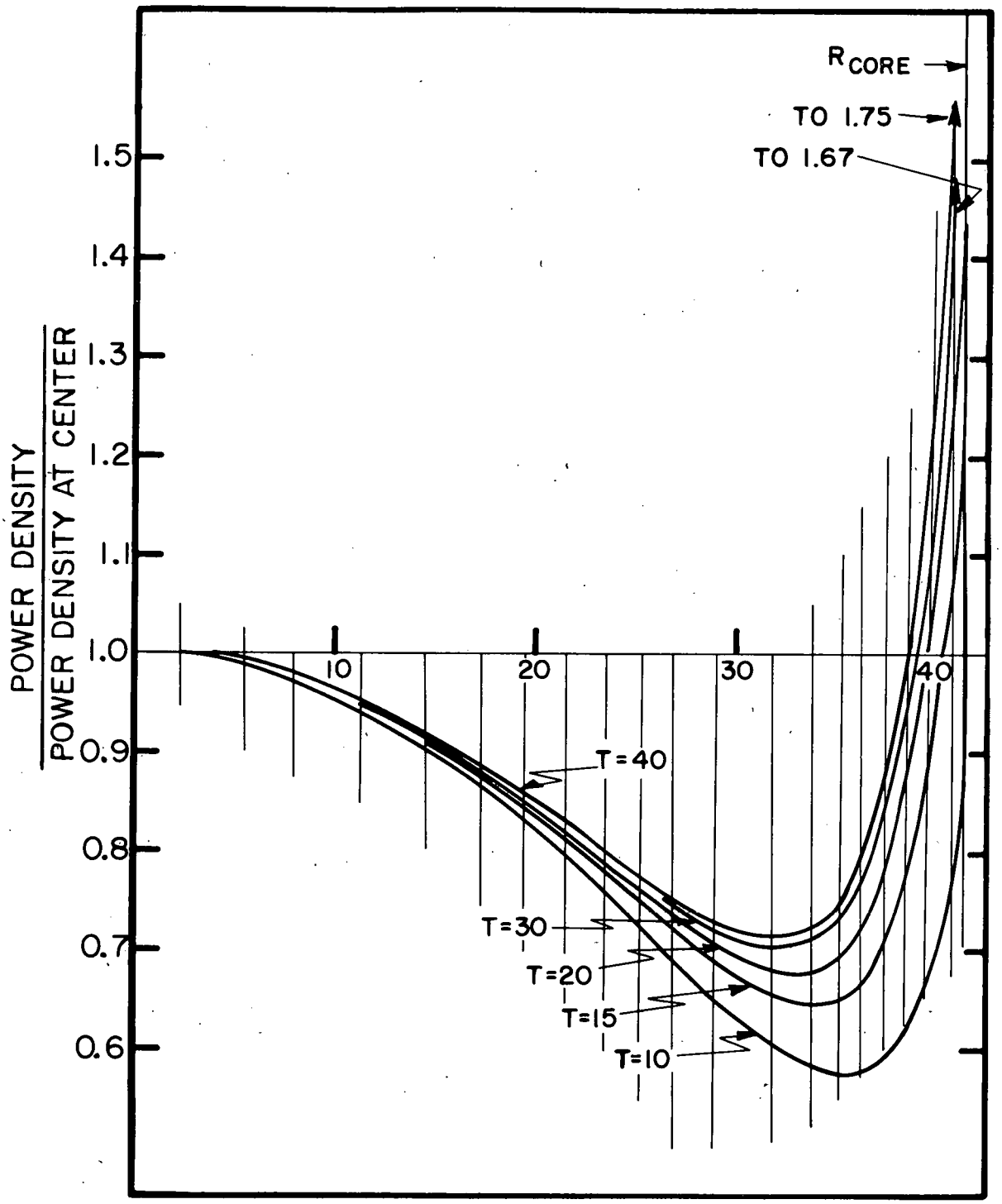

Fig. I-2. Power density versus radial position (core uniformly loaded).

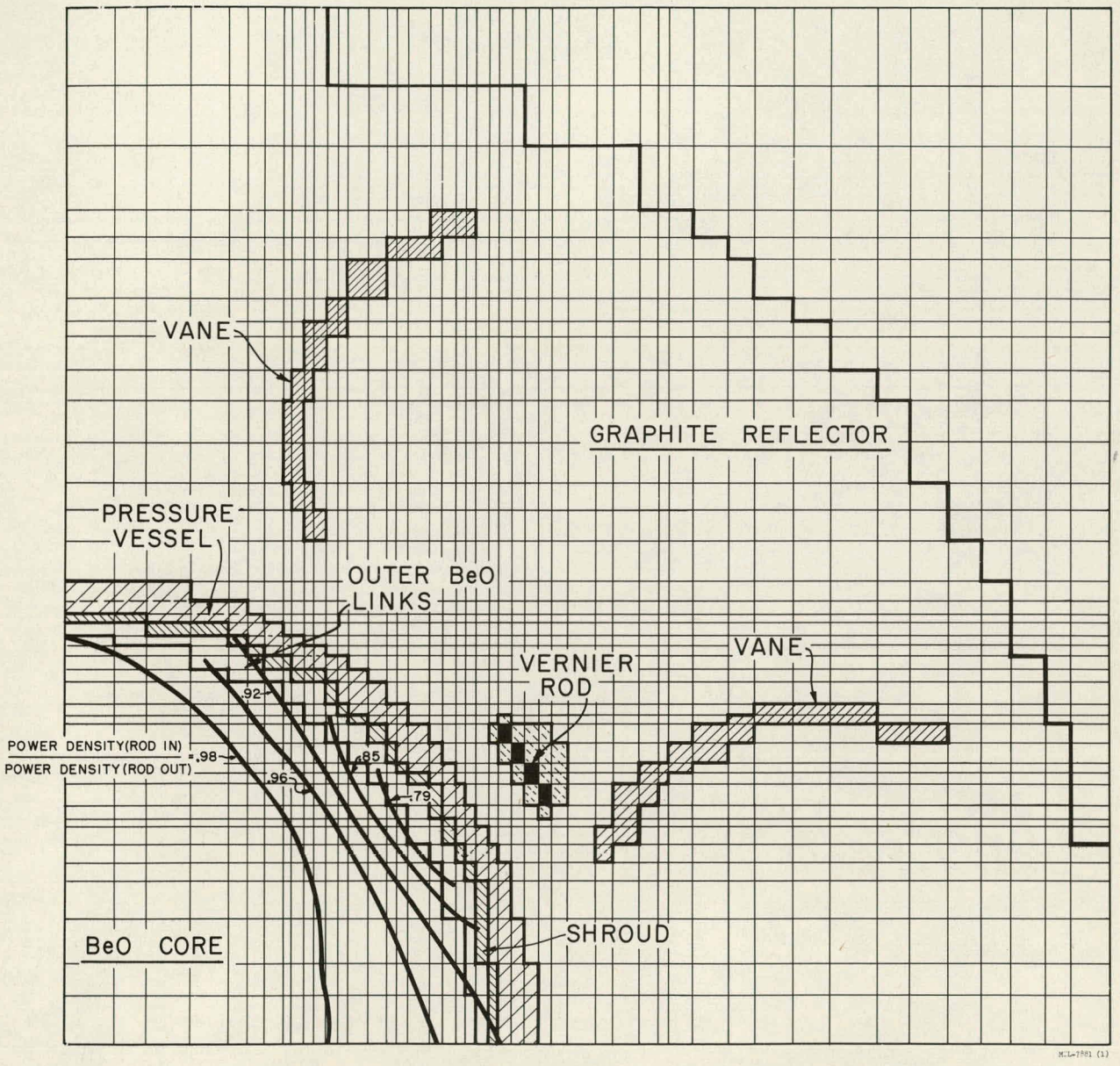

Fig. I-3. Representation of Tory II-A, vane angle 80°. Effect of vernier rod on power density.

density of as much as 20% is observed. If one relates the two-dimensional calculation to the one-dimensional Zoom through equal k_{eff}, it is seen that the 80° vane angle is equivalent to a reflector thickness of 17.4 cm.

Spade- Bare BeO-Moderated Systems

The experimental data on bare BeO systems is described in report UCRL-5369. These are accurately represented in the one-dimensional code, Zoom. Using the best available cross sections and transfer coefficients, reasonable agreement is realized with experiment, Fig. I-4. A maximum deviation of two percent in reactivity is found in the more dilute systems. The experimental uncertainty in critical height of ±0.2 inch has been represented in terms of reactivity.

The calculation employed self-shielding corrections to the fission and capture cross sections of the U^{235}. Cohen's method[1] was applied to each energy group, and individual sets of self-shielding corrections were computed for different foil thicknesses and spacings. The clustering of points in loadings suggest the validity of the self-shielding corrections.

The output of the Zoom calculations incudes the spectra along with other pertinent information. From this was derived the median fission energy of the various BeO-moderated assemblies. The curve in Fig. I-5 applies to assemblies with homogeneous fuel loading. The Zoom code assigns a median fission energy of 20 ev to an assembly with BeO/U^{235} = 120:1 (i.e., about the average loading in Tory II-A).

Snoopy- Bare Graphite-Moderated Systems

The Snoopy series of experiments have been described in UCRL-5175. In addition, an assembly with a C/U^{235} = 9550:1 has been studied. The results from Zoom is shown in Fig. I-6. The agreement with experiment is clearly not as good as in the case of BeO assemblies. In the Snoopy calculations, no need for self-shielding correction was necessary because experimental self-shielding corrections were made to the experimental critical buckling. Especially in the case of the most thermal reactor the disagreement is apparent. Part of that discrepancy may be due to an improper assignment of nuclear poisons in the code. One part per million of boron in the graphite would affect the reactivity by about one percent. The uncertainty in chemical determination is at least twice this amount, and is indicated on Fig. I-6. An experimental uncertainty of ±0.3 inch implies only ~±0.003 in k_{eff}.

[1] Nuc. Sci. and Eng. 4, p. 255-6 (1958)

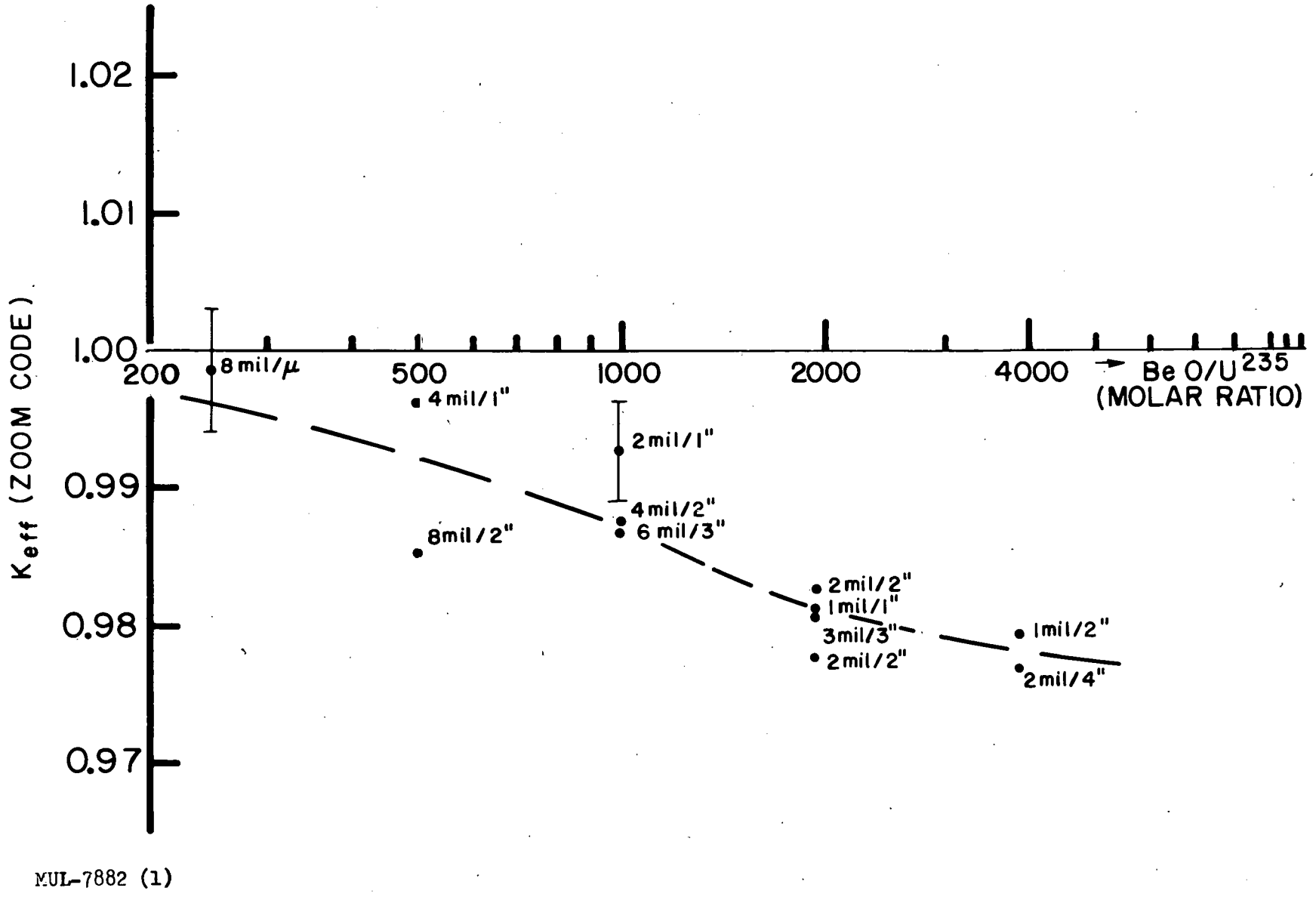

Fig. I-4. Spade – K_{eff} versus BeO/U^{235} for bare assemblies.

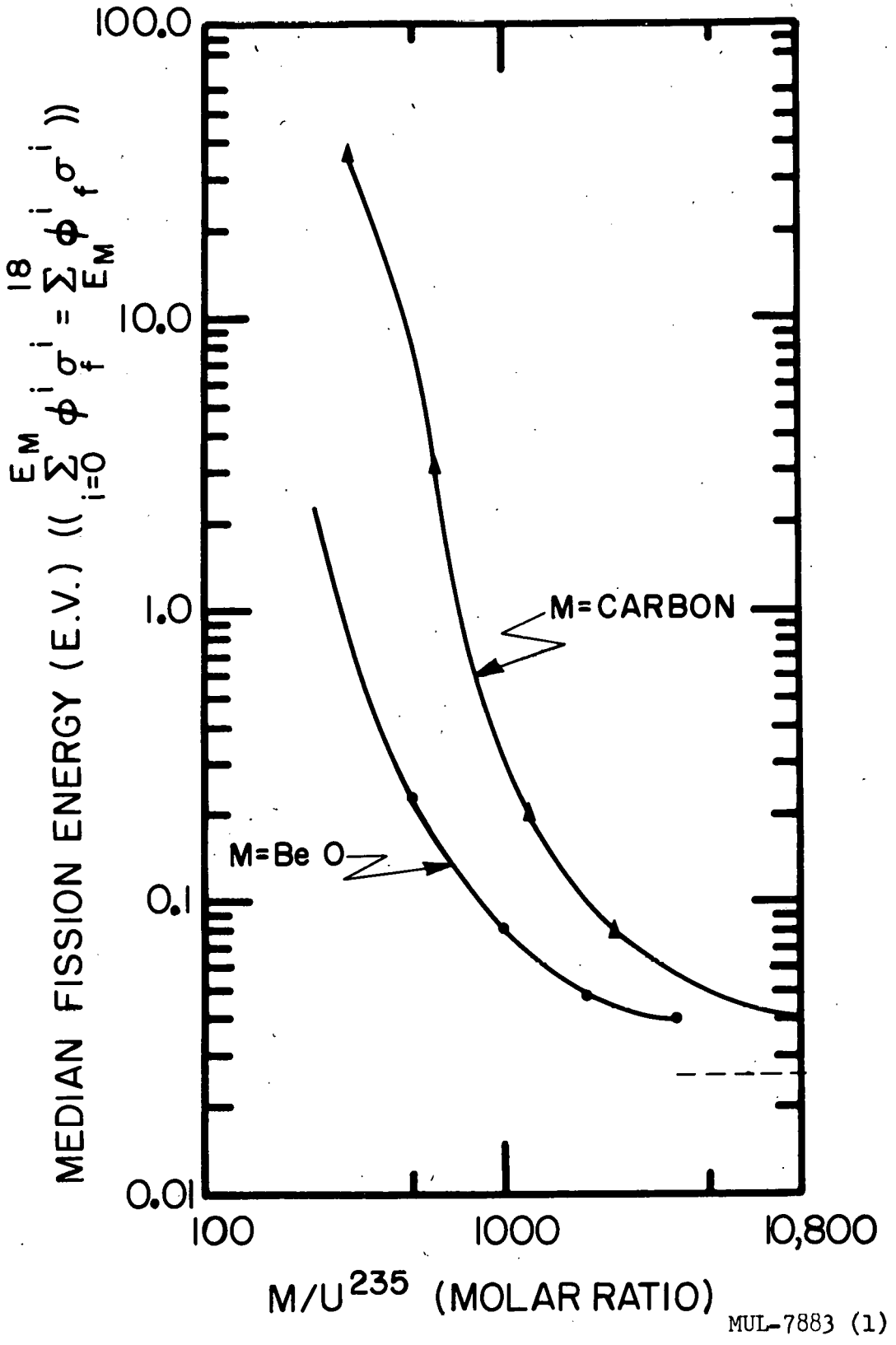

Fig. I-5. Median fission energy versus molar ratio of moderator to fuel.

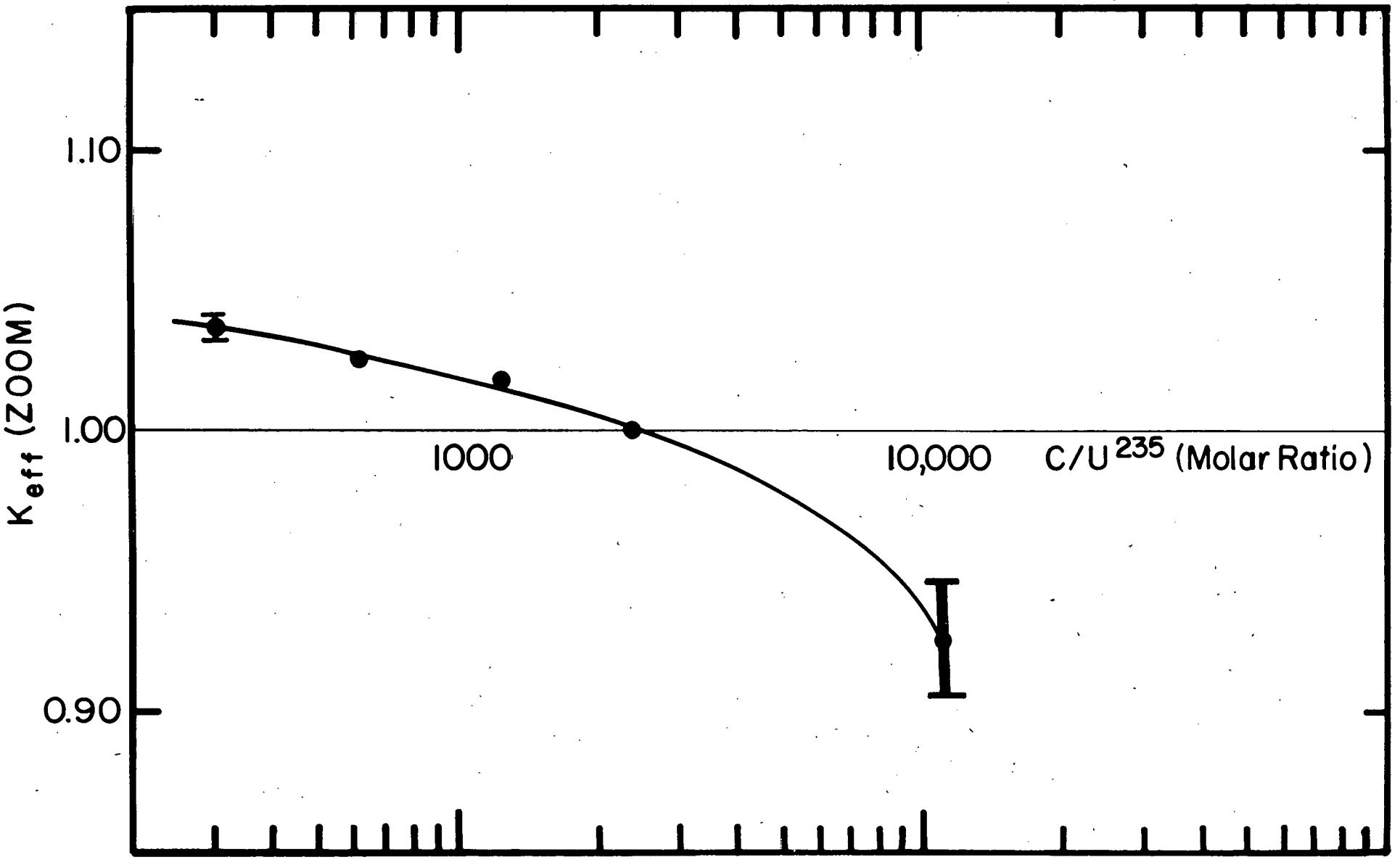

MUL-7884 (1)

Fig. I-6. Calculated K_{eff} from Zoom of various bare graphite (Snoopy) critical assemblies.

Fig. I-5 also shows the median fission energy for various Snoopy assemblies (corrected to a bare homogeneous system). These values are derived from Zoom.

Spade- Molybdenum, Hastelloy, and Gold

The experiments to which reference has been made earlier are summarized in Table I-1. The geometric arrangement is shown in Fig. I-7. Slabs of material are placed in approximately the center of the core of the assembly or at the core-reflector interfaces. The graphite reflector was of density: 1.70 g/cc, and the ρ_{BeO} = 2.86 g/cc. The BeO/U^{235} was 247:1. The foil thickness is 8 mils and spacing is one inch. Zoom calculations show the median fission energy in the center of the core to be 0.8 ev.

Table I-1

	Slab Material	T_E (in.)	T_C (in.)	h (in.)	H_C (in.)	k_{eff} $\left(\frac{\Delta k_{eff}}{\Delta x(\text{in.})} = 0.023\right)$	$2\sigma^i \times 10^{24}$* (cm^2)	$a\Sigma L$*
1	none	-	-	-	14.35	1.0083	-	-
2	Au	0	.0099	7.5	17.4	1.0178	(i=6) 138	
3	Au	0	.002	7.5	15.45	1.0122	(i=6) 306	
4	Hastelloy	0	.159	7.5	15.8	1.0060		.0680
5	Hastelloy	0	.0795	7.5	15.13	1.0065		.0836
6	Hastelloy	.0795	0	-	14.85	1.0050		.0836
7	Mo	0	.120	7.5	16.35	1.0096	(i=8) 8.75	
8	Mo	0	.080	7.5	15.8	1.0084	(i=8) 9.55	
9	Mo	0	.040	7.5	15.2	1.0070	(i=8) 11.96	
10	Mo	.040	0	-	15.0	1.0120	(i=8) 11.96	

*Energy Group 6 and 8 contain 1.15 lethargy units each. Therefore $I(\text{eff}) = 1.15\, a\sigma^{6 \text{ or } 8}$

These have been studied through the Zoom code, and it is found that a rather large resonance absorption must be assigned to molybdenum. Fig. I-8 shows the results of the calculations. Particular values of cross sections and the resultant k_{eff} is also given in Table I-1. The lack of agreement between the findings from the 40-mil sheet at the center and 40-mil sheets at the interfaces may be due to an experimental uncertainty in critical height of ±0.15 inch.

Two additional experiments were done with gold sheets. Insofar as the

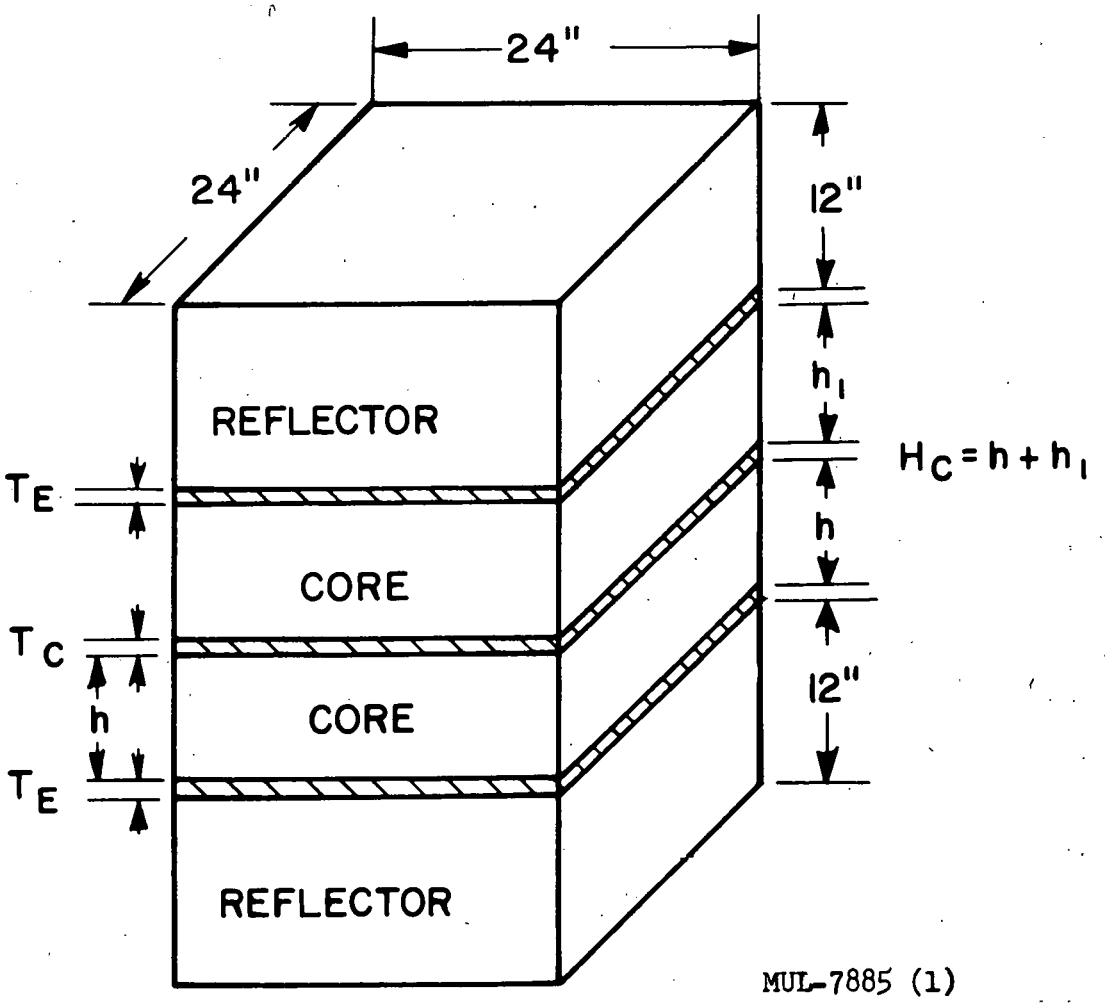
24"
24"
12"
h_1
REFLECTOR
$H_C = h + h_1$
T_E
h
CORE
T_C
12"
h
CORE
T_E
REFLECTOR
MUL-7885 (1)

Fig. I-7

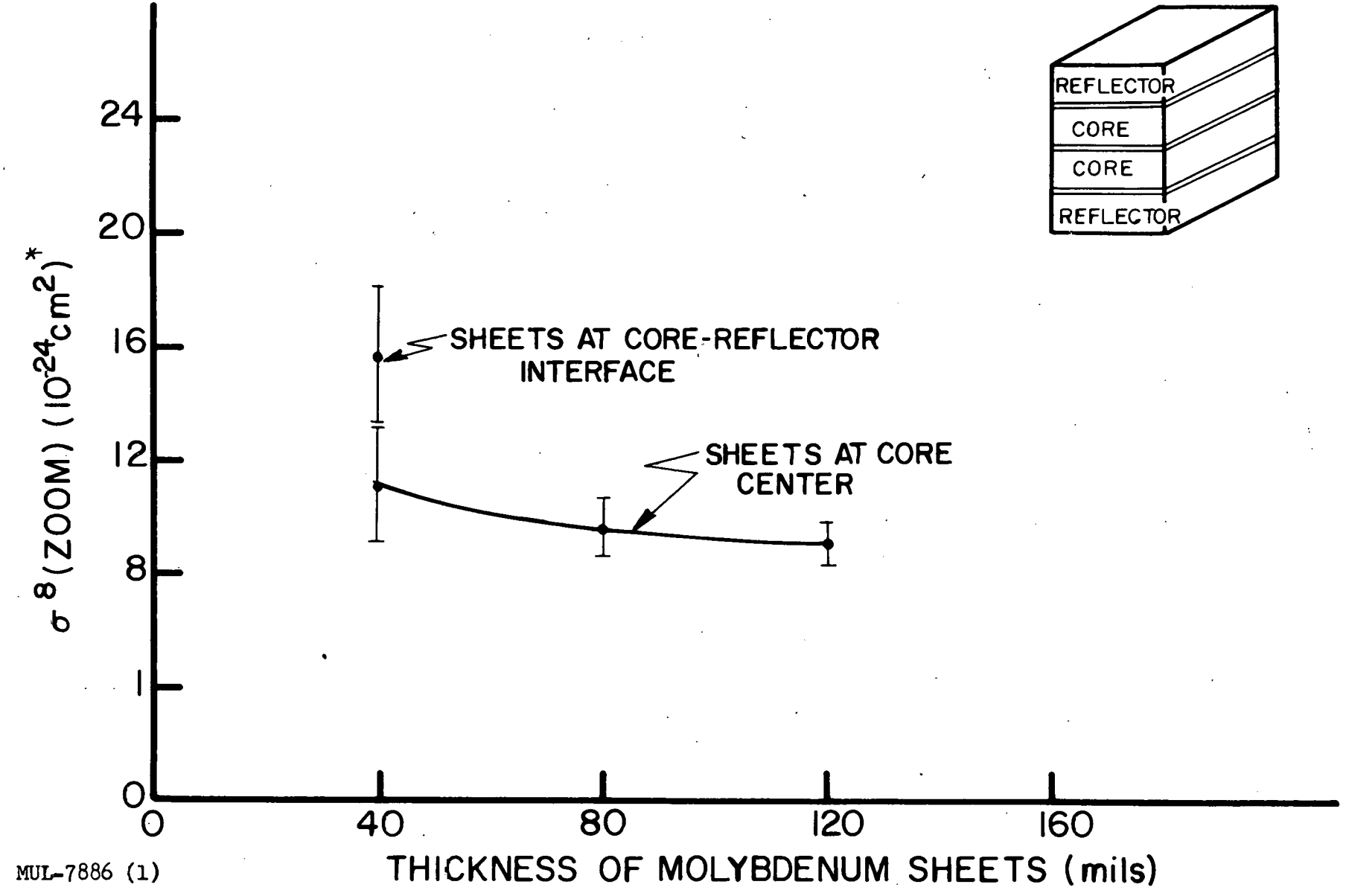

Fig. I-8. Resonance absorption cross section of molybdenum versus thickness of molybdenum sheets derived from Spade measurements.

5-ev gold resonance is a standard,[2] with a resonance integral of 1558 barns, it is very convenient to see how well the Zoom code duplicates the experiment. Table I-1 shows the results. Conventional slab self-shielding corrections were made.[3] It was reassuring to observe that for the 10-mil Au thickness, 87% of the change in critical height was accounted for, while for the 2-mil foil, 85% was accounted for by the calculation. The latter disagreement could be due entirely to the ±0.15 inch uncertainty in critical height.

Additional experiments performed with hastelloy R-235 could not furnish useful information concerning molybdenum (i.e., R-235 contains 5.5% Mo). However, it is seen in Table I-1 that the code now represents hastelloy very accurately if not slightly conservatively.

---

[2] Progress in Nuclear Energy, Vol. 1, Series 1, p. 187

[3] G. M. Roe, "The Absorption of Neutrons in Doppler Broadened Resonances," Knolls Atomic Power Laboratory report KAPL-1241, Oct. 15, 1954.

CHAPTER II. MATERIALS DEVELOPMENT AND PILOT PLANT ACTIVITIES

CERAMICS

Materials Studies

1. Pure BeO Preparation and Sintering

Preparation of BeO. This study is an attempt to determine how some factors can be varied to increase the densities of relatively pure BeO bodies formed by isostatic pressing and sintering in hydrogen. The BeO powder was prepared by ammonia precipitation from a $BeSO_4$ solution and subsequent calcination of the hydroxide. The variables considered were these: concentration and kind of anion added to the beryllium sulfate-water solution before ammonia precipitation, carrier gas added along with the ammonia, washing of the dried hydroxide-salt mass, calcining temperature, and sintering temperature. Not yet considered are $BeSO_4$/water ratio, ammonia/carrier gas ratio, ammonia addition rate, pressing pressure, calcining atmosphere, and sintering atmosphere. Optimum calcining and sintering times have not been established.

The method used to prepare the samples is as follows. 300 grams of $BeSO_4 \cdot 4H_2O$ and 10 grams of E. D. T. A. (Versene) are made up to 10 liters with distilled water in a polyethylene tank. The plastic agitator is turned on and NH_3 plus N_2 or O_2 are added at the rate NH_3/carrier gas of 1000 cm^3/min/ 4000 cm^3/min until the hydroxide-salt slurry reaches pH 8.5. The gas flow and stirrer are turned off and the mass is vacuum-filtered until it is no longer gelatinous but quite firm. The cake is removed from the filter paper, partially broken up, and further dried under heat lamps until it is apparently bone-dry, after which it is screened through a 20-mesh, stainless steel sieve and split into two parts. One part is set aside and the other is put into a fritted glass filter and washed with distilled water until the washings give no indication of sulfate when tested with barium chloride solution. The washed precipitate is then dried under heat lamps as before. The requisite amounts of the washed and unwashed portions are then put into the air calciner, brought up to temperature in about four hours, held at temperature for four hours, and then allowed to cool to room conditions. The powders are then hand-packed into rubber tubes and isostatically pressed at 30,000 psi. The pressed mass is placed in a tungsten furnace, heated to temperature in hydrogen (about 2 hours),

held there for three hours and cooled to ambient temperature in another 2 hours. The densities of the fired pieces are determined by the hanging thread-water immersion methods. Some of the samples are to be analyzed spectrographically for cation impurities. UOX, a commercially pure BeO, was pressed and sintered along with the ammonia-produced specimens as a control since it has less than 0.1% impurities, has given reasonably consistent density results, and is now employed in other experimental studies at LRL.

The preliminary work, which involved the sintering of more than 80 pieces, indicated that for densities greater than 95% of theoretical:

1. Sintering in hydrogen should take place above 1500°C.
2. Sintering at temperature for three hours appears sufficient.
3. Calcining for four hours at 900-1000°C is suitable.
4. Low sulfate is preferred in the $Be(OH)_2$ precipitated.
5. The combination of certain anions and carrier gas during the precipitation are helpful.

The following table (II-1) gives the conditions for precipitation, calcining and sintering as well as the sintered densities. The figure of merit, Fig. II-1, refers to sample density/UOX average density. Also, the figures of merit are plotted against added salt concentration. Since the final sample density is apparently not a strong function of calcining temperature in the 900-1000°C range, samples calcined at both temperatures are averaged. The oxgyen curves will be rechecked because of their odd character.

2. Fuel Retention Studies

Mechanism of Fuel Loss. As part of a continuing study of fuel loss processes, concentration profiles were obtained to show the distribution of UO_2 within $BeO-UO_2$ samples. Data were taken for two samples, one as sintered and one after fuel loss testing. The results are compared below with the calculated profile assuming a volume diffusion loss process. We are now obtaining additional data for samples having better fuel retention properties.

The attached graph, Fig. II-2, shows UO_2 distribution as a plot of concentration ratio, C/C_0, versus position ratio, x/l, where C_0 and l are the initial uniform concentration and half thickness of the disc-shaped samples respectively. The experimental values were obtained by x-ray attenuation measurements of the remaining sample after each successive removal of a layer of material. The volume diffusion profile was calculated assuming the sample to be a semi-infinite slab with zero surface concentration. This

Table II-1

SAMPLE PREPARATION AND FIRED DENSITIES OF BeO PIECES SINTERED IN HYDROGEN 3 HOURS AT 1750°C

Sample	Anion	Anion Conc. Mols/L	Carrier Gas	Calcine Temp. °C	Fired Density g/cm	% Theo. Density	Figure of Merit	Remarks
26-B	none	0	N_2	980	2.888	96.0	0.994	B's were washed
33-A	none	0	O_2	1000	2.927	97.3	1.008	A's were not washed
33-B	none	0	O_2	1000	2.901	96.5	0.999	
27-B	Cl^-	0.187	N_2	900	2.899	96.4	0.998	
34-B	Cl^-	0.187	O_2	1000	2.898	96.4	0.998	
28-B	Cl^-	0.561	N_2	900	2.927	97.3	1.008	
35-B	Cl^-	0.561	O_2	1000	2.940	97.8	1.012	
29-A	NO_3^-	0.125	N_2	1000	2.888	96.0	0.994	
29-B	NO_3^-	0.125	N_2	900	2.892	96.2	0.996	
36-A	NO_3^-	0.125	O_2	1000	2.901	96.5	0.999	
30-B	NO_3^-	0.375	N_2	900	2.926	97.3	1.008	
31-B	acetate	0.130	N_2	1000	2.896	96.3	0.997	
32-B	acetate	0.389	N_2	1000	2.919	97.1	1.005	
39-B	acetate	0.389	O_2	900	2.879	95.7	0.991	
UOX					2.915			As purchased
UOX					2.893			As purchased
UOX average					2.904		1	
26-A	none	0	N_2	1000	2.897	96.3	0.991	
33-B	none	0	O_2	900	2.895	96.3	0.991	
27-B	Cl^-	0.187	N_2	1000	2.928	97.4	1.002	
34-B	Cl^-	0.187	O_2	900	2.898	96.4	0.992	
28-B	Cl^-	0.561	N_2	1000	2.914	96.9	0.997	
35-A	Cl^-	0.561	O_2	1000	2.909	96.7	0.996	
35-B	Cl^-	0.561	O_2	900	2.924	97.2	1.001	
35-B	Cl^-	0.561	O_2	1000	2.936	97.6	1.005	
35-B	Cl^-	0.561	O_2	1000	2.946	98.0	-	Refired: 6 hrs at temp. total
29-B	NO_3^-	0.125	N_2	1000	2.909	96.7	0.996	
36-B	NO_3^-	0.125	O_2	900	2.916	97.0	0.998	
36-B	NO_3^-	0.125	O_2	1000	2.915	96.9	0.998	
37-B	NO_3^-	0.375	O_2	900	2.924	97.2	1.001	
37-B	NO_3^-	0.375	O_2	1000	2.929	97.4	1.002	
31-B	acetate	0.130	N_2	900	2.918	97.0	0.999	
38-A	acetate	0.130	O_2	1000	2.914	96.9	0.997	
38-B	acetate	0.130	O_2	900	2.903	96.5	0.993	
38-B	acetate	0.130	O_2	1000	2.895	96.3	0.991	
UOX					2.913			As purchased
UOX					2.920			As purchased
UOX					2.933			As purchased
UOX average					2.922		1	
33-A	none	0	O_2	1000	2.908	96.7	1.000	
$33\text{-}B_1$	none	0	O_2	1000	2.920	97.1	1.010	
33-B	none	0	O_2	1000	2.915	96.9	1.008	Subscript 1 is check in same firing
$27\text{-}B_1$	Cl^-	0.187	N_2	1000	2.908	96.7	1.006	
27-B	Cl^-	0.187	N_2	1000	2.901	96.5	1.003	
28-A	Cl^-	0.561	N_2	1000	2.852	94.8	0.986	
$28\text{-}B_1$	Cl^-	0.561	N_2	1000	2.912	96.8	1.007	
28-B	Cl^-	0.561	N_2	1000	2.915	96.9	1.008	
35-B	Cl^-	0.561	O_2	1000	2.914	96.9	1.008	
35-B	Cl^-	0.561	O_2	1000	2.950	98.1	-	Refired: 9 hrs at temp. total
30-B	NO_3^-	0.375	N_2	900	2.919	97.1	1.009	
30-B	NO_3^-	0.375	N_2	1000	2.901	96.5	1.003	
37-A	NO_3^-	0.375	O_2	1000	2.899	96.4	1.002	
37-B	NO_3^-	0.375	O_2	1000	2.917	97.0	1.009	
32-B	acetate	0.389	N_2	1000	2.880	95.8	0.996	
UOX					2.884			As purchased
UOX					2.890			As purchased
UOX					2.893			As purchased
UOX					2.891			As purchased
UOX average					2.892		1	

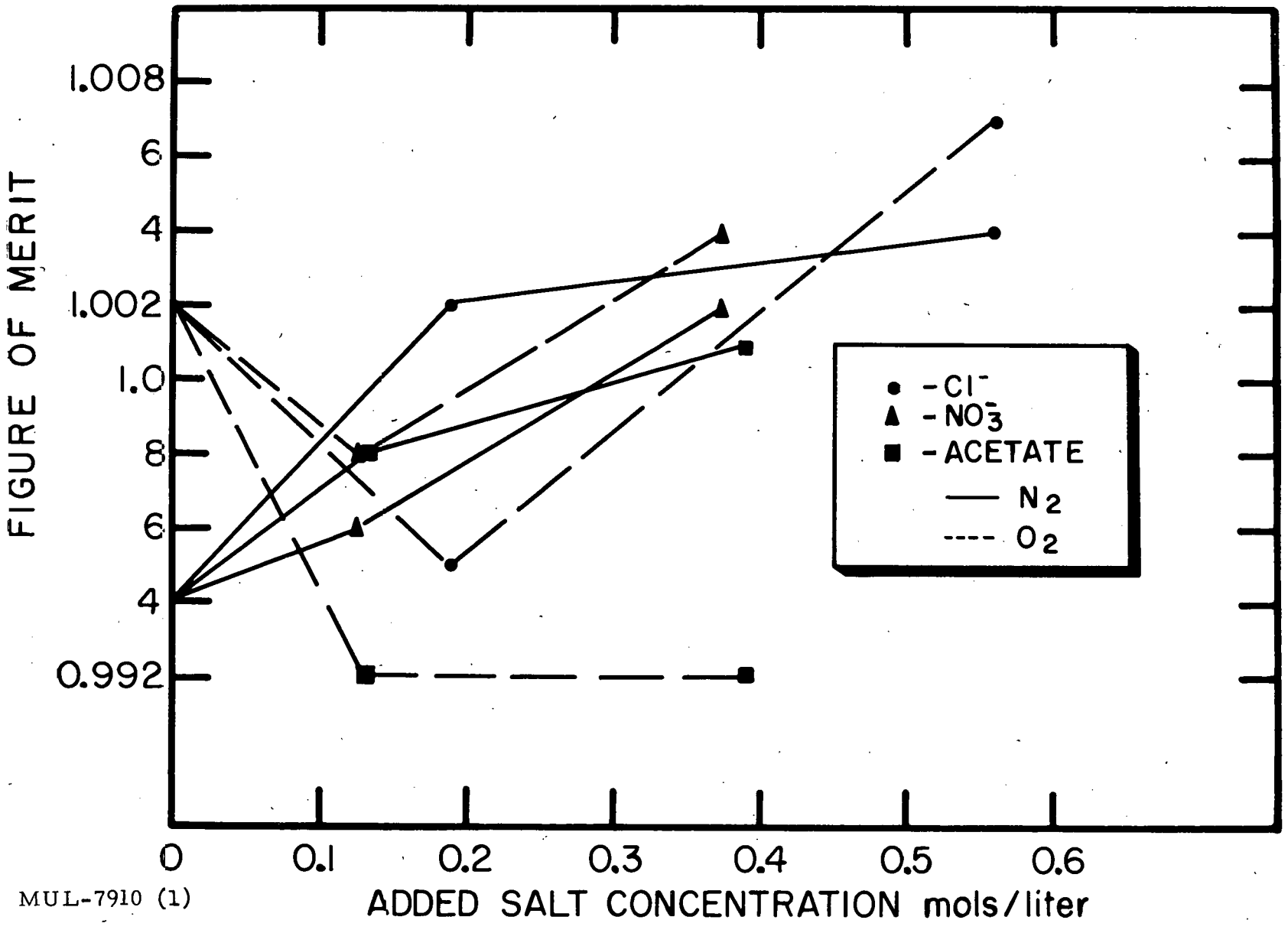

Fig. II-1. Figure of merit versus added salt concentration for O_2 and N_2 carrier gases.

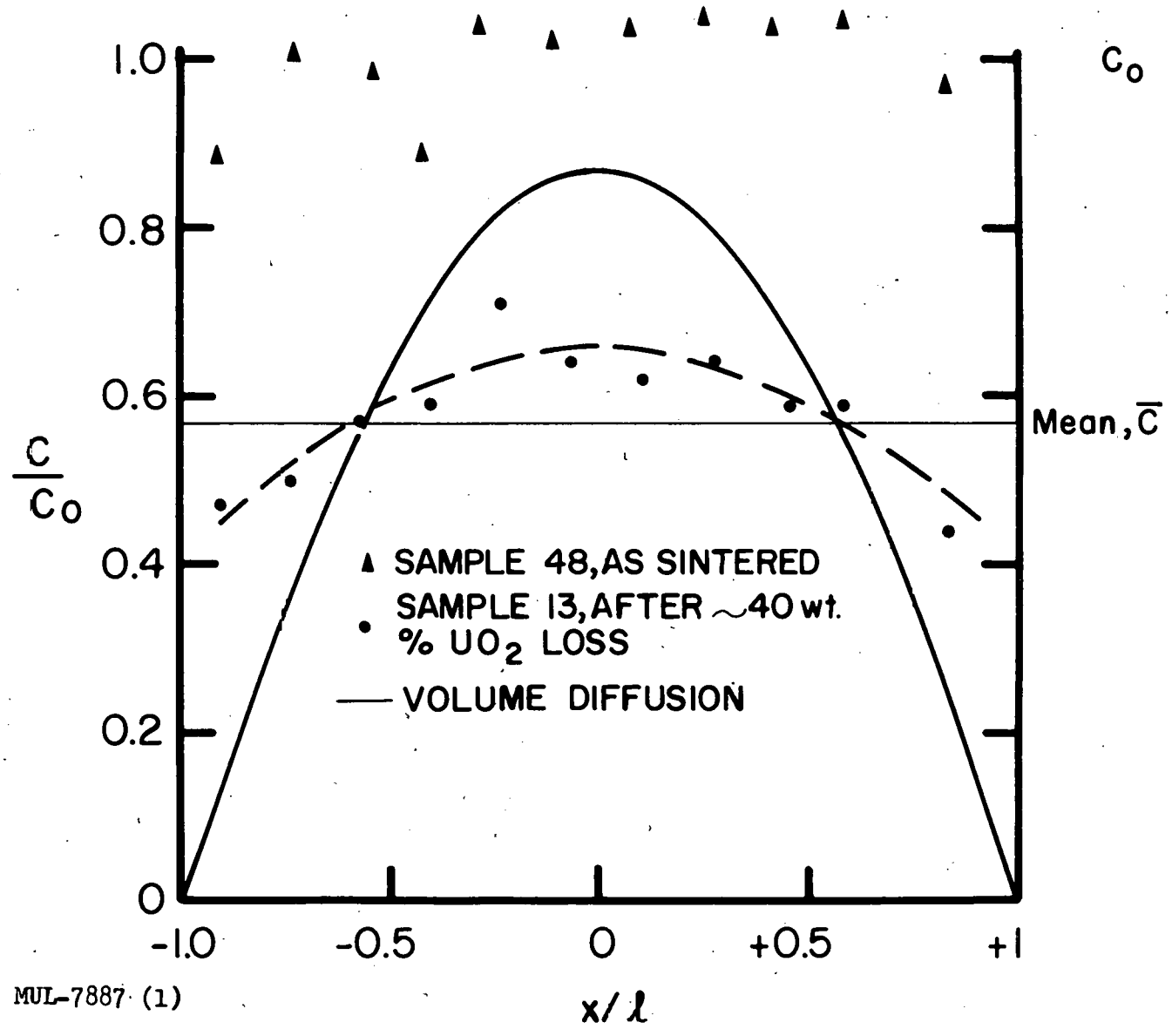

Fig. II-2. UO_2 distribution in BeO-UO_2.

profile represents a distribution of UO_2 having the same mean value of concentration as in the sample after loss testing.

The graphed data indicate: (1) The initial concentration is essentially uniform through these samples from face to face. (2) The concentration profile of the sample which had lost approximately 40 wt % of its UO_2 is markedly flatter than the profile for volume diffusion with the above-stated conditions.

Data are not adequate to determine the relative importance of the loss mechanisms that may combine to effect such a profile. Possible combinations include grain boundary and parallel lattice diffusion, and solid diffusion combined with reaction to form UO_3 and surface evaporation. Additional UO_2 distribution data as well as data from other experimental studies are being obtained to clarify the loss mechanisms.

Sample Descriptions

No.	Density % theor.	Initial Thickness cm	Type BeO	Initial wt % UO_2	Wt % UO_2 after loss test, mean.
48	95.0	0.296	UOX	4.7	not tested
13	91.2	0.309	LOH (1-2% impurities)	2.0	1.14*

*After 5 hrs in flowing dry air at 1520°C.

The expressions used to obtain the volume diffusion profile were:

$$1 - \frac{\bar{C}}{C_0} = 2 \frac{\sqrt{Dt}}{\ell} \left[\frac{1}{\sqrt{\pi}} + 2 \sum_{n=1}^{\infty} (-1)^n \, \text{ierfc} \, \frac{n\ell}{\sqrt{Dt}} \right]$$

which for values of $1 - \bar{C}/C_0 < 0.45$ reduces to

$$1 - \frac{\bar{C}}{C_0} = \frac{2}{\sqrt{\pi}} \frac{\sqrt{Dt}}{\ell}$$

The expression $100 (1 - \bar{C}/C_0)$ approximately equals the wt % of UO_2 lost.

$$\frac{C}{C_0} = 1 - \sum_{n=0}^{\infty} (-1)^n \operatorname{erfc} \frac{\ell}{\sqrt{Dt}} \left(\frac{2n + 1 - \frac{x}{\ell}}{2} \right) - \sum_{n=0}^{\infty} (-1)^n \operatorname{erfc} \frac{\ell}{\sqrt{Dt}} \left(\frac{2n+1 + \frac{x}{\ell}}{2} \right)$$

where $\overline{C}$ is the mean value of concentration C,

t is time,

D is a diffusion coefficient.

The first expression permits the evaluation of $\sqrt{Dt}/\ell$, and by use of this value in the second expression, C/C_0 can be computed for values of x/ℓ. The series in both expressions converge very rapidly.

Fuel Loss Determination by Gamma Pulse Spectrometry. After a preliminary investigation it was decided that fuel losses of UO_2-BeO tubes could be measured by gamma pulse spectrometry. The advantage of this method is that the sample is surrounded by a crystal well and eliminates alignment problems which occur in measuring restricted areas of samples. The disadvantages are that the well is only 1-5/8-in. deep while the fuel element is 4-in. long and that the counter operates close to electronic instability.

The percent error for a typical tube against counting time is given in Fig. II-3. A counting time of 20 minutes has been used on tubes measured thus far giving a percent error of 0.25%. In the first samples the fuel loss obtained from weight loss measurements has been 2 to 4.5 times as great as fuel loss by counting (see below), although correlation between the two methods seems reasonably consistent. We are checking further using wet chemical analysis.

Variables in Fuel Retention of Tubes. A preliminary investigation was made to determine the effect of sintering temperature-time and grain size on urania loss at temperatures above 1250°C. The materials used were designated as Y — UOX beryllia ball-milled 24 hours and passed through a 270-mesh sieve, and as Z — UOX beryllia, 100-mesh as received from supplier.

Nominally 7-1/2 wt% urania was added using LRL's standard precipitation method. Tubes were extruded and sintered in hydrogen. The soaking time of samples sintered at 1650°C was varied to change the grain size of the beryllia. However, the maximum grain sizes desired (over 25 μ) were not obtained.

Initially urania losses were to be determined by weight loss only. However, at the lowest testing temperature (1250°C) there was some weight gain in the samples, and it became necessary to use a gamma counting techinque also.

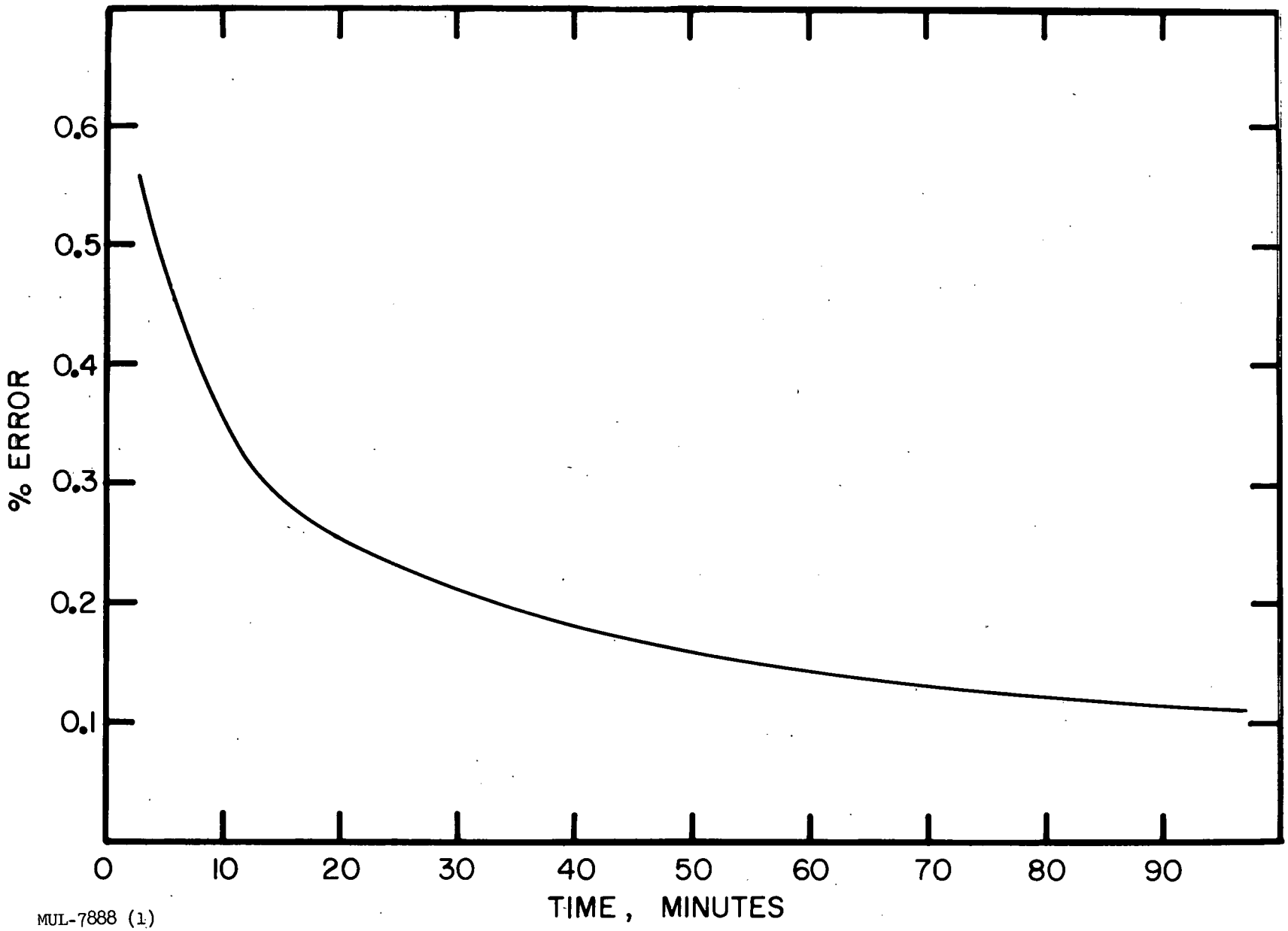

Fig. II-3. Percent error versus counting time for sample with 1,000,000 counts/hr and background of 500 counts/min.

Table II-3

SUMMARY OF 1650°C LOSS DATA

Tube Type	H_2 Sintering Temp °C	H_2 Sintering Time hr	Average Density % Theor.	U Loss from Weight 4 hr	U Loss from Weight 10 hr	U Loss from Weight 20 hr	U Loss from Count 4 hr	U Loss from Count 10 hr	U Loss from Count 20 hr
Y	1650	5	97.2	5.5	12	18	1.9	4.5	4.6
Y	1650	10	97.6	3.4	10	14.6	0.9	3.3	4.2
Z	1725	3	97.2	3.7	10.6	18	1.2	3.8	4.9
Z	1650	5	92.6	4.3*	19	20	2.7	4.3	4.3
Z	1650	10	95.5	3.9	8.1	8.8	1.2	2.9	2.4

* This sample had a density of 96% theor. unlike the 10- and 20-hr samples in its class (92.6%).

Table II-4

Sample No.	Tube Type	Sintering Temp., °C	Time hr	Density % Theor.	BeO grain size(μ) Range	BeO grain size(μ) Average	UO_2 grain size μ*
78	Z	1725	3	97.8	6-18	10.5	1/4 -- 1.5
109	Z	1650	5	95.6	3-10 (part of outer rim 6-16	6.5 9)	1/4 -- 2
86	Z	1650	10	95.3	3-11	6	1/4 -- 1
79	Y	1725	3	----	6-24	12.5	1/4 -- 3
92	Y	1650	5	97.8	5-16	10	1/4 -- 2
89	Y	1650	10	97.8	4-9	6.5	1/4 -- 1
90	X	1650	10	95.4	7-22 (center and inner rim)	12	-------
					8-32 (outer rim)	16	

* Note: all specimens show yellow color, presumably due to UO_2 grains smaller than can be resolved optically (< 1/4 μ).

At the highest testing temperature (1650°C), the urania loss assuming the weight change was entirely due to UO_2 lost was 3 to 4 times higher than the loss by gamma counting. It is thus not possible to specify the loss unequivocally, but we can set maximum limits by using the weight changes. The results are shown in Tables II-2, II-3 and Fig. II-4.

We can draw some conclusions, however.

1. Losses of UO_2 at 1258°C are negligible.

2. Losses of UO_2 at 1526°C are at most 2-3% even after 20 hours in dry air.

3. The effect of somewhat lower density (92-93% of theoretical) is not clear. However, tubes of this density had significantly higher early losses (up to 10 hours) but only slightly higher 20-hour losses (as judged by weight changes).

4. The effect of ball-milling is not clear. Generally lower densities were achieved at 1650°C sintering temperature. However, both lower and higher fuel losses were experienced than for the "as received" BeO. Ball-milled material sintered for 10 hours had the lowest fuel loss of all material tested.

5. Losses of UO_2 at 1650°C for 10 hours ranged from 8 to 12% (calculated from weight change) except for a low density sample (92.5% theor.). Corresponding losses by counting were 3 to 4.5%. Even the higher figures look promising.

6. Longer soaking times in hydrogen appear to give better fuel retention.

Future work will be to obtain larger-grained samples, and to verify urania losses by wet chemical analysis.

Dependence of Grain Size on Sintering Time (Tubes). Grain size measurements were made on a series of Z-tubes and Y-tubes (described above) which had been sintered in hydrogen for 3, 5 and 10 hours. About half the tubes were uniform in grain size, but others showed gradation across the tube (i.e., in a radial direction, from inner rim to outer rim), and one showed variation in grain size along the outer rim. It is conceivable that this variation is related to freedom of access of hydrogen or to local temperature environment. The apparent decrease in size of the BeO grains with increasing time may be attributable to unrecorded variation in the firing conditions. Note that separate specimens were used for different soak times instead of exposing a single specimen to increasing soak times (Table II-4).

Table II-2

VARIABLES IN FUEL RETENTION OF TUBES

Tube Type *	Hydrogen Sintering °C	Hydrogen Sintering Hrs.	Density g/cc.	Density % theor.	Wt. Loss % of Total **	Uranium Loss, % by Weight Change	Uranium Loss, % by Count **	Loss Tested in Air Time Hrs.	Loss Tested in Air °C
Y	1650	5	3.11	97.8	0.005	0.066	-	4	1258
Y	1650	5	3.11	97.8	0.016	0.210	0.09	10	1258
Y	1650	5	3.11	97.8	0.005	0.066	0.32	20.4	1258
Y	1650	10	3.11	97.8	0.006	0.080	0.96	4	1258
Y	1650	10	3.12	98.1	0.011	0.014	0.99	10	1258
Y	1650	10	3.12	98.1	0.002	0.026	0.79	20.4	1258
Z	1725	3	3.11	97.8	0.029	0.399	1.19	4	1258
Z	1725	3	3.11	97.8	0.019	0.250	(0.47)	10	1258
Z	1725	3	3.11	97.8	0.016	0.210	1.42	20.4	1258
Z	1650	5	3.04	95.6	(0.028)	0.370	(0.12)	10	1258
Z	1650	5	3.04	95.6	(0.006)	0.080	(0.15)	20.4	1258
Z	1650	10	3.03	95.3	(0.046)	0.610	(0.34)	4	1258
Z	1650	10	3.02	95.0	(0.088)	1.170	0.32	10	1258
Z	1650	10	3.02	95.0	(0.038)	0.501	2.46	20.4	1258
Y	1650	10	3.12	98.1	0.079	1.050	(1.21)	4	1526
Y	1650	10	3.11	97.8	0.104	1.383	1.06	10	1526
Y	1650	10	3.11	97.8	0.179	2.39	1.00	20	1526
Z	1725	3	3.12	98.1	0.123	1.64	-	4	1526
Z	1725	3	3.11	97.8	0.141	1.87	(0.41)	10	1526
Z	1725	3	3.11	97.8	0.203	2.70	0.95	20	1526
Z	1650	10	3.04	95.6	0.188	2.50	0.84	4	1526
Z	1650	10	3.05	95.9	0.277	3.01	1.32	10	1526
Z	1650	10	3.07	96.5	0.263	3.50	0.64	20	1526
Y	1650	5	3.09	97.2	0.415	5.51	1.94	4	1650
Y	1650	5	3.10	97.5	0.916	12.02	4.53	10	1650
Y	1650	5	3.08	96.9	1.332	17.70	4.59	20	1650
Y	1650	10	3.11	97.8	0.254	3.38	0.89	4	1650
Y	1650	10	3.10	97.5	0.741	9.88	3.29	10	1650
Y	1650	10	3.10	97.5	1.097	14.60	4.21	20	1650
Z	1725	3	3.10	97.5	0.277	3.69	1.25	4	1650
Z	1725	3	3.09	97.2	0.799	10.62	3.81	10	1650
Z	1725	3	3.08	96.9	1.346	17.92	4.91	20	1650
Z	1650	5	3.07	96.5	0.320	4.26	2.72	4	1650
Z	1650	5	2.94	92.5	1.415	18.85	4.32	10	1650
Z	1650	5	2.95	92.8	1.520	20.22	4.31	20	1650
Z	1650	10	3.06	96.2	0.295	3.93	1.250	4	1650
Z	1650	10	3.02	95.0	0.610	8.13	2.93	10	1650
Z	1650	10	3.03	95.3	0.656	8.80	2.44	20	1650
X	1650	10	2.87	95.4	0.00	-	-	20.4	1258
X	1650	10	2.87	95.4	0.011	-	-	20	1526
X	1650	10	2.87	95.4	0.027	-	-	20	1650

* X tubes - "as received" UOX BeO unfueled.

Y tubes - "as received" UOX BeO · 7-1/2 w/o UO_2.

Z tubes - ball-milled UOX BeO · 7-1/2 w/o UO_2.

** Values enclosed by ( ) were apparent gains instead of losses.

MUL-7876 (1)

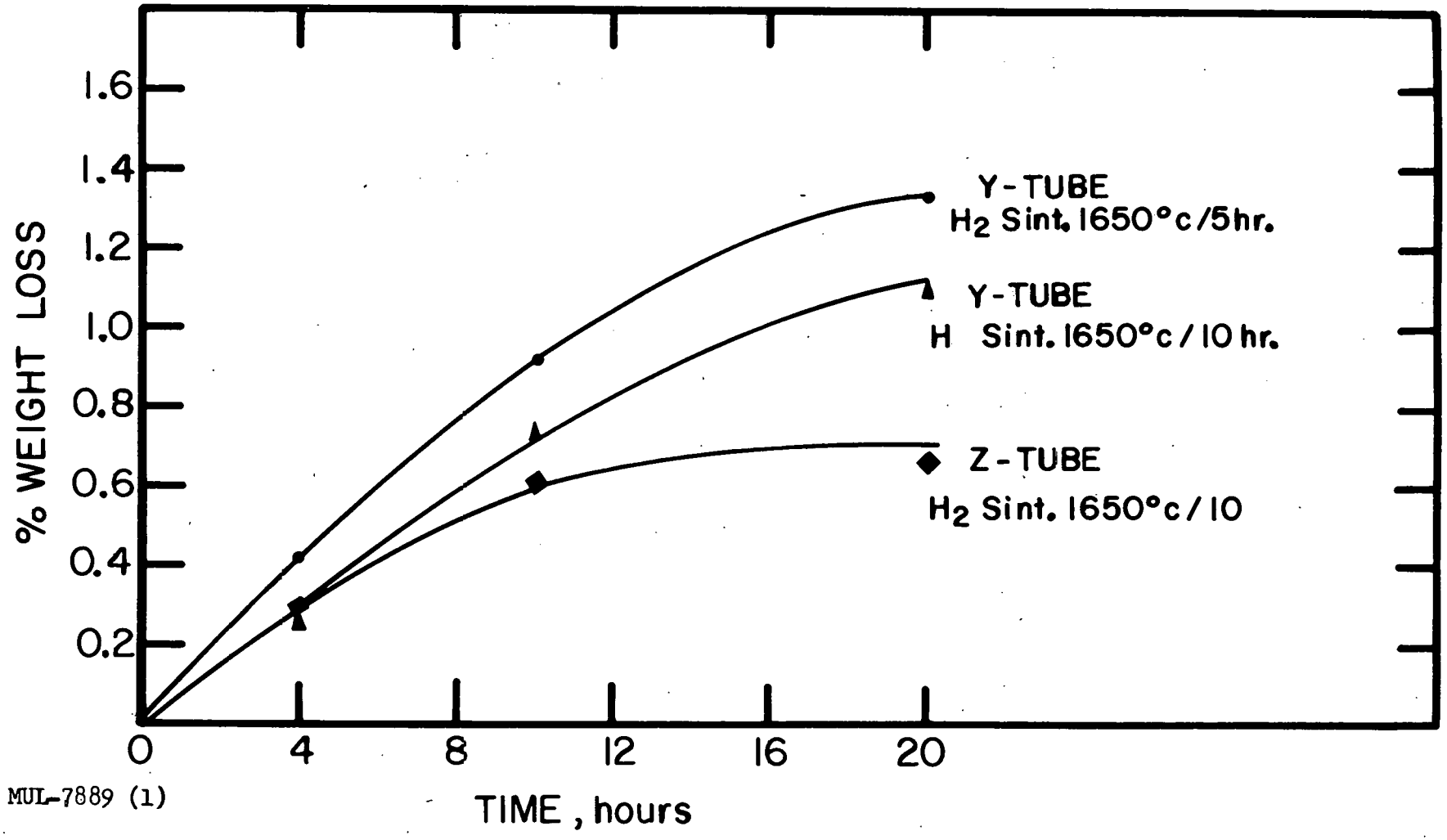

Fig. II-4. Weight loss versus time, $BeO-UO_2$ in air at 1650 °C.

In the six loaded tubes, the urania is rather evenly distributed. In all of them, the BeO grains are almost opaque, and are golden in color in thin section under plane-polarized light; presumably the color is caused by many fine-grained inclusions of UO_2, which are too small to resolve optically. The larger UO_2 grains occur both enclosed in BeO grains and along grain boundaries. In both the Z- and Y-tubes heated for 5 hours at 1650°C (#109, #92), however, there is some tendency for the larger UO_2 grains to concentrate along grain boundaries.

Sintered Samples Reheated in Air. Samples of a Z-tube which had been sintered 3 hours in H_2 at 1725° were fired in air at 1525°C for 4, 10 and 20 hours. There was no significant change in grain size of the BeO even after 20 hours. The boundary between oxidized and (relatively) unoxidized material is marked by a color difference from black (oxidized) to brown in these tubes: the 4-hour sample is brown with black inner and outer rims, the 10-hour sample is black except for lenses of brown material in the interior of the tube, and the 20-hour sample is entirely black. It is interesting to note by comparison that a sample of a Z-tube which was sintered 5 hours in H_2 at 1650°C and then fired only 4 hours in air was totally black.

Urania in the two fired tubes which are totally black is almost all present as large grains (1-3 μ) located along grain boundaries. There is probably some very fine-grained (< 1/4 μ) urania retained in the BeO grains, as they have a grayish tinge. In narrow zones along the edges of the sample, the BeO grains are clear, and there are very few urania grains even along grain boundaries. Throughout the sample there are many small spheroidal voids within grains, and large elongate and triangular voids along grain boundaries.

In each of the two samples which are part black and part brown, there is a narrow transition zone (50-100 μ) between the brown area and the black area. The prevailing color in the transition zone is black; the interstitial urania grains are small (< 1 μ). Going from the transition zone toward the edge of the sample, the size of the interstitial urania grains increases gradually from ~ 1 μ to 2-3 μ (See Fig. II-5).

Effect of Grain Size on Sintering Time (Cylinders). Samples used for this purpose were 3/4-in. diameter cylinders. They were isostatically pressed and sintered in hydrogen at 1650°C for 1, 3, and 5 hours. Density as well as grain sizes of both BeO and UO_2 increased with time.

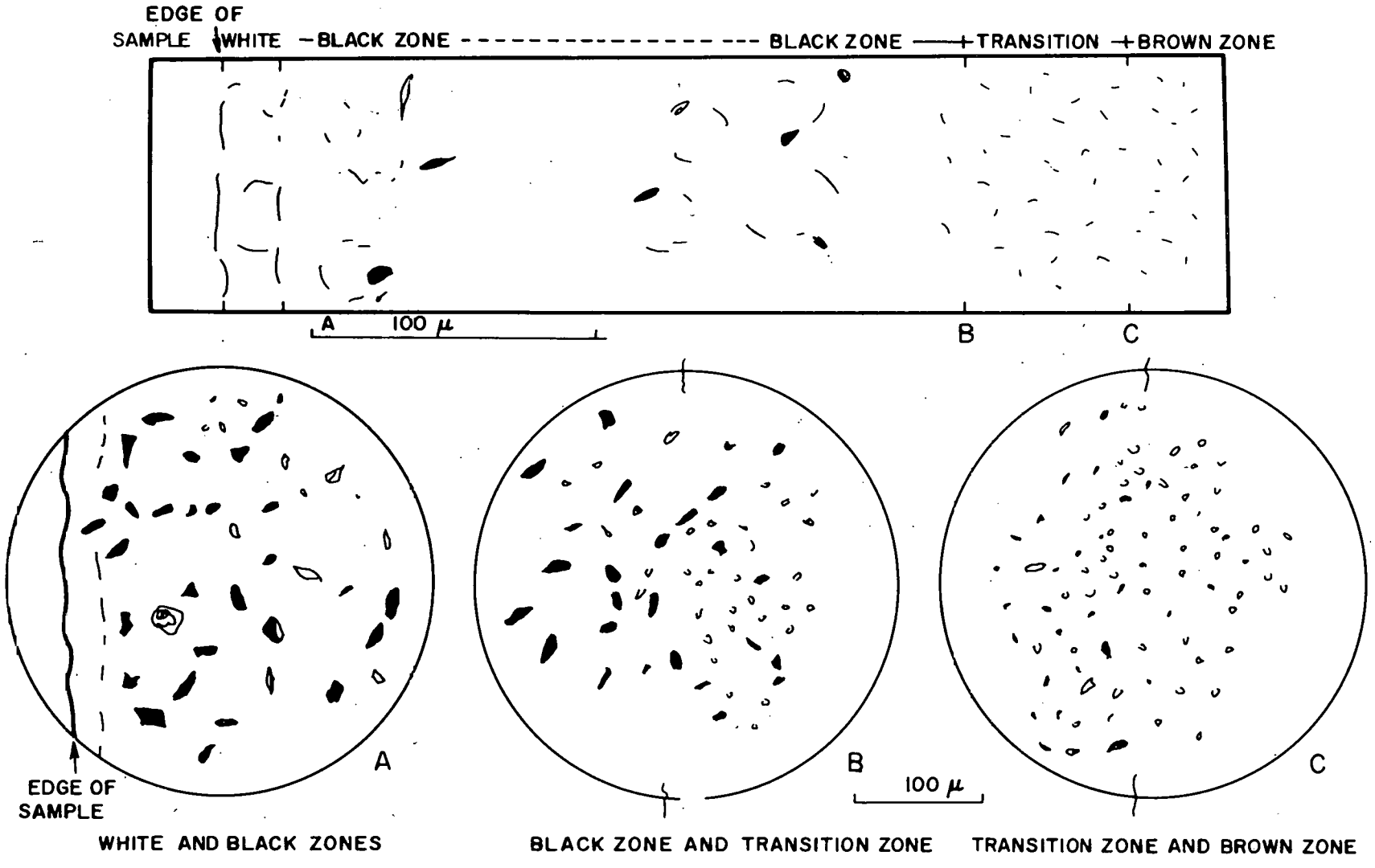

MUL-7890 (1)

Fig. II-5. Diagrammatic sketches of black and brown zones, and transition zone, in a thin-walled tube (thin section #99) which has been fired in air to test fuel loss. Sketches as seen in plane polarized light. Black spots are urania grains. White spots (in A and B) are voids; white spots (in C) are chiefly urania, a few are voids. BeO grain boundaries are not visible but are roughly marked by urania grains in A and the left side of B.

Grain Size, Microns

Time, hrs	BeO	UO_2	Density % theor.	Fuel loss 1525°C - 4 hrs
1	1 - 4 μ	< 1/2	92.9	25%
3	10 - 20	up to 1	96.1	18
5	10 - 20	up to 1.5	96.5	4

We have since determined that considerable improvements in densities and fuel loss can be made by sintering thin-wall extruded specimens (e.g., tubes).

General Petrographic Observations. In addition to the variations in grain size and distribution of urania, certain other features have been noted. In all samples, there are vugs* lined with BeO crystals which lack urania inclusions. Rectangular areas filled with coarse-grained (~3-5μ) urania are common in the extruded tubes. Areas of BeO grains which are slightly larger, and lower in urania content than the rest of the sample, are presumed to be the result of incomplete mixing; they have been observed in the cylinders but not in the tubes. The "border zones" containing very fine-grained urania observed previously are generally present in the cylindrical specimens but have not been found in the tubes. The interpretation of some of these inhomogeneities may provide clues to the mechanisms of diffusion.

Testing of Suppliers' tubes. The results of four tubes tested for fuel loss are given in Table II-5. The counting of the tubes was done by the gamma pulse spectrometer for a total of 1,000,000 counts per sample. Also a DXT run was made on each sample before and after testing to determine uniformity of fuel loading along the length of the tube. Before the fuel loss test all samples showed a variation of less than 0.5%. However, after the test the variation increased in all tubes up to 6%. Test conditions were 1525°C for 4 hours.

The 4.51% UO_2 tubes showed severe eruptions on the surface while the 8.23% UO_2 tubes did not. The discrepancy between fuel losses by weight and losses by counting is unexplainable at this time.

3. Petrographic Work

Sample Preparation. During the past three months, the thin-section saw and cutoff saw have been completed and put into operation. Subsequent

*Vug is a cavity or hollow in a rock, often lined with crystals which project into the cavity.

Table II-5

	T-120-A	T-120-B	T-237-A	T-237-B
Density before, g/cc	3.179	3.178	3.066	3.045
Density after, g/cc	3.138	3.144	3.144	3.056
% Density change	-1.28	-1.06	-0.32	-0.29
% Weight loss	0.90	0.79	-0.211	-0.386
% Fuel loss by weight change	10.8	9.60	-4.68	-8.56
% Fuel loss by counting	3.94	3.48	1.46	1.78
% Fuel loading	8.23	8.23	4.51	4.51

Note: Minus sign signifies gain.

repairs have also been required. The completion of the most recent batch of thin sections has demonstrated that thin sections can be produced at the rate of 4 to 5 per day, starting with an uncut tube and going through the whole process including application of the cover glass. .

It has been demonstrated that a good preliminary surface, without pull-outs, can be obtained on various BeO samples by grinding with 400-mesh SiC abrasive on the bronze lap.

Petrographic Examination Techniques. A method for the measurement of grain size which is rapid and internally consistent has been developed, using a grid eyepiece and measuring maximum grain diameters of 40 grains along selected traverses. The results show that a difference of 2 to 3 μ in the average value (ca. 6-16 μ) obtained by this method is significant and can readily be detected by optical inspection.

Thin-section technique has so far proved good for the location of voids and urania inclusions, and for distinguishing voids from inclusions, if the oil immersion objectives are used (magnification of 1250 x). This technique also indicates that unresolvable urania grains are present in many BeO grains, since the presence of finely divided urania imparts a golden or grayish color to the BeO, as viewed in transmitted light. Additional advantages are the ability to distinguish individual grains of BeO clearly and to note grain orientation.

4. Coating of BeO (Process and Material Development Section)

Two coatings have been applied to fueled (10% UO_2) BeO tubes of high density (above 98% of theoretical). Coating No. 1 (90% silica, 10% ball clay)

did not protect well. It softened at too low a temperature (1500°C) and was probably too fluid at the test temperature of 1650°C allowing uranium loss through the coating. Silica also has a fairly high vapor pressure at these temperatures and much of the coating apparently evaporated. Coating No. 2 (90% $ZrSiO_4$, 10% ball clay) looks like a good coating. Test conditions (approx. 1 hr at 1700°C) were not as severe as for Coating No. 1. Coating No. 2 softened at a higher temperature (1700°C) and covered well. This coating will be tested more extensively in the future.

5. Coating of Graphite

The large vacuum coating furnace has been checked out and has proven satisfactory to temperatures of 2000°C. Preliminary coating work was done on cylindrical samples of ATJ graphite, approximately 1-1/2 in. diameter and 1 in. high. No problems developed in coating these samples although only one sample was successful. However, ATJ is not considered a coatable grade of graphite and was used only to check out the procedure.

Two cylindrical samples of Grade "A" graphite with dimensions of 4 in. diameter and 2.4 in. high were then coated. The first sample was damaged in testing; the second, however, has been exposed to static air at 1350°C, and has so far withstood oxidation for 353 hours. It will be tested to failure.

Since no cracking or flaking of the coating on the larger samples occurred, the coating process probably would not be the limiting factor for even larger coated graphite pieces. During the coating procedure the sides of the sample reach the melting point of silicon before the cooler ends. However, the sample has been completely covered with powdered silicon which remains more or less in place after melting. Since the entire sample need not reach the melting temperature simultaneously, long rods could probably be coated by passing them through a comparatively small hot zone.

6. Beryllium-Boron System

The objective of this study is to explore this poorly-known system from a fundamental viewpoint, which includes completion of the Be-B phase diagram and investigation of compound properties within this system. Note that beryllium borides obtained from pure B^{11} would be possible moderators for a Pluto reactor.

Compounds were prepared from mixtures of Be (-170 to 325 mesh) and boron (-325 mesh). Stoichiometric proportions were crudely mixed by hand and isostatically pressed at 50,000 psi prior to heat treatment. Pressed

samples were outgassed at 1000°C and approximately 10^{-4} to 10^{-5} mm Hg before introducing one half atmosphere of argon for the final heat treatment. Preliminary impressions of melting points were noted during preparation (characterized by edge-rounding of pellet specimen). A microscopic phase analysis was made after heat treatment. These results are listed in Table II-6.

Table II-6

Be/B Ratio	Melting Pt. (°C)	Remarks (Visual, x-ray, microhardness) After heating
6/1	1200°C	Two phases present; one appears to be Be
2/1	1400°C	One phase (Be_2B) present as copper-red crystals
1/2	1750 - 1910°C	One phase (BeB_2) present as black crystals
1/6	1910°C	One phase present as reddish single crystals, very likely BeB_6

Microhardness tests were run on the samples mentioned above. They are listed in Table II-7. Note the unusual hardness of the BeB_2. For comparison several hard substances are listed.

Table II-7

Be/B Ratio	Phase	20-g Load	50-g Load	100-g Load
6/1	Be	690	-----	-----
	Eutectic	-----	2000	-----
2/1	Be_2B	-----	-----	2160
1/2	BeB_2	-----	-----	3490
1/6	BeB_6	-----	-----	2590
Diamond*		-----	-----	7000
B_4C**		-----	-----	3050
Boron**		-----	-----	2410

* HANDBOOK OF CHEMISTRY AND PHYSICS

** Cline, C., "An Investigation of SiB_6," Jour. of Electrochemical Soc., Vol. 106, No. 4, p. 322 (1958).

Single crystals were found for the compounds Be_2B, BeB_2 and BeB_6. The structure of Be_2B has been reported by Markovsky et al, as having an anti-florite (C1) structure. Our x-ray single crystal analysis has established the crystal system of BeB_2 as hexagonal. The calculated density is 2.337 g/cc and the lattice parameters are $a_0 = 9.76$ Å and $C_0 = 9.51$ Å. A chemical analysis of the BeB_2 sample is given in Table II-8.

Table II-8

Element	Wt. % Calculated	Wt. % Analyzed
Be	29.4	29.3
B	70.6	70.8

Fabrication Studies

1. Extrusion Variables

Attempts are being made to determine how moisture and urania content affect the sintered shrinkage and density of thin-walled beryllia tubes. When completed, the information should permit prediction and make it possible to extrude BeO-UO_2 fuel elements to dimensional tolerances.

The data collected so far are presented in Table II-9 and Fig. II-6. When data are complete, we will have relationships between total combustibles and (a) green shrinkage and sintered shrinkage, (b) green bulk density and sintered density. With these relationships, it should be possible to predict the sintered shrinkage for an extrusion mix and thus to select the proper extrusion die size. Also, it may be possible to check the fuel elements after the organic burnout phase to see if they could possibly meet the final sintered dimensions. So far, the points seem to correlate reasonably well. However, we are seeking considerably more data.

2. Fuel Element Fabrication Facility (Building 192-C)

The procedure to be used for the manufacture of Pluto reactor fuel elements is as follows: Beryllium oxide-water slurry will be mixed with uranyl nitrate solution. The uranium will be precipitated using NH_4OH and the solids filtered and dried. The dried mixture will be weighed and a measured amount of binders and water will be added. This mixture will be mixed, aged, then extruded to shape, cut and dried. The dried tubes will be heated in air at

Table II-9

Sample	% UO_2	Lot No.	Organic Burnout Shrinkage* %	Organic Burnout Density (gm/cc)	Organic Burnout Density (% theor)	Sintered Shrinkage* %	Sintered Density (gm/cc)	Sintered Density (% theor)	Initial Moisture %	Total Combustibles** %
V3-1	0	100 W 5	2.05	1.5891	52.84	22.70	2.9551	98.26	28	28.02
V3-2	0	100 W 5	2.23	1.5686	52.16	22.68	2.8496	94.76	28	27.94
V3-3	0	100 W 5	2.22	1.5773	52.45				28	27.67
V3-4	0	100 W 5	2.14	1.5744	52.35	22.71	2.9545	98.24	28	27.48
V14	5	100 W 5	3.44	1.6060	51.47	24.64	3.0873	98.94	34.82	29.60
V15	5	100 W 5	2.20	1.6003	51.29	22.89	3.0158	96.66	33.73	27.74
V16	5	100 W 5	2.50	1.6251	52.08	23.57	3.0650	98.24	31	28.35
V20	5	100 W 5	3.55	1.5542	49.81	25.36	3.0836	98.82	32	30.53
V6	7-1/2	30	3.37	1.6265	51.15	24.42	3.1391	98.71	27	29.11
V7	7-1/2	30	3.32	1.6656	52.38	23.87	3.1311	98.46	29	28.30
V8	7-1/2	30	3.28	1.6196	50.93	24.68	3.1447	98.89	31	29.09
V17	10	100 W 5	4.41	1.7220	53.11	24.81	3.2225	99.39	27	29.18
V18	10	100 W 5	2.91	1.7631	54.38	23.12	3.2293	99.60	29	26.93
V19	10	100 W 5	4.73	1.6738	51.62	25.73	3.1940	98.52	31	30.38
V21	15	100 W 5				28.91	3.3111	98.12	39	36.30
V22	12-1/2	100 W 5				25.77	3.2824	99.25	34	33.62
V27	10	100 W 5				26.58			29	31.80
V28	10	100 W 5				22.94			30	27.08
V29	5	100 W 5				24.93			30	29.58
V30	7-1/2	100 W 5				22.23	3.1757	99.86	27	25.88
V31	7-1/2	100 W 5				23.69	3.1769	99.90	28	28.36
V32	7-1/2	100 W 5				24.57	3.1660	99.56	29	30.38

* Shrinkage based on extrusion die hole size.

** Total combustibles determined by change in weight from extrusion through organic burnout. Based on extruded weight.

MUL-7877 (1)

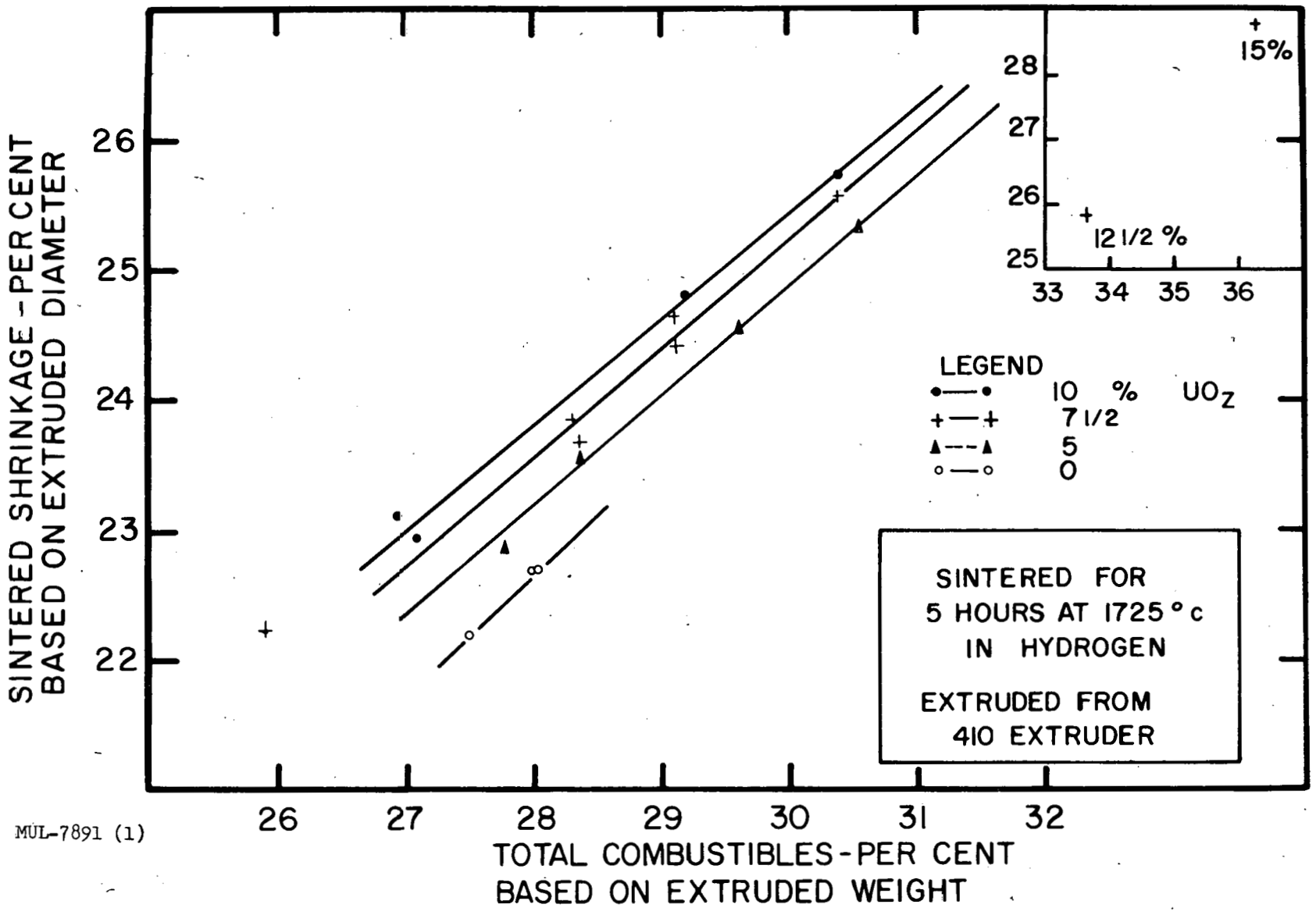

MUL-7891 (1)

Fig. II-6.

1500°F to remove binder, then fired in hydrogen at 1500°C to final density.

The status of equipment to perform the above operations is as follows: In general, all major components for the blending, mixing, extruding and drying systems are installed. Certain refinements are yet to be made. Several test runs have been made utilizing unfueled BeO, and no major difficulties have been encountered.

Mechanical Properties

1. Thermal Stress (Process and Material Development Section)

The extreme environmental conditions under which the Tory II reactors will operate necessitates a knowledge of the resistance of beryllium oxide ceramics to thermal stresses. Equipment for evaluating the steady-state thermal stress resistance of fueled and unfueled beryllium oxide has been described in UCRL-5515. In this method the power required to fracture a hollow cylinder is measured. The cylinder is heated by an electrical heater in the central hole. A thermal stress resistance parameter can be evaluated from the measured power. This parameter is denoted by the symbol R' and is equal to $\sigma_f k(1-\mu)/E\alpha$

where σ_f = failure stress
k = thermal conductivity
E = elastic modulus
α = coefficient of thermal expansion
μ = Poisson's ratio

Using this material parameter the data obtained as above may be compared with samples tested in the Blowpipe.

Recent data obtained is shown in Table II-10. These data are compared with the Tory II thermal stress parameter in Fig. II-7. The majority of the specimens contained 5 wt % UO_2 dispersed in a beryllium oxide matrix. The tests were performed at an outer wall (minimum) temperature of 1000°C (1832°F) since it was felt that this would be the most drastic temperature insofar as materials parameters were concerned.

A comparison was also made between samples having two different firing histories (1725°C and 1800°C respectively). In addition, an attempt was made to increase the grain size without changing the bulk density of the material. Examination of the microstructure, however, indicated that there was no significant change in grain size.

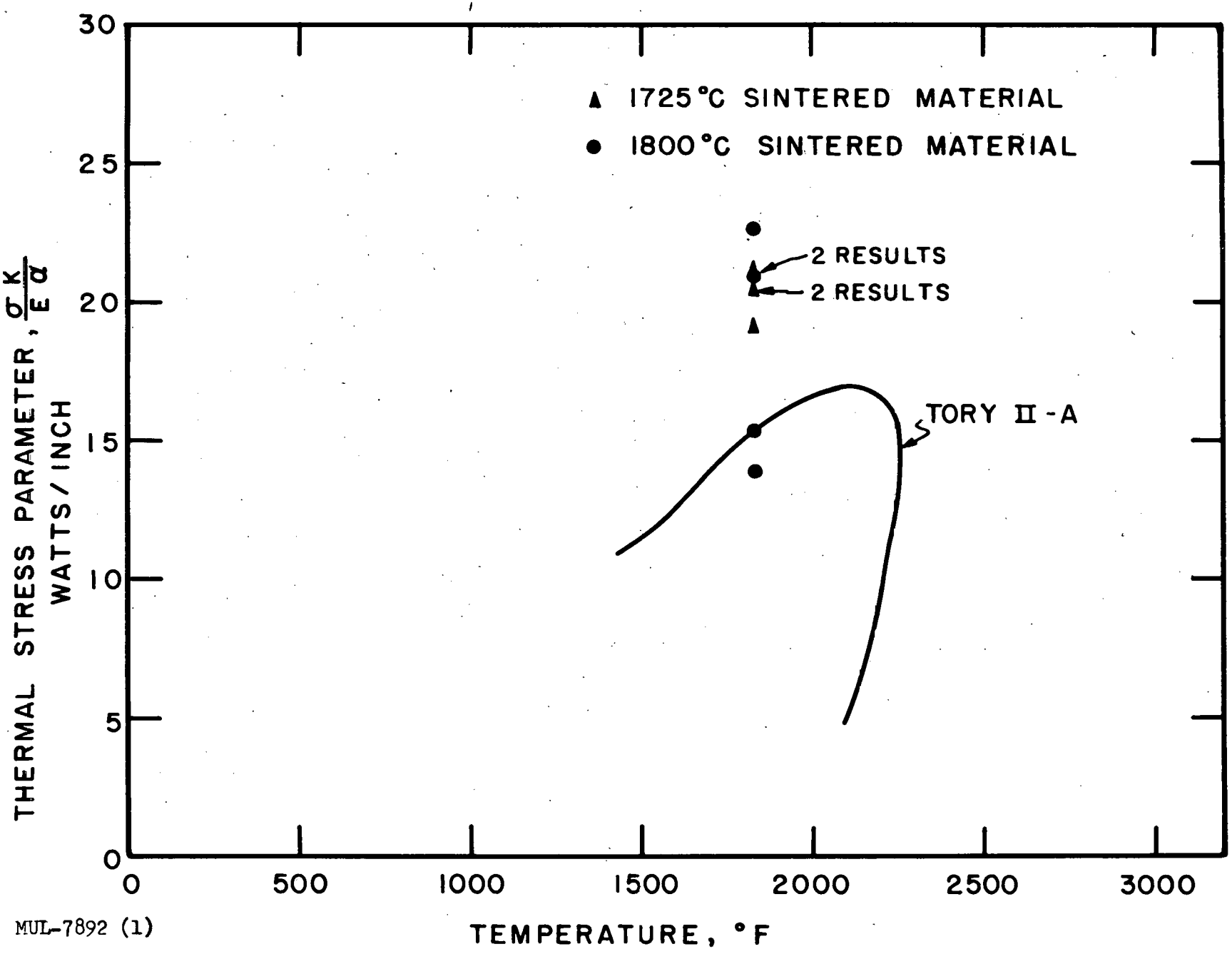

MUL-7892 (1)

Fig. II-7.

Table II-10

Sample	Sintering Conditions No.	Temp. (°C)	Hold time	Density % of Theor.	Power input (watts/in.)	Inner Wall Temp. °C Initial	Failure
2B	1800	5 hrs		95.18	>200	800	1000
2A	"	"		98.27	217	"	950
2C	"	"		(98.)	133	"	1100
4A	"	"		98.0	>116, <150	"	1000
6A	"	"		98.0	>180, <200	"	1000
1A	1725	"		97.89	183	"	950
1B	"	"		98.0	>194, <333	"	1350
1C	"	"		98.0	207	"	1000
1D	"	"		98.0	194	"	1000

Evaluation of the data indicates several important factors of which the following are the most pertinent:

a. The material fired at 1725°C had a more consistent thermal stress parameter at 1000°C than the material fired at 1800°C.

b. Material of slightly lower density (95%), appears to have a higher resistance to thermal stress than the 98% dense material.

c. Cracks propagate much further and deeper in the 98% material than they do in the 90-95% material previously tested.

2. Compressive Creep

We have run several compressive creep tests on commercially procured "High Purity" hot-pressed BeO (indicated as 99^{+}% pure). The samples were hot-pressed at 3150°F and 2000 psi. The average grain size for these specimens ranged from 20 to 34 microns as received.

Creep is a thermally activated process in which a material strains with time under a constant stress. The amount of primary creep in BeO appears small. This would indicate that the material work hardens very little and attains the steady-state secondary creep rate rapidly. Secondary creep is dependent upon the structure, S, and the applied stress, σ. Secondary creep rate, $\dot{\epsilon}$, can be described by the following rate equation

$$\dot{\epsilon} = f(S,\sigma)\, e^{-\Delta H_c/RT}$$

where S = Structure factor which includes grain size, dispersions, solid solution effects, and imperfections such as dislocations and vacancies.

ΔH_c = activation energy for creep

R = gas constant

T = absolute temperature

Assume steady-state secondary creep is established at a given temperature and stress. By rapidly changing the temperature a small amount at constant stress, we can assume negligible change in structure, S. A comparison of the creep rates and temperatures permits calculation of the activation energy for creep (Fig. II-8).

$$\ell n \frac{\dot{\epsilon}_1}{\epsilon_2} = - \frac{\Delta H_c}{R} \left(\frac{1}{T_1} - \frac{1}{T_2} \right)$$

A series of runs were made using the following procedure: All specimens were preconditioned at 2850°F for 12 hours in air. Specimens BC-BH-25 and BC-BH-31 were heated to the lowest test temperature, and the load was applied. The testing temperature for each specimen was successively raised 100°F in approximately 3 minutes after 24 hours or 1% creep, whichever occurred first. The remaining specimens were raised to the single test temperature, the load was applied, and the temperature was held for 10 hours or 4% creep (whichever occurred first).

The following is the experimental data:

Specimens	Density g/cc	°F	°C	$\dot{\epsilon}$ in./in./hr	1/°K
BC-BH-25	2.82	2250	1232	0.0000217	0.0006644
BC-BH-31	2.84	2300	1260	.000022	.0006523
BC-BH-25		2350	1288	.0000318	.0006407
BC-BH-31		2400	1316	.0000953	.0006295
BC-BH-25		2450	1343	.000181	.0006187
BC-BH-31		2500	1371	.00636	.0006083
BC-BH-23	2.81	"	"	.00083	.0006083
BC-BH-28	2.82	"	"	.00021	.0006083
BC-BH-30	2.80	"	"	.00088	.0006083
BC-BH-33	2.79	"	"	.00061	.0006083
BC-BH-25		2550	1399	.001200	.0005981
BC-BH-31		2600	1427	.002690	.0005883
BC-BH-34	2.84	2700	1482	.010300	.0005697

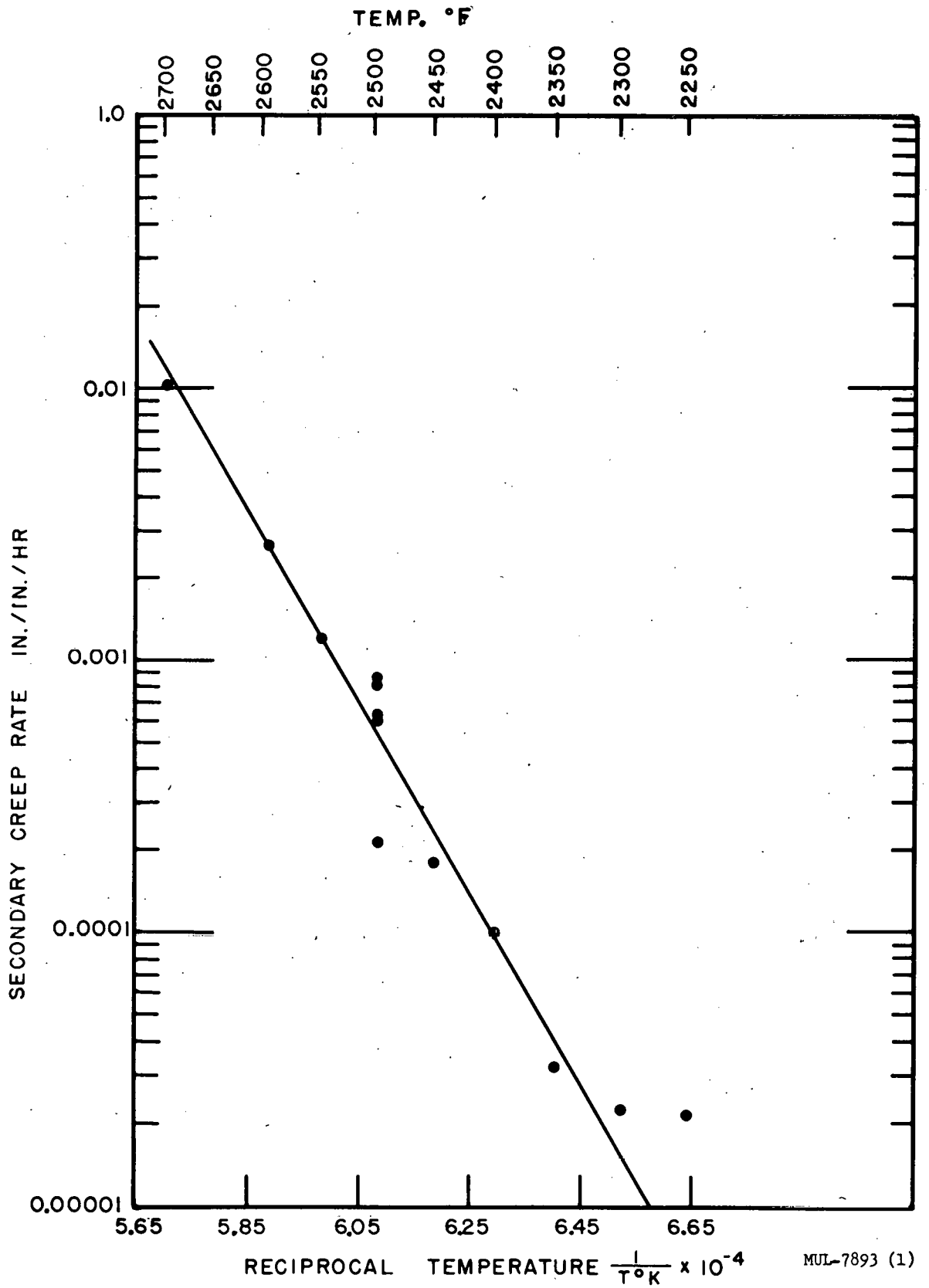
TEMP. °F
2700
2650
2600
2550
2500
2450
2400
2350
2300
2250
1.0
0.01
0.001
0.0001
0.00001
SECONDARY CREEP RATE IN./IN./HR
5.65
5.85
6.05
6.25
6.45
6.65
RECIPROCAL TEMPERATURE $\frac{1}{T°K} \times 10^{-4}$
MUL-7893 (1)

Fig. II-8.

The creep data are plotted as

$$\ln\dot{\epsilon} \text{ vs } 1/T \text{ , where the slope is } \Delta H_c/R \text{ .}$$

The lowest points do not fit the straight line. At these very slow creep rates, the measured strains approach the experimental error of the system. By taking abscissae from the straight line at $\dot{\epsilon}_1 = 0.01$ and 0.00001 (extrapolated), ΔH_c may be calculated as 160,000 cal/mol.

This experimental activation energy is considerably higher than the activation energy for self-diffusion of 106,700 cal/mol or the high-temperature low stress activation energy for creep of 114,000 cal/mol, found by Chang (NAA-SR-2458). However, verbal communication from another source indicates a diffusion activation energy of nearer 150,000 from sintering data.

Although a high activation energy for creep indicates a resistance to creep, this holds only when comparing specimens with the same structure at the same stress. It is possible for a material to have a lower activation energy and have it creep at a lower rate than a high activation energy material due to structural changes, such as grain size, dispersions (amounts, distribution).

THERMAL FRACTURE OF BERYLLIA FUEL ELEMENTS (BLOWPIPE)

Tubular beryllia specimens, about the same size as the Tory II-A fuel elements, are subjected to high temperature and thermal stresses in the "blowpipe" apparatus. A specimen is heated by thermal radiation from a graphite heater surrounding it. The heat is removed by forced convection cooling at the inside surface using helium.

70 tubes containing between 5 and 10% urania have been tested since the last report. Specimens have been subjected to thermal stresses up to 3 times those expected in Tory II-A, and temperatures up to 3200°F. Testing conditions have varied, but for most tests the specimen was brought to maximum temperature and thermal stress in 2 to 3 minutes, held at steady conditions for about 5 minutes, then brought back to room temperature and zero stress in about a minute. The thermal stress level and temperatures at which the specimens were tested is shown in Fig. II-9. The thermal stress parameter, $\sigma k/E\alpha$, represents the severity of the test and may be compared with that to which the actual Tory II-A fuel elements are to be subjected, shown by the curve in Fig. II-9.

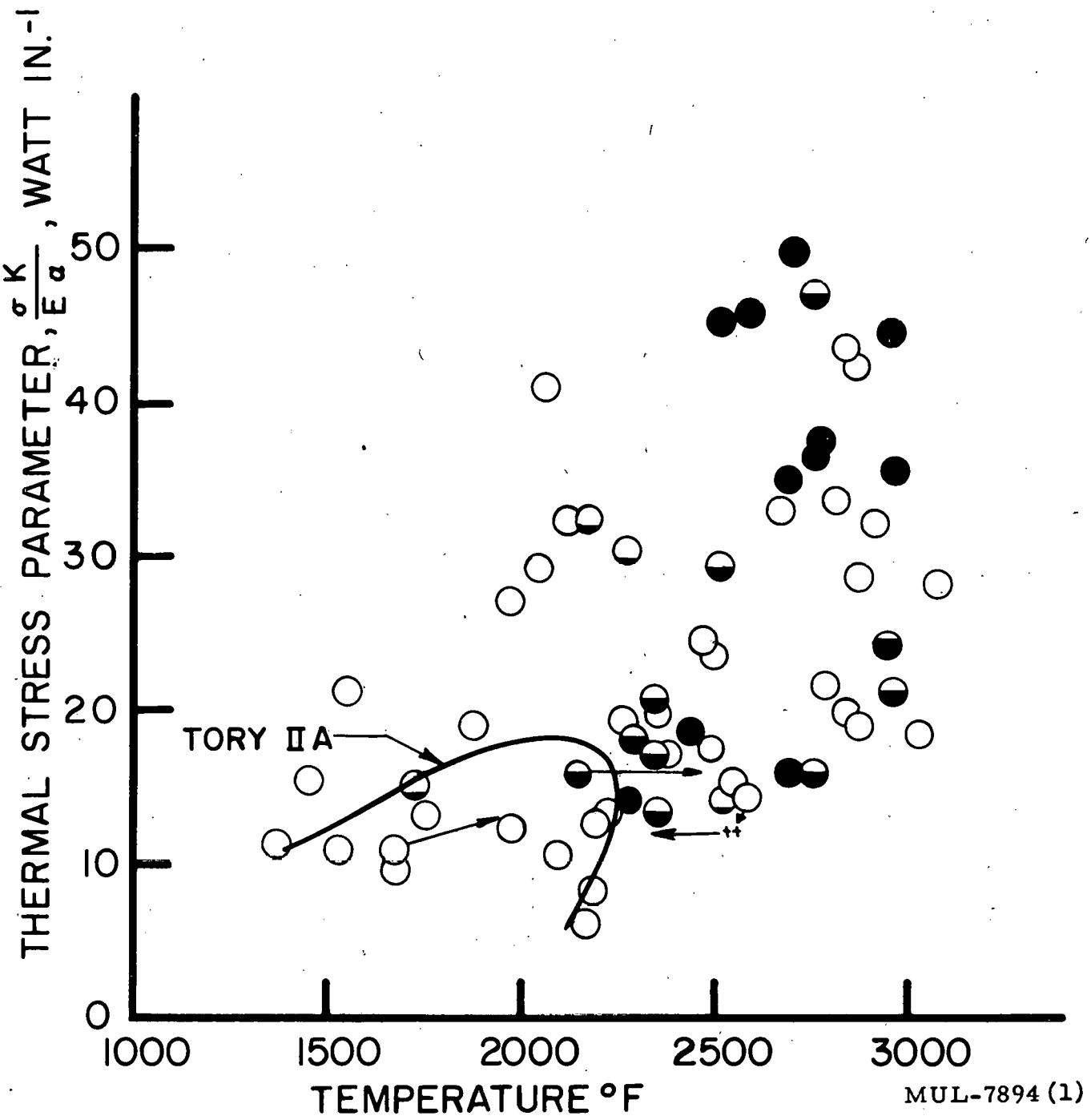

Fig. II-9. Thermal stress test results.

Condition of tubes before and after testing was determined by visual, x-ray and Zyglo inspection. The degree of damage ranges from "none" denoted by the symbol O to "severe" denoted by ⊙. "Severe" denotes at least a network of many interconnecting cracks, and in some cases, fragmentation of the specimens. The half-filled symbol ⊖ corresponds to a tube with one or two longitudinal cracks and perhaps one or two circumferential cracks. Failure seldom occurred when the Tory II-A conditions were not greatly exceeded.

METALLURGY

Coatings on Ti-Moly

Two 1/2 Ti-Moly tubes were electroplated for Lawrence Radiation Laboratory with 0.001" Cr on the Moly followed by 0.003" Ni on the Cr. The tube was then subjected to the following cyclic heating and cyclic loading conditions.

No. of Cycles	Room Temp to °F to Room Temp	Stress psi	Hold Time at Each Temp Cycle
4	700°F	8,000	10 minutes
4	700°	14,000	5
4	700	21,000	2
12	1400	6,000	10
3	1600	11,000	5
3	1900	21,000	2

The specimen withstood these conditions with no visible failure. The coating was still intact.

Tensile Creep

We have completed the vacuum system on the 6 Arc-Weld Model-"EE" creep machines. They will hold a vacuum better than one micron at 1800°F. We have run several high temperature (1800°F) stress strain curves on 1/2 Ti-Moly and René 41 with the following results.

	Yield Strength	Ultimate Strength	Elongation
1/2 Ti-Moly	62,000 psi	65,000 psi	9%
René 41	40,000	45,000	15%
LRL Spec. MEL-280	50,000	60,000	10%

The 1/2 Ti-Moly exhibited high yield and ultimate strengths at the expense of elongation. René 41 does not have the high strength to warrant further effort.

ANALYTICAL CHEMISTRY

Spectrochemical Determination of Impurities in BeO

A method has been developed which provides for the determination of the following elements with the limits of detection indicated:

Ag	2 ppm	Cr	4 ppm	Ni	1 ppm
Al	10	Cu	4	Pb	<4
B	2	Fe	10	Sb	4
Ba	1	Li	10	Si	<10
Bi	4	Mg	< 4	Sn	< 4
Ca	< 10	Mn	< 4	Ti	< 4
Cd	4	Mo	4	Zr	20
Co	4	Na	10	Hf	20

Gd 20 ppm, Sm 100 ppm, Eu 50 ppm, Dy 100 ppm.

The method is divided into three separate procedures in order to achieve the stated limits of detection. All three procedures utilize the dc arc excitation technique. The first is a total energy procedure primarily for the determination of refractory elements. The second is a carrier distillation procedure for the determination of low and intermediate boiling elements. Finally the alkali metals require a separate excitation in a different region of the spectrum. The accuracy and the precision of the method have not been determined pending the acquisition of reliable standards and high-purity base material. To date, approximately forty samples of BeO raw material, extruded shapes, and test specimens have been analyzed by this method.

Electron Microscopy

1. Characterization of BeO powders

Electron microscope examination was completed on two samples of BeO powder prepared from $Be(OH)_2$ and calcined at 800°C. Although the precipitation was performed differently, no significant difference was found between the two. An ultrasonic generator was successfully used to break up agglomerates and obtain a thin dispersion of BeO particles for this study.

The "puff-ball" appearance (predicted by others) to be characteristic of BeO made from the hydroxide was not observed. However, if the "puff-balls" had been present, they probably would have been broken up by the dispersing procedure, since the goal at that time was to observe individual particles if possible. Nondispersed material was not examined because the "puff-ball" information had not reached the laboratory at the time the work was being done.

2. Replicating method for BeO

The technique used by Stanley Bartram at GE ANP for replicating BeO has been tried, using Al_2O_3 for simplicity at first. Most details of the procedure have now been worked out successfully. Recent discussion with Mr. Bartram has clarified the remaining points. The method makes it possible to study the way in which particles are stacked in agglomerates and to observe the detail of particle surfaces that are not visible when whole particles themselves are magnified in the electron microscope.

HIGH-TEMPERATURE CHEMISTRY

Preparation and Phase Studies of Beryllides

Synthesis and determination of the crystal structure of a number of metal-beryllium compounds have been reported previously (UCRL-5309, 5432, 5517 and 5562). During this reporting period the following new compounds were prepared and their structure identified:

Compound	Structure	Cell Dimensions, A	Density
$HfBe_2$	hexagonal	a = 3.787 c = 3.159	8.32 g/cm^3
$HfBe_5$	hexagonal	a = 4.519 c = 3.465	6.06
Hf_2Be_{17}	rhombohedral	a = 7.49 c = 10.93 (hexagonal cell)	
$HfBe_{12}$	hexagonal	a = 7.44 c = 7.35	
$HfBe_{13}$	face-centered cubic	a = 10.00	
$TiBe_2$	face-centered cubic	a = 6.455	3.14
$TiBe_3$	rhombohedral	a = 4.49 c = 21.32 (hexagonal cell)	
Ti_2Be_{17}	rhombohedral	a = 7.39 c = 10.79	2.43

Titanium-Beryllium Phase Diagram

In addition to the structure work on the Ti-Be system, rough melting points of the five Ti-Be compounds were determined by visual observation of samples heated in BeO crucibles. The melts were pulverized and x-ray powder-diffraction patterns taken. The results are summarized below:

Composition	Melting Point	Phases identified in melt
Ti_3Be_2	1020°C ± 50°	$TiBe_2$ plus "X"
$TiBe_2$	1425 ± 50°	$TiBe_2$ plus "X" (very very weak)
$TiBe_3$	1480 ± 50°	$TiBe_3$ plus "X"
Ti_2Be_{17}	1685 ± 50°	Ti_2Be_{17}
$TiBe_{12}$	1595 ± 50°	$TiBe_{12}$ plus Ti_2Be_{17} ,

where "X" is a face-centered cubic structure with a = 10.62 A, isomorphous with the unidentified phase in the metal rich compositions of the Nb-Be and Ta-Be systems.

Fabrication of Beryllides

Several 1 in. × 1 in. cylinders of beryllides, both $ZrBe_{13}$ and $(Zr-U)Be_{13}$ have been formed by vacuum hot-pressing at ~1500°C and 4000 psi. Under these conditions specimens of ~100% theoretical density are obtained. The dies and the rams were of graphite, in some cases lined with Mo foil to prevent reaction of the pressing with the die. No particular difficulties have been encountered in the hot-pressing operation. Modifications of the hot press are in progress to allow fabrication of cylinders of 2 in. × 2 in.

Protective Coatings on BeO (General Chemistry Section)

The work on a water-vapor-resistant coating on BeO continues. A testing furnace capable of operation in humid atmospheres at temperatures >1600°C has been constructed and is now in operation.

Attempts to utilize SiO_2 as a protective coat have been completely unsuccessful. Two high-fired BeO specimens coated with SiO_2 were tested in water vapor at one atmosphere and ~1485°C for a total time of 433 minutes. An uncoated BeO piece was tested simultaneously as a control. The coated specimens lost weight more rapidly than the uncoated one by a factor of two. Further tests on SiO_2 and other coatings are planned.

Protective Coatings on Beryllides

The investigation of oxidation-resistant coatings which are suitable for application to beryllide pieces continues with the major effort being applied to the $MoSi_2$ on Mo combination. It has been necessary to use molybdenum as the base material since no beryllide pieces have been available. A considerable amount of time has been devoted to deposition of the coats by electrophoresis. As deposited, the coats have been smooth and adherent, but most have cracked or flaked upon sintering. No coating yet obtained has been successful.

Oxidation Resistance of Pure Silicon

When graphite is coated with silicon metal, the protection obtained is actually due to the formation of a "skin" of adherent SiO_2, which forms on the surface of the silicon. This SiO_2 is extremely resistant to the inward diffusion of oxygen, and thus the silicon metal is protected and with it the graphite beneath.

It has been observed recently that the presence of impurities in the silicon (leading to yielding impurities in the SiO_2 skin) may greatly increase the rate of diffusion of oxygen. Measurement of the rate of oxidation of extremely pure transistor-grade silicon shows it to be ~ 1/50 that of the rate given in the literature. The purity of the silicon used to obtain the literature value is given as 99.95%. It thus appears that by careful control of the purity of silicon used, the lifetime of coated pieces will be lengthened. Work is under way to establish the rate of diffusion and the heat of activation of the diffusion process on the purest silicon obtainable.

CHAPTER III. HOT BOX

EXPERIMENTS AND RESULTS

Initial criticality measurements were performed on a BeO critical assembly during the week of June 1-6. The BeO was in the form of 6.000" × 6.000" × 1.000" blocks which had slots on one face 5-3/8" wide and 0.015" deep. These had been used in the Livermore Spade experiments. The slots in fact are used in the present assembly as heating passages.

The experimental layout is shown in Fig. III-1. The BeO blocks are stacked on edge in four graphite boxes separated by graphite vane guide plates. In this assembly 2-mil oralloy foils were placed every inch giving a BeO/U ratio of 1130:1, and were suspended in a vertical direction. The depth of the assembly is 24.00 in. The lower surface of the assembly is raised 5 in. above the base layer of the low-mass table by graphite risers which are spaced 6 in. apart and run north to south. The vane guide plates are 1-in. thick; the side walls are 3/4-in. graphite while the pusher plates at the north and south ends are 1/2-in. thick. The graphite density is 1.74 g/cm^3.

In the initial experiment, the critical dimensions of assembly were determined by inverse multiplication variation with length. In the process, it was found that the fine vane was equivalent to 0.8 ± 0.1 in. of BeO in the north-south dimension. Also, Vane No. 4 was found to be worth ≥ 5 in. of BeO in the N-S dimension. The critical dimensions at 29°C were found to be: 26-23/32 ± 1/32 in. wide (including graphite walls), 37-1/32 ± 1/32 in. long (including pushers), and a depth of 24.00 in. Two qualifications exist; the fine vane was not completely out nor was the source removed. The fine vane had 3.5% of its reactivity worth in the assembly, which is equivalent to 0.03 in. of BeO in the N-S dimension. The source was seen to act as a neutron absorber as well. In fact, it was worth 18.5% of the fine vane, or 0.14 in. in BeO in the N-S direction. Therefore, the length should be reduced from 37-1/32 in. to 36.86 in. One layer of BeO (i.e., the southern-most layer) was of half-inch thickness. Seventy 2-mil fuel foils were used. The fuel mass was 8.566 kg of 93.2%-enriched oralloy.

Transient studies involving motion of the fine vane were performed to find the reactivity worth of the fine vane. A value of $0.72 was obtained for the "fine vane unit" for this loading. To establish the nuclear hazard associated with a man falling on the assembly, paraffin was placed on the top of half

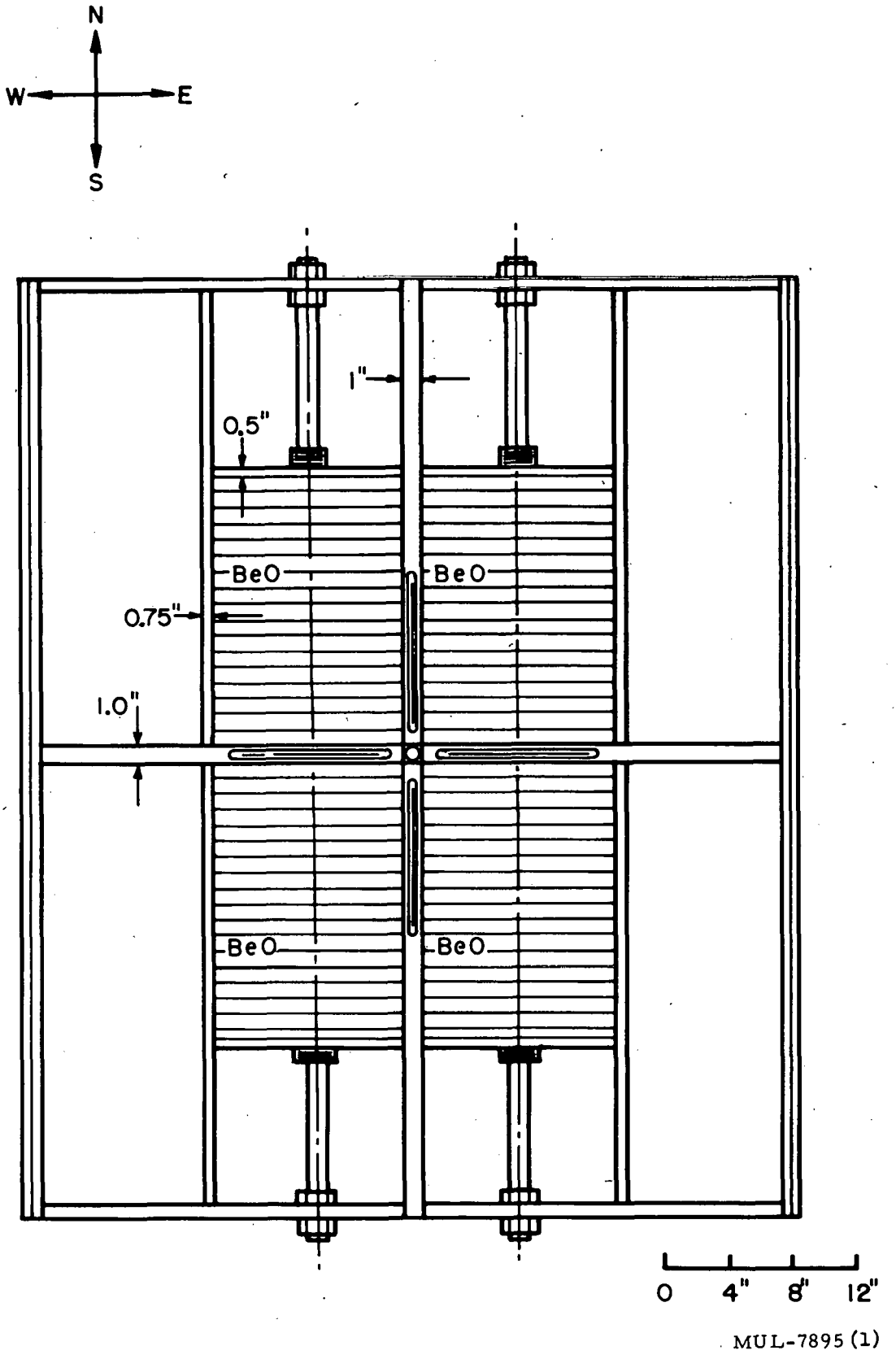

Fig. III-1. View from above of BeO critical assembly, depth 24.0 in.

of the assembly. The fine vane fully inserted and 6.8% of the Vane No. 4's worth compensated for a 6-in. thickness (i.e., 78 lb) of paraffin. Therefore, ample negative reactivity is available in the vanes to compensate for possible accidents involving reflection of neutrons from a man very near the assembly.

The core was increased in length by 3-1/2 in. of BeO to see what the vane positions would be at the start of a hot run. To compensate for the decrease in buckling, the fine vane was inserted, and 36% of Vane No. 4 was necessary for criticality. Six inches of paraffin on half of the top required an additional 30% of Vane No. 4. Since Vanes Nos. 2 and 3 are also inserted during loading, an ample safety margin exists.

The above critical assembly may be converted to a simplified buckling description for comparison purposes. In the present case, the vane cruciform complicates the calculation, and one might anticipate a serious streaming correction. In order to homogenize the core for calculation of buckling the 1-in.-thick half-void graphite cruciform, the 0.50-in. graphite pusher plates, and the 0.75-in. graphite side walls must be converted to their BeO equivalents. Comparison of Livermore cold criticality BeO and graphite experimental results for M/U of 2300 and for M/U of 570 indicates that graphite is neutronically equivalent to BeO with a density 0.897 of the graphite density. The graphite cruciform walls and pusher plates were converted to BeO on this basis. Furthermore, the density effect of the cruciform is averaged, disregarding notions of importance, over the whole reactor. The effect is to give a buckling of $B^2 = 5.61 \times 10^{-3}$ cm^{-2} at a density of $\rho_{BeO} = 2.64$ g/cm^3 for the BeO/U ratio of 1130:1. All buckling calculations include the assumption that the extrapolation length is 0.55 in. The buckling is then, when one transforms to a system whose density is $\rho_{BeO} = 2.86$ g/cc, $B^2 = 6.58 \times 10^{-3}$ cm^{-2}. The requirement for constancy of mean-free paths causes the reduction of the buckling to a standard density to be accomplished by multiplying it by the square of the density ratio.

From June 17 to June 19, several cold critical runs were made on a bare BeO system with a BeO/U^{235} ratio of ~565. This was achieved by placing two 2-mil foils in each space between BeO blocks. The critical dimension was found as before. It was found that the fine vane was equivalent to ~0.3 in. of BeO in length. The neutron source was seen to be worth ~0.06 in. of BeO. The average fuel mass per foil is 122.6 g, 93.2% of which is U^{235}. A flux-weighting calculation gives an average foil mass of 128.9 g. The overall

critical dimensions, including the graphite side walls and pusher plates are: ℓ = 31.85 in., w = 26.72 in., h = 24.00 in., corrected for the presence of the fine vane and source. In this critical assembly, there would be 29.25 in. of BeO in length. The total volume it would occupy would be 24.00 × 24.00 × 29.25 in.^{3}, and in this volume, ρ_{BeO} = 2.86 g/cc. The vane cruciform plates are 1.00 in. thick, and the vane slots ~ 1/2 in. × 10 in. in each arm. The source tube passes vertically through the center of the assembly. The assembly temperature was 31.5°C.

The average BeO density, calculated with the conversion of the cruciform to BeO, is $\bar{\rho}_{BeO}$ = 2.636 g/cc. If further, the retaining wall thicknesses are altered according to the above estimate, the buckling is found to be 5.939 × 10^{-3} cm^{-2}. This buckling, converted to the basic block density of ρ_{BeO} = 2.86, is 6.991 × 10^{-3} cm^{-2}.

A peak radiation field of ~ 10 mr/hr was registered at the oven wall during operation.

Transient studies were performed with the neutron source removed. The fine vane was found to be worth \$0.52 ± ~ 7%.

A nuclear safety test involving placement of 8 in. of paraffin on half of the assembly's top surface showed it to be worth ~ 22% of Vane No. 4. If the ratio of worths of Vane No. 4 to the fine vane is taken as 20:1 (see below), the paraffin is seen to be worth ~ 1.3 in. BeO addition to the length of the assembly.

The critical height experiment was repeated for the same assembly with more space, or "slop," between blocks. This was achieved by using 10-mil stainless steel sheets as spacers which were removed prior to going critical.

A technique which proved time-saving was to calibrate, for a particular loading, Vane No. 4 against the fine vane and thereby stipulate in "fine-vane units" the extent to which the assembly was over-critical. It was found from two runs that the fine vane was worth 0.36 in. of BeO in length. This is in reasonable agreement with the earlier determination. In one loading, Vane No. 4 was worth 16 times the fine vanes and in the second loading the ratio was 24.4. The latter value should be more reliable since the flux was not suffering as large a perturbation.

The overall critical dimensions were: ℓ = 33.42 in., w = 26.72 in., h = 24.00 in. The BeO length was 30.10 in. The correction for source poison has been included. The average BeO density is $\bar{\rho}_{BeO}$ = 2.573 and the buckling is 5.805 × 10^{-3} cm^{-2}. This becomes 7.172 × 10^{-3} cm^{-2} at ρ_{BeO} = 2.86,

and it is not in good agreement with $B^2 = 6.991 \times 10^{-3}$ which identifies the more dense critical assembly. This 2.6 difference in buckling is equivalent to a ~14% difference in fuel loading, or ~2.1 in. in BeO length.

The disagreement is likely due in large part to a non-uniformity of BeO density within the boxes. It is obvious that great care must be taken to assure that the BeO blocks are spaced uniformly within the retaining walls and that this spacing is preserved during the experiments.

On June 24 a bare BeO critical assembly (First Assembly, Fig. III-2) was set up. The intention was to make a basic assembly with the proper and reproducible amount of void to allow for the thermal expansion of the BeO to 1200°F. Two 2-mil fuel foils were put in each space between BeO blocks, yielding a BeO/U^{235} ratio of about 565. The proper spacing was obtained uniformly throughout by inserting two 10-mil stainless-steel foils in each slot with the fuel foils, clamping down with the pusher plates, then removing the stainless foils without disturbing the blocks.

The next assembly (Second Assembly, Fig. III-2) was similarly arranged but with the addition of an extra inch of BeO and a set of foil pairs at each end to enable the assembly to go critical at an elevated temperature. Four extra foil pairs were added at the south end of the core and tied with wires to the remote foil extraction apparatus. A room-temperature criticality run was made with this assembly before heating.

The second assembly was next heated to 1100°F, and the four extra foil pairs were extracted remotely without incident to demonstrate the ability of the retraction system to remove reactivity at high temperatures. Six foil pairs at the center of the core were then tied to the foil extraction apparatus for safety while still at 1100°F before the vanes were withdrawn. As soon as it was found that the core was quite subcritical with all the vanes removed, the heater was shut off and the temperature lowered. A count rate at 1050°F gave a crude estimate of the subcriticality. The core was cooled below the temperature of criticality and three critical runs were made at 760, 840 and 920°F as the critical temperature was approached again from below. It was found by extrapolation (Fig. III-3) that the core would be just critical with all vanes and the source removed at 950 ± 5°F. During cooldown a final critical run was made at 300°F.

On July 7, a critical run repeating the first assembly (Fig. III-2 length = 34-13/32 instead of 34-5/16 in.) was made to check the reproducibility of the spacing arrangement.

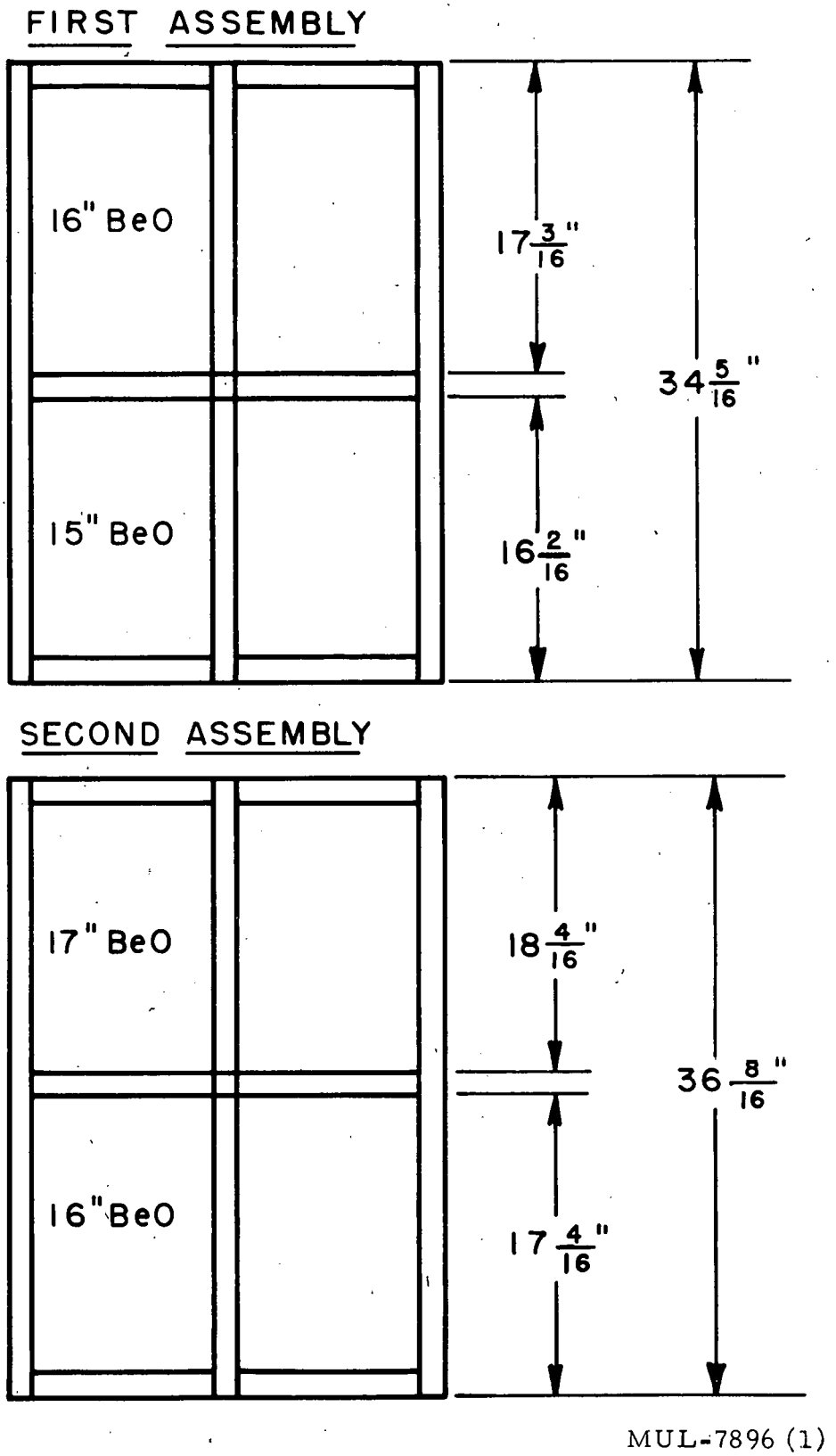
FIRST ASSEMBLY
16" BeO
15" BeO
17 3/16"
16 2/16"
34 5/16"
SECOND ASSEMBLY
17" BeO
16" BeO
18 4/16"
17 4/16"
36 8/16"
MUL-7896 (1)

Fig. III-2.

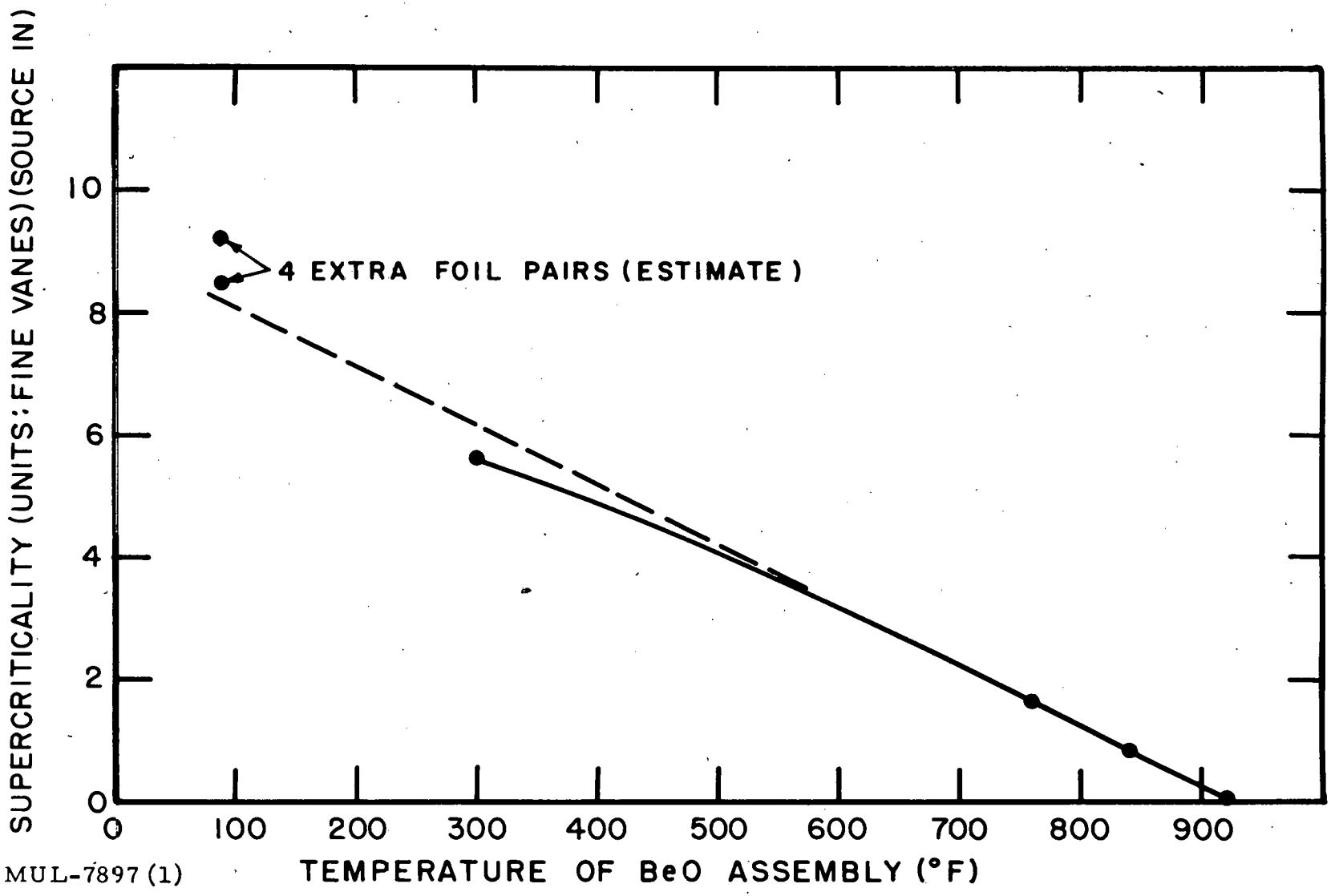

Fig. III-3. Supercriticality of BeO assembly of 6/25/59 versus assembly temperature (length at room temp. = 36.50 in.).

A summary of the neutronic results of the above experiments is given in Table III-1. Linear extrapolation from the 920° point through the 300°F point to 90°F gives an estimate of the supercriticality of that temperature; and comparison with the 2-in. shorter first assembly gives a worth of the fine vane of 0.345 in. of assembly (cf. previous results: 0.30 — 0.36 in. of assembly). Comparison with the room temperature run of the second assembly gives an apparent worth of the four extra foil pairs or 1.7 fine vanes or about three times an estimate based on more accurate considerations. The flux in the cold second assembly was quite highly perturbed by the deep insertion of Vane 4, however, and the results of this run are therefore not very significant.

The critical length is based on a fine-vane worth of 0.345 in. of assembly and a source worth of 0.08 in. of assembly. Calculation of the BeO/U^{235} ratio is based on the flux-weighted average fuel foil weight of 128.9 g. A summary of the results of the calculations for the two similar assemblies, the room temperature assemblies of 6-24 and 7-7, and the high-temperature assembly of 6-25 are given in Table III-2. Better agreement between the reduced bucklings of the assemblies of 6-24 and 7-7 is seen to be obtained than between the previous week's assemblies.

During period of July 13 to Sept. 4, thirty-six criticality determinations were made. Table III-3 lists the experiments by date. The table gives the degree of supercriticality for each determination in fine vane units with all vanes removed and the source in; and, where the measurement was made, it gives the number of fine vanes equivalent to Vane 4 and to the source, and the equivalence between fine vane units and dollars or inches of BeO.

The basic bare BeO assembly of 6-24 and 7-7-59 (Fig. III-2, First Assembly) was brought to criticality seventeen times in this period, for normalization purposes preliminary to other experiments. These other experiments were mainly measurements of differential effects which were in general smaller than the total variation in criticality of the basic core itself. The supercriticality of the basic assembly with all vanes out and source is varied mainly from 0.70 to 1.45 fine vanes, with two measurements outside this range at 0.16 and 1.78 fine vanes. The previous measurements gave 1.16 fine vanes supercriticality. The variation is probably attributable to lack of reproducibility of core-block spacing and the sensitivity of the fine vane unit.

The neutronic effect of the supporting base layer (1-1/2 inch thick graphite

Table III-1

Neutronic Results	T (°F)	Supercrit with source in** (fine vanes)	Vane 4 worth** (fine vanes)	Fine vane worth ($)	Fine vane worth (°F)	Source worth** (fine vanes)	Source worth (°F)	Temp. coefficient of reactivity (¢/°F)	Overall critical length w/ source out (in.)
I First Assembly	91	1.16	18.5			0.2			33.83
I' Repeat First Assembly (3/32 in. longer)	82	1.15	19.6	0.45 0.49					33.93
II Second Assembly (w/4 extra foil pairs)	91	9.2*	21.4						
III Second Assembly	1050	-(1-3)							
IV Second Assembly	760	1.68	17.5	0.50					
V Second Assembly	840	0.86	12.8		98			0.49	
VI Second Assembly	920	0.090		0.48 0.47	103	.2-.25	20-25	0.46	36.43
VII Second Assembly	300	5.6*	18.5	0.27*	112*	.07-.27	7-27	0.43*	
Adopted Value			19.0	0.48	100	0.22	22	0.48	

* Results perturbed by insertion of Vane 4 more than half its travel.

** Fine vane = 0.345 in. of assembly at room temperature.

Table III-2

Geometry	Previous Week 'High'-Density Assembly	Previous Week 'Low'-Density Assembly	First Assembly (6-24)	Repeat First Assembly (7-7)	High-temperature (Second) Assembly (6-25)
T (°F)	89	89	91	82	950
ρ_{eff} (BeO) (g/cm^3)	2.636	2.573	2.586	2.579	2.565
Critical dimensions (homogenized) with all vanes and source out					
LENGTH (in.)	31.44	33.03	33.43	33.53	36.14
includes BeO-equiv graphite (in.)	0.59	0.61	0.60	0.60	0.60 + 0.04 thermal exp.
WIDTH (in.)	26.11	26.13	26.13	26.13	26.16
includes BeO-equiv graphite (in.)	0.89	0.91	0.91	0.91	0.91 + 0.03 thermal exp.
HEIGHT (in.)	24.00	24.00	24.00	24.00	24.10 (Incl. 0.10 thermal exp.)
B^2 (10^{-3} cm^{-2}) (2 Δ = 1.10 in.)	5.939	5.805	5.775	5.767	
B^2 reduced to ρ = 2.86 g/cm^3 (10^{-3} cm^{-2})	6.991	7.172	7.063	7.092	
ρ (stainless steel) (g/cm^3)				0.03736	0.03723
BeO/U^{235} (actual – based on flux-weighted average foil)				568.8	567.8

Table III-3

SUMMARY OF RESULTS, PERIOD OF JULY 13 to SEPTEMBER 4, 1959

DATE	ASS'Y	LENGTH (in.)	TEMP (°C)	SUPERCRIT (bare f.v.)		VANE 4** (f.v.)	SOURCE (f.v.)	FINE VANE	EFFECT
7-15	basic	34-13/32	33.5	1.06					
7-16	basic	34-13/32	31.8	0.97		19.6[c]			
Base Layer Effect Experiment									
7-29	basic	34-13/32	31.8	1.21					
	plywood	34-13/32	32.1	1.54					plywood = 0.33 f.v.
	graphite	33-13/32	32.7	-1.12	-1"BeO				graphite = 1"BeO-2.66 f.v.
7-30	basic	34-13/32	30.7	1.45					
	plywood	34-13/32	30.7	1.89					plywood = 0.44 f.v.
7-31	basic	34-13/32	28.4	1.36					
	plywood	34-13/32	28.8	1.75					plywood = 0.39 f.v.
	graphite	34-13/32	29.0	2.56				0.29"BeO	graphite = 0.81 f.v.
Reflector Experiment									
8-3	1"+0"	33-12/32'	27.8	1.37	-1"BeO			0.286"BeO	1" graph = 1.02"BeO
	3 + 0	32-11/32	28.0	4.23	-2"BeO				
8-4	3 + 3	29-8/32	28.4	-1.6	-5"BeO				
	4 + 4	29-8/32	28.8	0.41	-5"BeO				
	6 + 6	28-7/32	28.9	0.16	-6"BeO				
8-5	8+8(-)*	28-3/32	28.5	1.62	-6"BeO	8.2[c]	0.070	$0.95	
	8+8	28-3/32	28.8	3.32	-6"BeO				wings - 1.7 bare f.v.
8-17	basic	34-13/32	29.9	1.78					
8-18	basic	34-13/32	27.7	1.00		17.1[v]			
8-19	basic	34-13/32	23.9	0.83		14.7[v]			
	basic	34-13/32	24.0	0.86		15.1[v]	0.29		
	SW 3 out	34-13/32	24.2	0.20					foil SW-3 = 0.66 f.v.
Box Worth Experiment									
8-20	SW-3 out	34-13/32	20.0	0.28			0.21		
	E+W box	34-13/32	20.0	1.85	1.79				
	E+W box	34-13/32	20.0	1.77		14.4[v]			1"gr E+W box = 0.92 f.v.
Activation Run									
8-26	Source, SW 3 out	34-13/32	27.1	0.22				$0.48	
Full Worth Experiment									
8-26	basic	34-13/32	27.5	0.70		18.3[v]	0.264		foil NE-0 = 0.524 f.v.
8-27	basic	34-13/32	26.1	0.73		19.0[v]	0.203		NE-1 = 0.655
8-28	basic	34-13/32	26.0	0.72		18.6[v]	0.234		NE-3 = 0.701
	basic	34-13/32	26.5	0.73		19.2[v]	0.264		NE-6 = 0.647
8-31	basic	34-13/32	26.0	0.71		19.3[v]	0.297		NE-9 = 0.455
9-1	basic	34-13/32	26.7	0.76		18.6[v]	0.244		NE-12 = 0.243
	basic	34-13/32	26.8	0.75		18.5[v]	0.261		NE-15 = 0.126
1" BeO Worth Experiment									
9-3	1"BeO	35-14/32	27.9	3.32		20.0[v]			
9-4	basic	34-13/32	27.4	0.16		20.1[v]			
	1"BeO	35-14/32	27.5	2.99		17.1[v]		0.33 in BeO	

* Reflector wings removed.

** c - coarse indicator, v - venier indicator, and f.v. - fine vane units.

MUL-7878 (1)

with an effective density of 1.67 g/cm^3, 5 in. below the bottom of the BeO blocks) was investigated by mounting a plywood platform to support 1 in. of standard Hot Box graphite (effective density of 1.46 g/cm^3) 5 in. above two quadrants of the assembly. The graphite was shown to be worth 0.81 fine vane units. Taking the fine vane to be equivalent to 0.30 in. of assembly in the N-S direction, and correcting for the number of quadrants covered and the relative graphite thickness and density, the base layer is found to be worth 0.83 in. of assembly in the N-S direction. From constancy-of-buckling considerations, the ratio of equivalent infinitesimal length increments in perpendicular directions is given by the inverse cube of the respective overall lengths including extrapolation lengths. With this correction, the base layer is found to be equivalent to an increase in assembly height of only 0.29 in. of BeO. In the above experiment, a value of the fine vane unit of 0.29 in. of BeO (N-S) was obtained as a by-product.

The effect of adding graphite reflectors on the East and West faces of the assembly was measured for reflector thickness from 1 in. to 8 in. Standard Hot Box graphite was used in 1-in. thicknesses along 48 in. of each side, and BeO blocks were removed from the assembly as the reflector was added. Figure III-4 is a graph of the effectiveness of each additional inch of graphite in terms of inches of BeO in the N-S direction, a kind of reflector savings determination. The first inch of this graphite on each side is seen to be closely equal to 2 in. of BeO in the N-S direction. The results are in good agreement, in the limit of zero reflector, with the constancy-of-buckling ratio-of-effectiveness of increments in perpendicular directions. The reflector addition does not start at zero in the experiment because the 1-1/2 in. of BeO and the 3/4-in. graphite walls to the East and West of the fuel foils are acting as reflectors also. For the 8-in. reflector another critical determination was made with the reflector length (N-S) reduced from 48 in. to the core length of about 29 in. The removed wings were found to be worth 0.85 fine vanes. Since the reactivity worth of the fine vane for this last system was found from transient experiments to be about \$0.95 or quite closely twice the \$0.48 obtained for the bare core, the wings are worth 1.7 bare fine vane reactivity units. From the series of reflector experiments a value of the (bare) fine vane unit of 0.286 ± 0.01 in. of BeO was obtained.

The reflection furnished by the outer box walls (graphite, density 1.74 g/cm, thickness 1/2 in.) was investigated by adding 1 in. of standard Hot Box

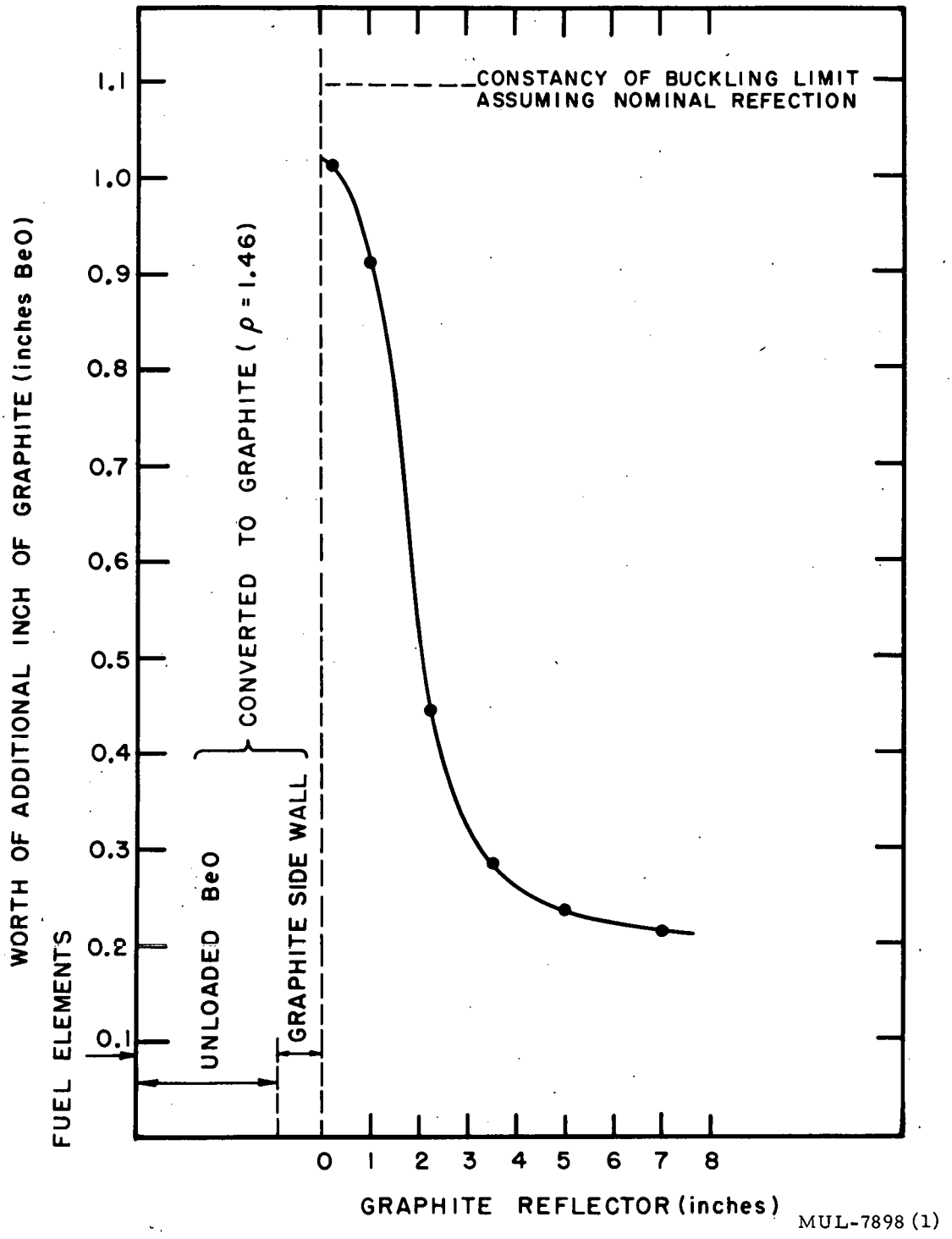

Fig. III-4. Relative effectiveness of each additional inch of reflector (for 1 in. BeO = 3.5 fine vane units).

graphite just outside and the full length of the East and West box walls. This additional graphite was found to be worth 0.92 fine vane units or 0.28 in. of BeO in the N-S direction or about one-eighth the worth of the same graphite immediately against the assembly. Correcting for the relative thicknesses and densities and assuming that the North and South box walls, which are closer to the core but see a smaller core face, are equal in effect to the East and West walls, we find a value of 0.33 in. of BeO (N-S) for the worth of the whole outer box.

Prior to the activation run, the foil pair in SW-3 was removed so that two activation foil ribbons could be put in its place. The worth of the foil pair was found by pulling it with the remote foil-retraction system while the core was critical with the source out. This obviated moving Vane 4 which would have been necessary if the foil had been pulled by hand. The foil pair was found to be worth 0.66 fine vanes.

The relationship between the γ-radiation at the RAMS meter at the oven wall and the total core power has been recalculated from different considerations but is found to be the same as originally calculated within 10%. For both the $6 \times 6 \times 5$ foot bare graphite assembly and the $2 \times 2 \times 2$ foot BeO assembly, about 220 mR/hr corresponds to 1 watt in core power.

For the activation experiment the core was run at 1100 mR/hr or 5 watts for one hour. Vane 4 was all the way out and the source was removed. The fine vane was about half-way out or only about one-fifth of its worth was effective (Fig. III-5). During the run the neutron flux at the fence due South of the core was approximately 200 in Rem/hr. Thirty minutes after shutdown the γ-radiation of the core was approximately 300 mR/hr, and the activation foils were about 3 R/hr at 3 in., about nine-tenths of which were betas. An hour and a half after shutdown the radiation at the oven wall was down to 10 mR/hr. Counting of the foils started about an hour and a half after shutdown and was completed in another hour and a half. No measurable radiation was indicated by the dosimeters carried by the persons handling the activation foils. A second count of the activation foils was made the succeeding day. The resulting flux plot in the vertical direction in the core is shown in Fig. III-6. The solid line is a best-fit cosine distribution. The dispersion of the experimental points corresponds to about 3% probable error. The extrapolation lengths are found to be 0.60 ± 0.1 in. at the top and 1.30 ± 0.1 in. at the bottom of the core, to be compared with 0.55 in. calculated for the bare core. The

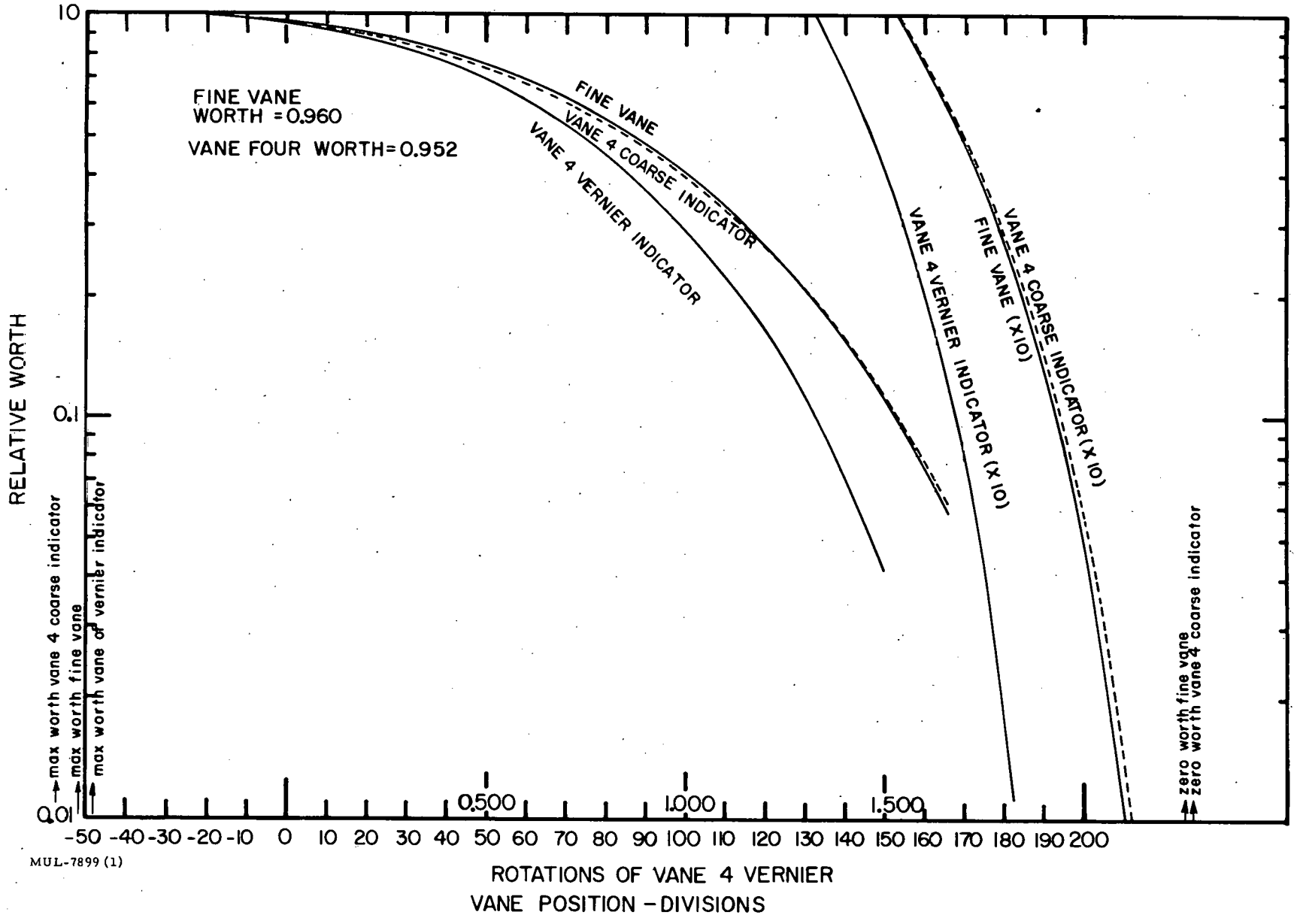
FINE VANE
WORTH = 0.960
VANE FOUR WORTH = 0.952
FINE VANE
VANE 4 COARSE INDICATOR
VANE 4 VERNIER INDICATOR
VANE 4 VERNIER INDICATOR (X 10)
FINE VANE (X10)
VANE 4 COARSE INDICATOR (X 10)
RELATIVE WORTH
10
0.1
0.01
max worth vane 4 coarse indicator
max worth fine vane
max worth vane 4 vernier indicator
zero worth fine vane
zero worth vane 4 coarse indicator
0.500
1.000
1.500
-50 -40 -30 -20 -10 0 10 20 30 40 50 60 70 80 90 100 110 120 130 140 150 160 170 180 190 200
MUL-7899 (1)
ROTATIONS OF VANE 4 VERNIER
VANE POSITION - DIVISIONS

Fig. III-5.

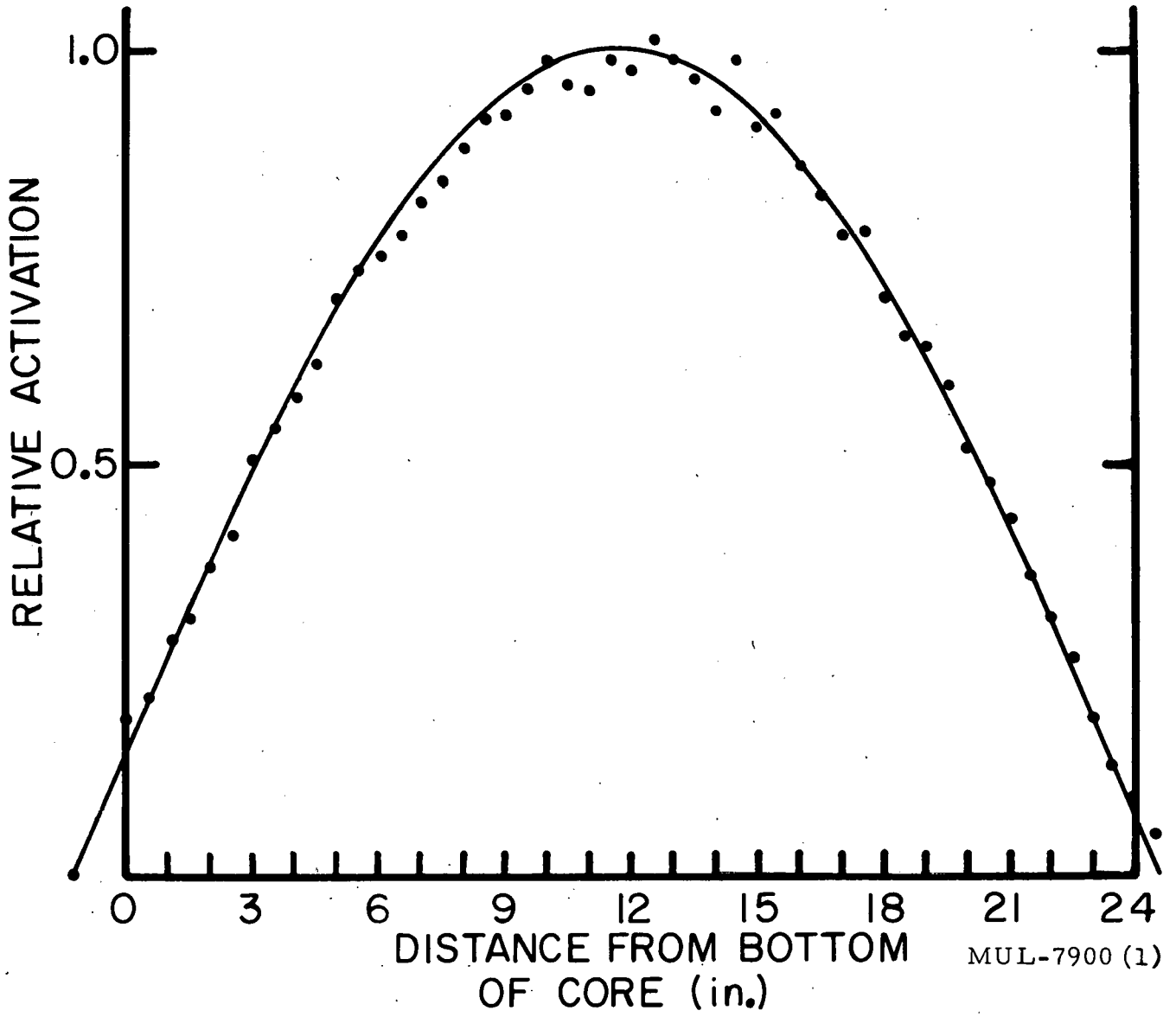

Fig. III-6. Flux plot in vertical direction, composite of activation foil counts.

extrapolation length at the bottom is seen to be increased by 0.7 in. showing that the reflection from the floor, low-mass table, and base layer is more than twice the base layer effect deduced previously.

During the 15-minute run-up from normal levels to 5 watts, a constant amount of excess reactivity in fine vane position was maintained yielding a very constant period of 191 seconds for the last 10 minutes prior to reaching power. Using the in-hour formula, we can find a value for the worth of the fine vane unit of $0.48 of reactivity.

The worth of fuel foils in the positions NE-0, -1, -3, -6, -9, -12, and -15 was evaluated by essentially the same method as that for SW-3 above. The original foil-pair was removed in each case in this series and replaced by a standard foil pair (840 and 793, combined weight 246.15 g) which was tied to the remote foil retraction system. The supercriticality of the basic core was redetermined each time with the standard foil pair in place of the regular foil pair. The source was then pulled to make the determination of the differential effect more precise, and also to remove some poison so that the core would still be critical with the fuel foil-pair removed. Finally, the standard foil-pair was remotely retracted when the assembly was just critical, and the compensating travel of the fine vane to bring the assembly back to criticality yielded directly the foil worth in fine vane units. Only about 1.5% of the Vane 4 worth was present in each case as a perturbation. The resulting worth plot in the N-S direction is shown in Fig. III-7. A cosine-squared curve based on the predicted extraoplation is shown also for comparison. Normalization to any other point than the one chosen would probably be just as meaningful. The flux is considerably depressed in the core center due to the vane slot, and unaccountably increased near the outside compared with the cosine-squared curve. The uncertainties in the experimental points in the figure are only from the errors in reading the fine vane position indicator and in finding the critical position.

The series of seven experiments above give a good feeling for the reproducibility of an assembly. Supercriticality varied only from 0.70 to 0.76 fine vanes and the Vane 4 worth varied from 18.3 to 19.3 fine vanes in good agreement with the previously adopted value of 19.0 fine values per Vane 4. The source worth, however, varied from 0.20 to 0.30 fine vanes indicating a possible unreproducibility in the full-in source position.

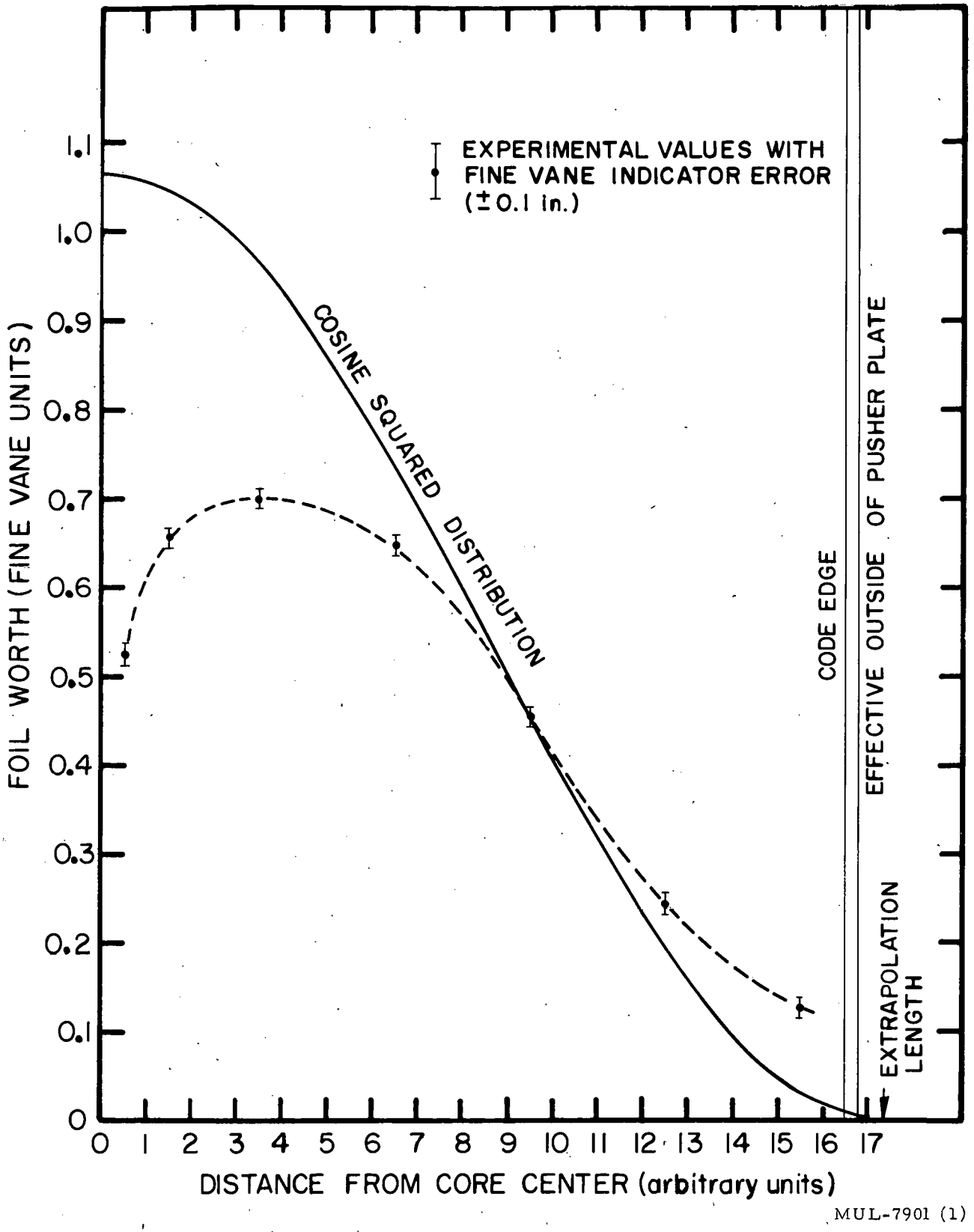

Fig. III-7. North-south foil worth plot (north-east quadrant).

The last experimental series ostensibly was a most precise determination of the equivalence of fine vane units and inches of BeO. One inch of BeO and two foil-pairs (SE-15 = 793, 840; SW-15 = 731, 712) were added to the south end of the basic core (Fig. III-2), and the degree of supercriticality determined. The BeO and foil pairs were then removed and the supercriticality of the basic core redetermined for normalization. Unfortunately and unaccountably, the supercriticality was 0.16 fine vane units compared with an expected value of 0.7. The one-inch addition was repeated showing fair reproducibility. The value obtained for the fine vane unit was 0.33 in. of BeO. The previous value of 0.30 in. of BeO is felt to be more nearly correct.

An effect noticed in the experiments was an increase in reactivity as Vane 4 was moved inward from its full-out position. The multiplication was observed to rise 10% before returning to its original value with the vane moved inward about 6 in. The boron nitride had penetrated slightly more than 2 in. into the core at that position. This effect is attributable to fast-neutron reflection from the boron. Its influence on the Vane 4 worth plot is not known.

The worth plots for the fine vane and the Vane 4 coarse indicator have been recalculated with more precision. A worth plot for the new Vane 4 vernier indicator has also been calculated. The three plots are shown in Fig. III-5. All are based upon the 0.55-in. extrapolation length. If the 0.60- and 1.30-in. extrapolation lengths at the top and bottom of the core were taken into consideration, the maximum change in the worth plot would be a decrease in worth of 10% of its value in the range in which the vane is worth 0.10 to 0.20.

From September 4 to September 25, the experimental operations were shut down for installation of a cooled reflector system for the BeO assembly.

With the corrections obtained from the different experiments above, the basic bare assembly and the high-temperature assembly may be described in terms of a bare BeO core with the half-density graphite cruciform all surrounded by infinite space. The basic assembly would have the dimensions ℓ = 33.67 in., w = 26.20 in., and h = 24.70 in. with an average BeO density of 2.579 g/cm^3. The 950°F assembly would have ℓ = 36.19 in., w = 26.23 in., and h = 24.80 in. with an average BeO density of 2.568 g/cm^3. An extrapolation length of 0.55 in. at each end must be added for buckling calculations.

The thermal expansion resulting in the change in the dimensions and the density, together with the difference in the starting densities of the two assemblies must be corrected for in order to get a true nuclear temperature

coefficient of reactivity. Removing these differences through buckling corrections is equivalent to substracting 0.6 ± .15 in. from the equivalent room temperature length of the hot assembly. The net length increase required to compensate for the nuclear effect of the 860°F temperature increase was therefore 1.9 ± 0.2 in. Through the fine vane unit equivalence of 0.30 in. of BeO and $0.48 of reactivity, the length increase becomes $3.04. The average nuclear temperature coefficient between 90°F and 950°F is therefore $0.35 per 100°F.

NEUTRONICS

Some preliminary calculations on Tory II-C neutronics have been completed. Prior to this period only a few exploratory calculations had been performed for the purpose of obtaining some explicit information. These calculations as well as those made during the quarter will be outlined below after a brief illustration of Tory II-C and the manner in which the neutronics calculations were made.

Tory II-C is a lightly reflected cylindrical reactor having holes running axially through the core. The core material is a homogeneous mixture of beryllium oxide and uranium dioxide. The amount of UO_2 present in the mixture is measured as a percentage of the total weight of the mixture. In some designs, molybdenum is used in the reactor as a structural material. The amount of molybdenum used is expressed as a percentage of the total volume of the core. When it is possible an average thickness of the molybdenum structural members will be quoted. Another number important in describing the reactor is the molecular moderator-to-fuel ratio M/U. Porosity refers to the cross-sectional void area divided by the core area (for core porosity) or divided by the reactor area (for reactor porosity). Since the early calculations have to do with generalized concepts of the reactor and not particular structural details, the void area is composed of not only the holes through which air is to pass to be heated but also any structural and core cooling voids that are necessary from an engineering standpoint. At present we are concerned only with reactor configurations which will be critical at 1700°K. Hence all points presented here will be points for which the particular configuration is critical at the above temperature.

All neutronic calculations used an 18-energy group* neutron diffusion code (Zoom) designed for use on an IBM 709 (UCRL-5293). This code is a one-dimensional code which treats cylindrical reactors with radial variations and has a provision which will include an axial buckling coefficient in the calculations. Thus while a total z-length may be stated, there is complete homogeneity in this direction. Thus there can be no end reflectors.

Most of the calculations prior to this period were made to determine what variations in reflector thickness and variations in radial fuel loading

* The neutron energy spectrum is divided into 18 separate groups

would produce a reasonably flat power level across the core. They showed that a 0.4-in. beryllium reflector on a 24-in.-radius core would give a flat power distribution, and that the inclusion of a small unfueled "island" region about 8/10 of the way out from center would level it still more. From these calculations we obtained some rough estimates of how such reactor parameters as the effective multiplication factor, the temperature coefficient of reactivity, and the worth of a small amount of molybdenum varied with side reflector thickness, M/U ratio, placement of unfueled annular cylindrical "islands," volume percentage of molybdenum, and core temperature. The "roughness" of these calculations was due to our rough cross-section values and energy transfer coefficients which have since then become more accurate and have been made to conform to critical experiments.

A specific calculation was made for a reactor 54 in. long by 52 in. diameter including a 3-in.-thick beryllium oxide reflector of 0.05 porosity. 1.5% of the cross-sectional reactor area was occupied by molybdenum structural trays, 50-mil average thickness. This configuration was calculated to be critical for an M/U ratio of 345 and a core porosity of 0.45. The critical mass was 70.3 kg of which about 55% (38.8 kg) was needed to offset the large resonance absorption cross section in energy group Eight, produced by the molybdenum trays. The critical mass could be reduced to perhaps 59.9 kg by the use of front and rear end reflectors. Figure IV-5 illustrates the flux depression in energy groups 5, 6, 7, and 8 caused by the molybdenum. The plots are of the middle annular section, the axial center section, and the interface between the core and the reflector. Another case of the above configuration was found to be very close to being critical with a core porosity of 0.50 and a moderator to fuel ratio of 200:1. Core temperature for both cases was 1700°K.

General calculations have been made on two basic systems, both with an axial length of 51 in. and at a temperature of 1700°K; one was a critical mass of 50 kg, and the other a critical mass of 100 kg. No molybdenum was present in either system. Around these basic cores were placed reflectors of beryllium oxide, 96% theoretical maximum density and 5% porosity. The reflectors were 2 and 4 in. thick. Unreflected cores were also studied and in the figures mentioned below these are labeled as cores with zero reflector thickness. All points shown on the graphs are for critical systems with the region above any particular curve being one of supercriticality and the region below being one of subcriticality. The variable parameters in this study were total core porosity and core radius. The results are shown in Figs. IV-6 to IV-14. In the figures, the dashed portion represents an extrapolation. Each circled point represents a separate calculation.

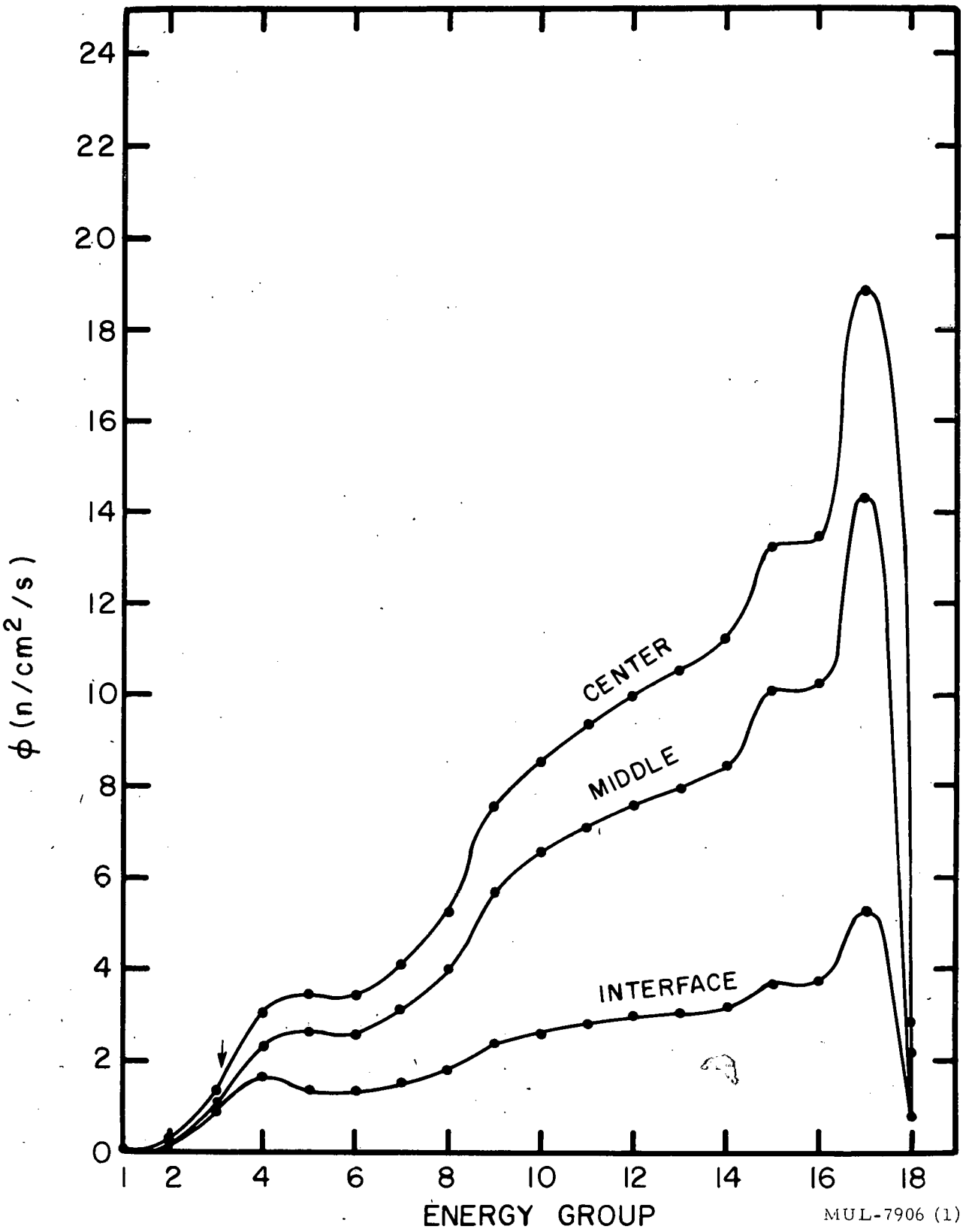

Fig. IV-5. Flux versus energy group (Γ = 0.45, M/U = 200).

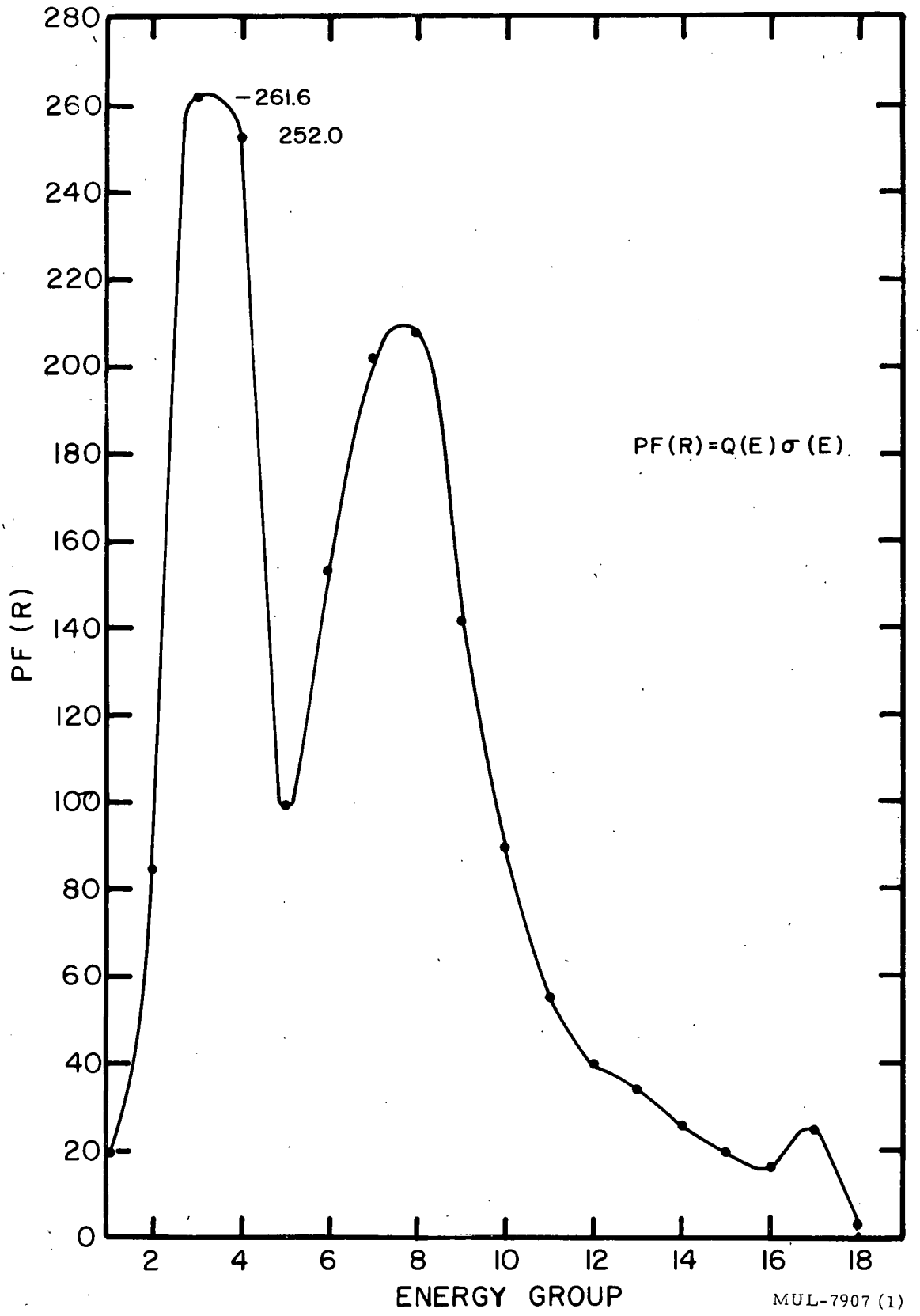

Fig. IV-6. Power fraction versus energy group for Tory II-C (Γ = 0.45, M/U = 200).

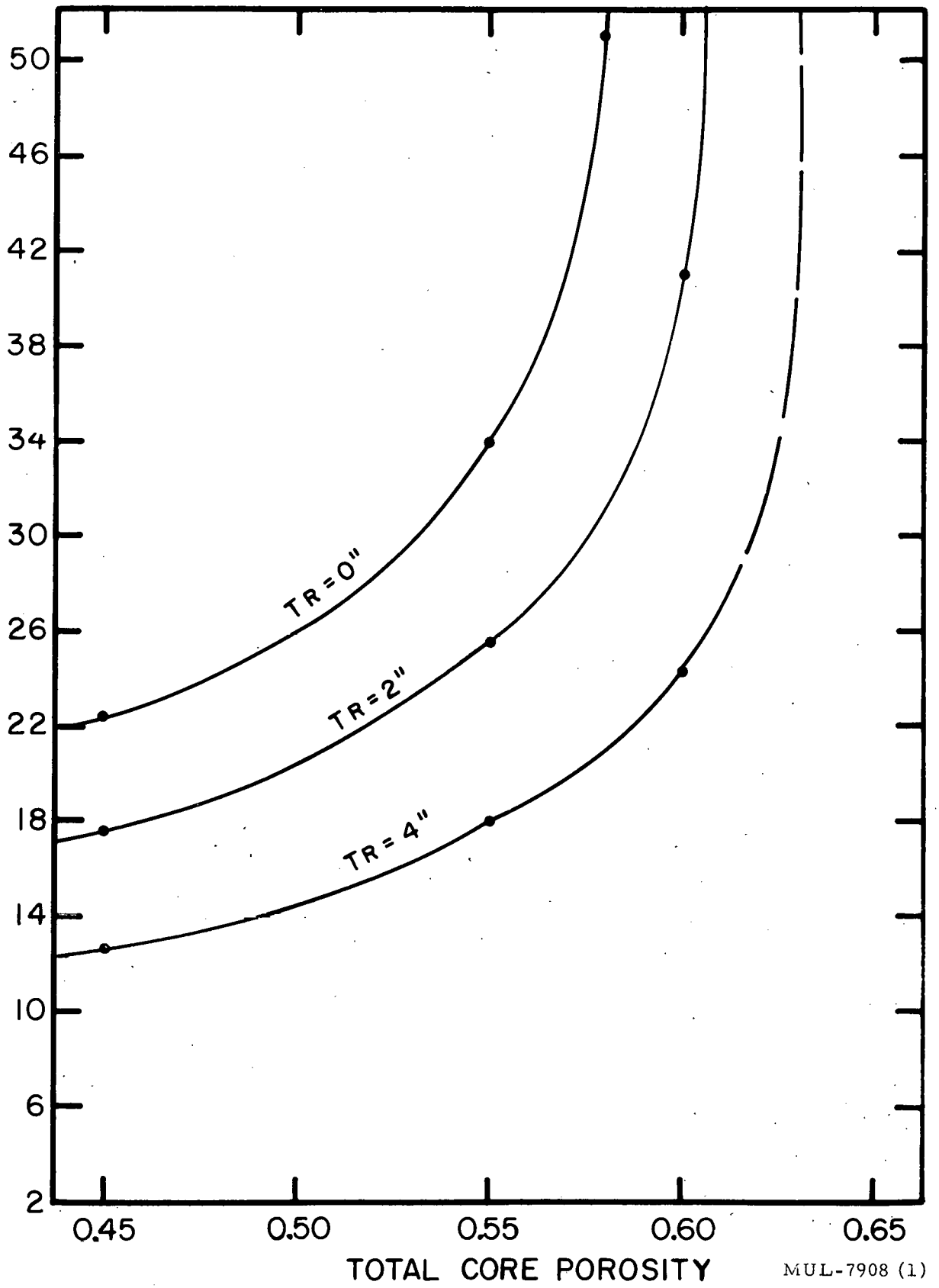

Fig. IV-7. Core radius versus total core porosity for critical mass = 50 kg.

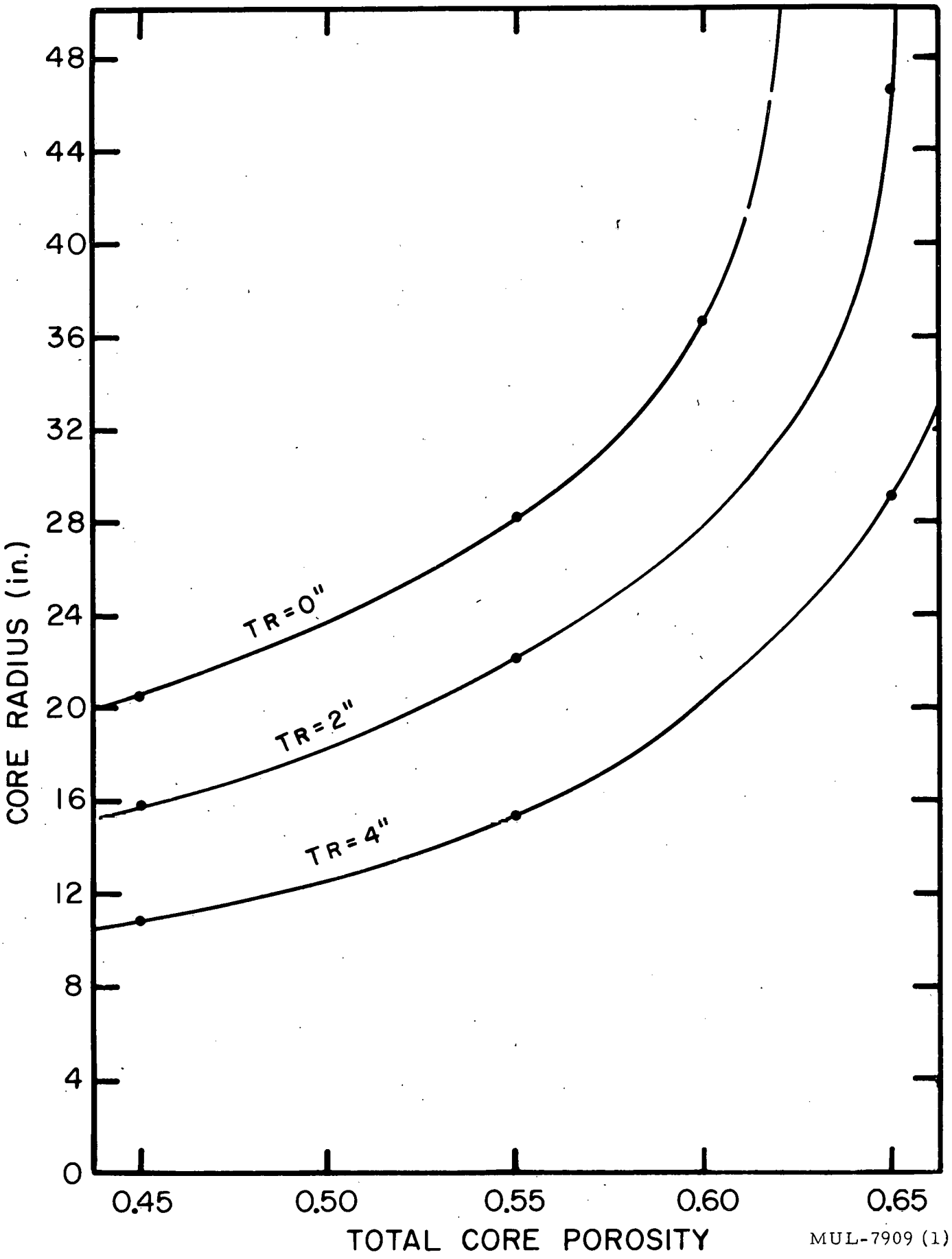

Fig. IV-8. Core radius versus total core porosity for critical mass = 100 kg.

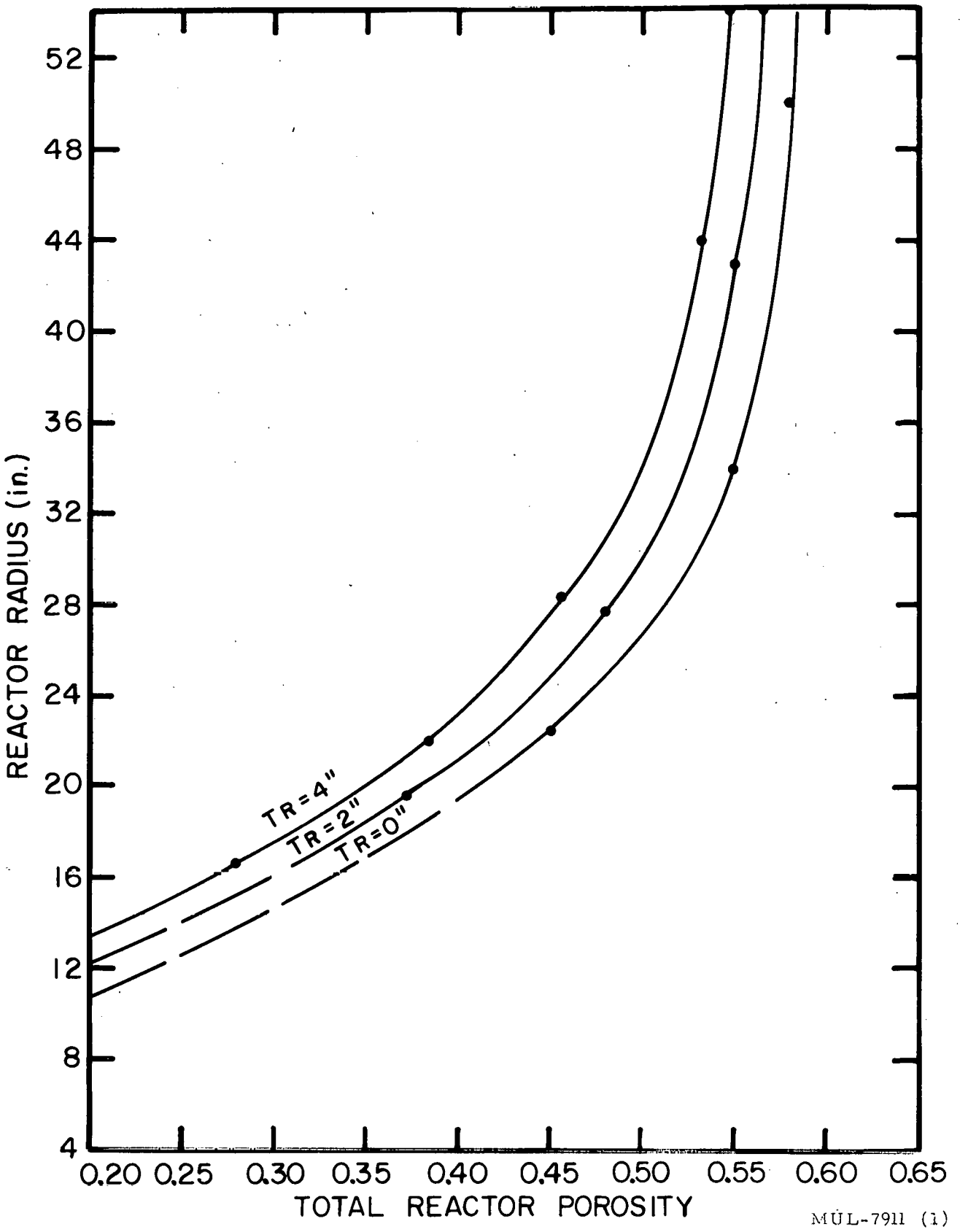

Fig. IV-9. Reactor radius versus total reactor porosity for critical mass = 50 kg.

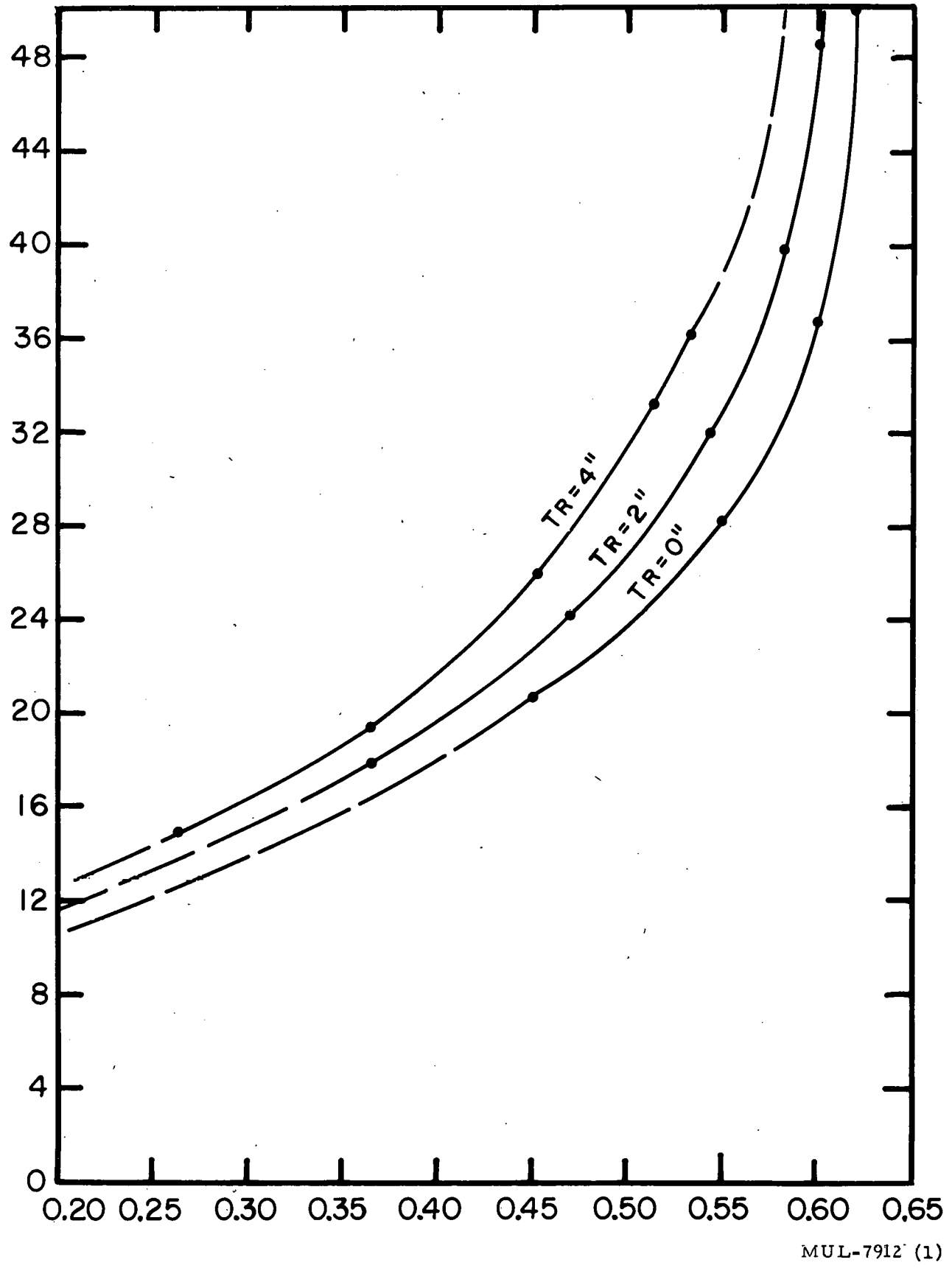

Fig. IV-10. Reactor radius versus total reactor porosity for critical mass = 100 kg.

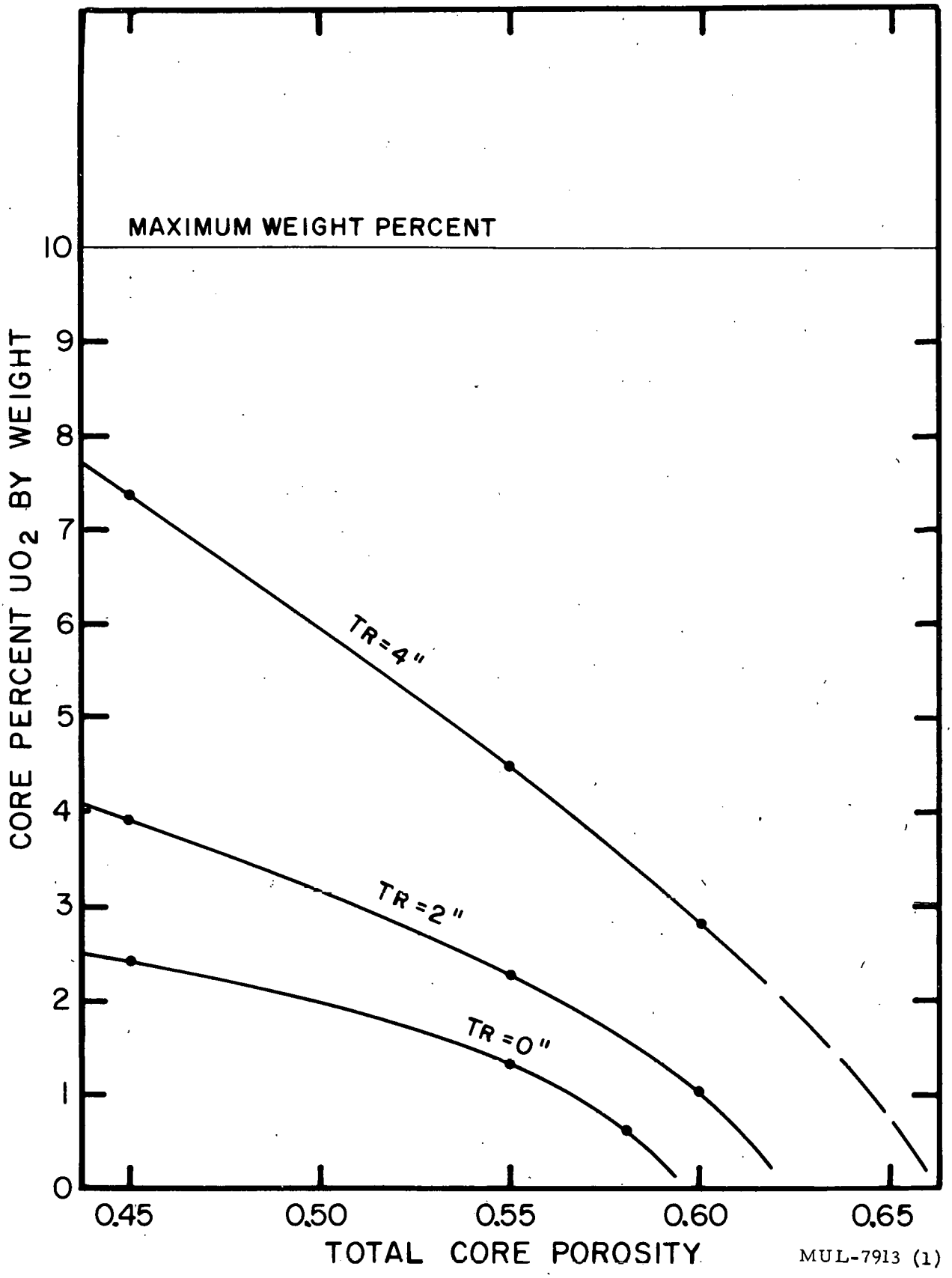

Fig. IV-11. Weight percent UO_2 versus total core porosity for critical mass = 50 kg and three reflector thicknesses.

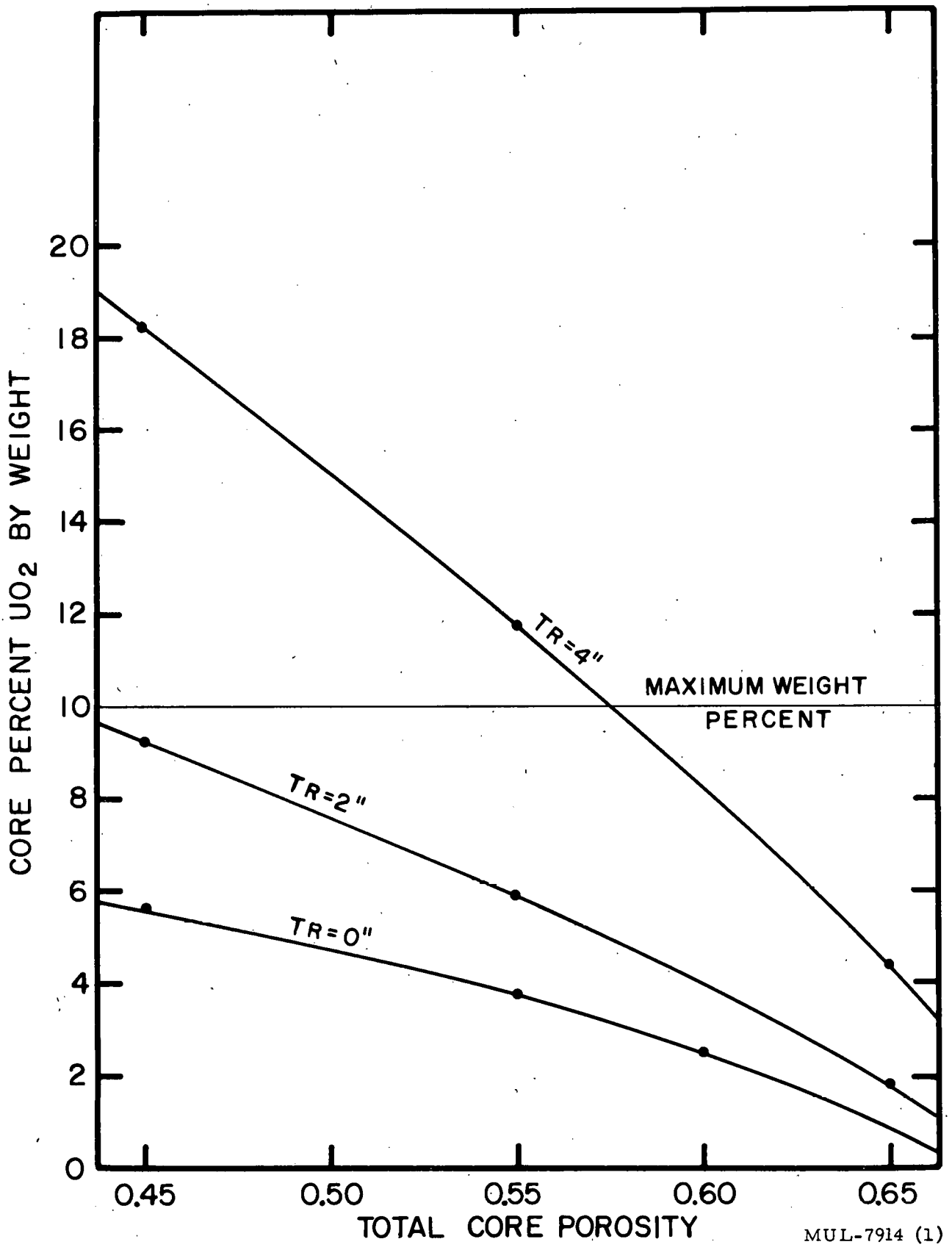

Fig. IV-12. Weight percent UO_2 versus total core porosity for critical mass = 100 kg and three reflector thicknesses.

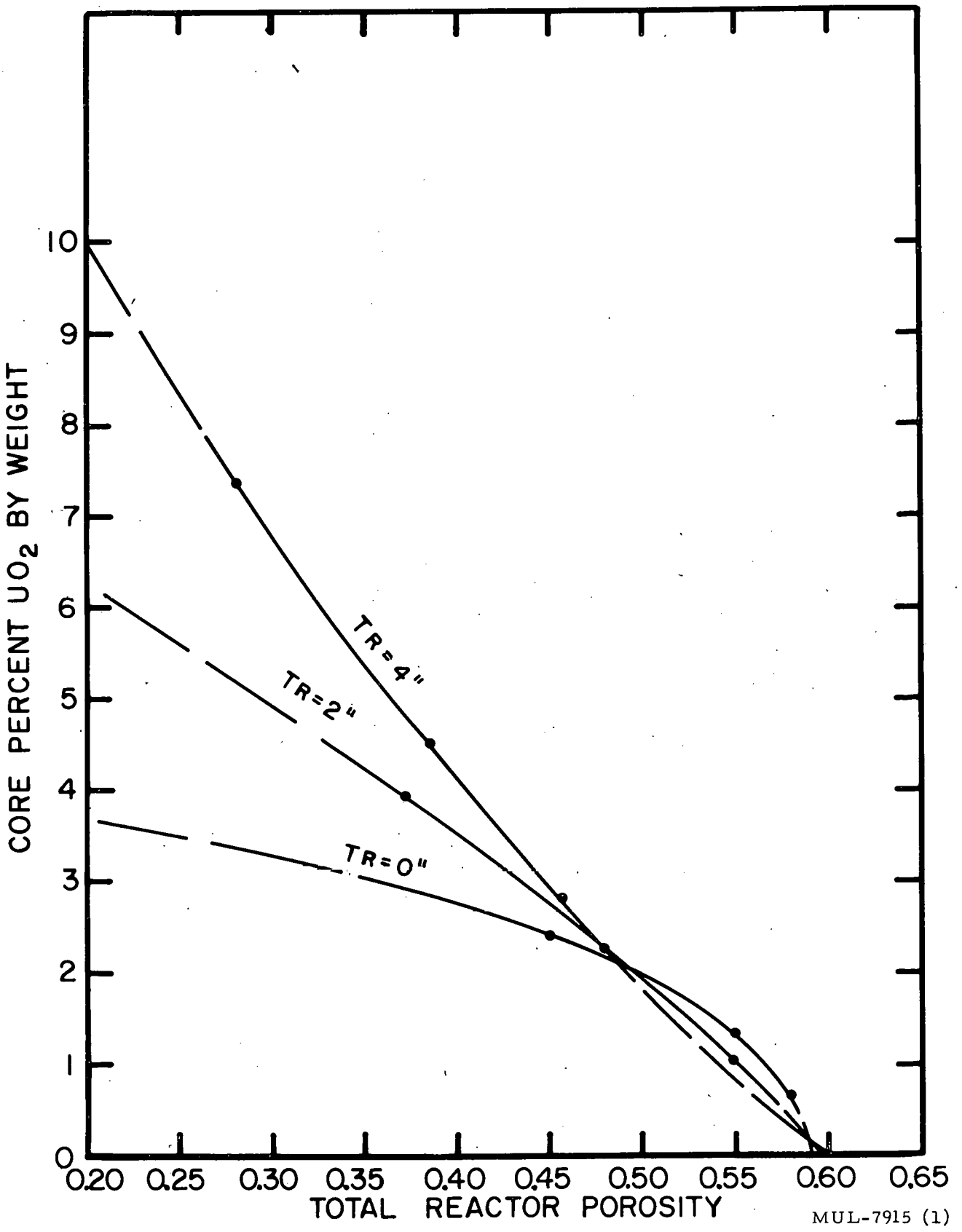

Fig. IV-13. Weight percent UO_2 versus total reactor porosity for critical mass = 50 kg and three reflector thicknesses.

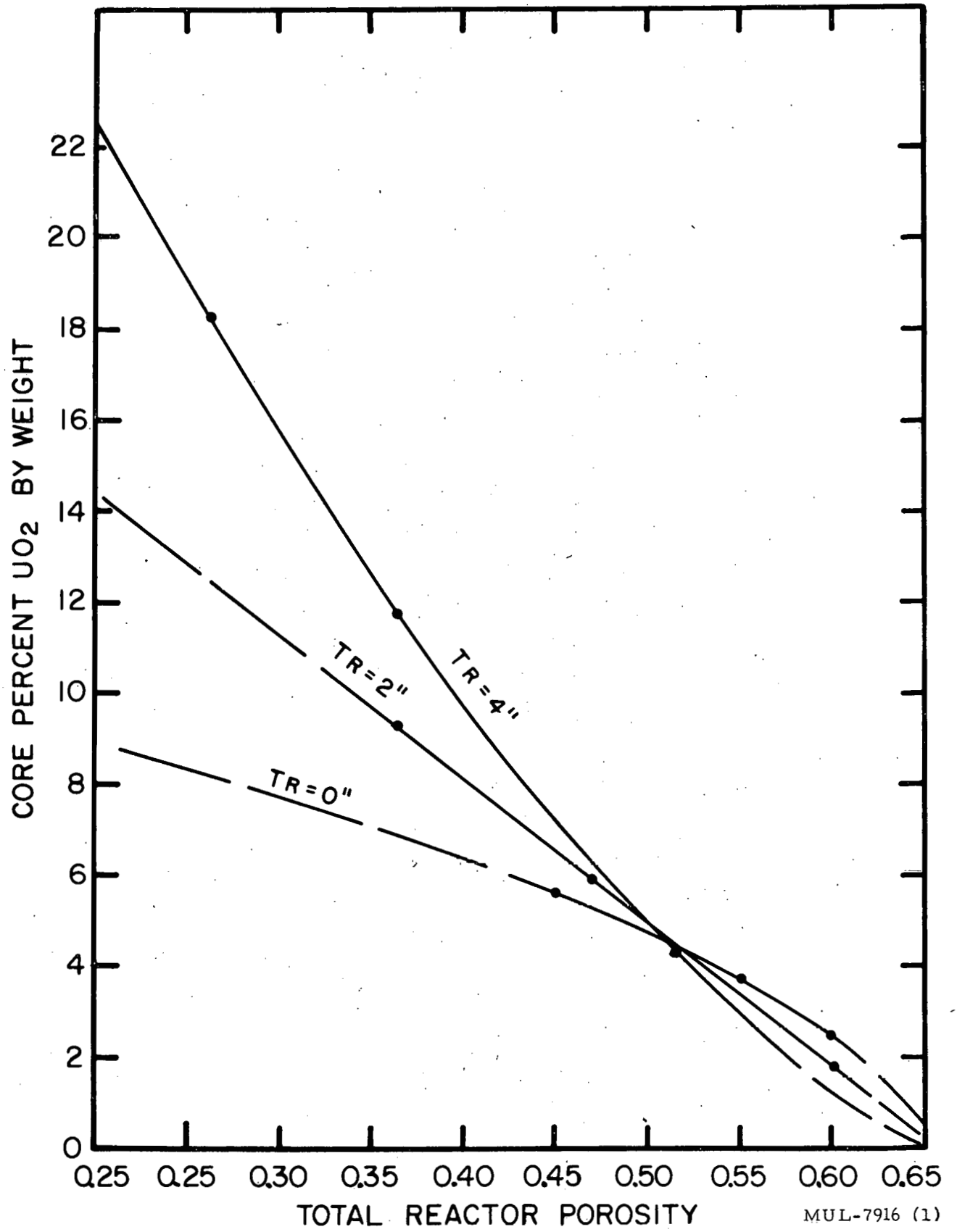

Fig. IV-14. Weight percent UO_2 versus total reactor porosity for critical mass = 100 kg and three reflector thicknesses.

CHAPTER V. FACILITIES

Livermore Construction Program: July 1, 1959 to September 30, 1959

Building 173-A Mezzanine — Core Assembly Building

This building was constructed for the Pluto program for the core assembly and assembly on the test vehicle.

The mezzanine, which is for the actual modular assembly of the core, was started August 21, 1959; and as of September 30 the job is approximately 10% complete, with the scheduled completion date of November 7, 1959 (original completion date, October 12, 1959--delayed by steel strike).

Building 173-B — Fuel Element Development Laboratory

This building is to house the Chemistry Engineering Group where all the ceramic development work for the program will be conducted.

The construction work was started March 16, 1959, and is scheduled for completion February 9, 1960. As of July 1, the building was about 7% complete, and as of September 30 the building is approximately 40% complete and appears to be on schedule.

Disassembly Building (Nevada)

Actual progress is now 27% as against a scheduled 61%. The carpenter strike (June 16 - 22 July) caused the delay. The contractor has been unable to produce barite concrete up to specified density.

The manipulator for the Livermore mockup arrived.

Railroad (Nevada)

Notice to proceed was given to the contractor on July 3, 1959, with work starting July 13. A delay in obtaining signal cable has resulted in an actual progress of 27% vs a scheduled progress of 61%. Scheduled completion date is 31 October 1959.

Miscellaneous Structures (Nevada)

Contract went out for rebid on 13 July 1959. Bids were opened August 4 and notice to proceed was given to the contractor on 18 September. The contractor has begun rough grading. Scheduled date for beneficial occupancy of the Control Building is December 15, 1959.

Test Bunker Complex (Nevada)

1. Test Bunker: Bids were opened on July 14, 1959, with award of bid to the contractor. Notice to proceed was given August 6 and construction began August 7. Rough excavation of the footings has been completed. Footings on

the Head House have been poured. The actual progress is now 10.5% vs a 12.6% schedule.

2. Compressor House: Footings have been poured, and forming is in progress for the compressor foundation. The scheduled beneficial occupancy is October 12, 1959.

3. Air Heater: Award of contract was made to the contractor on July 1, 1959. Notice to proceed was given on July 11. The actual progress is 3.4% vs 19.0% scheduled. The steel strike will delay this contract.

4. Compressors (IR XNH-4): The award of contract was made to the contractor on July 2, 1959, with notice to proceed given on July 7. The overhaul has proceeded very satisfactorily and is now approximately 80% complete. The compressors are scheduled for shipment to NTS on October 5, 1959.

5. Air Storage System: Award of contract was made on July 1, 1959, to the contractor, with notice to proceed given on July 11. The steel strike is delaying the delivery of materials sixty to seventy days after strike termination. Scheduled completion date was January 7, 1960.

6. LRL Procured Equipment: The Hydraulic Power Package and Air Relief Valves are on schedule. The shut-off valves, temperature-control valves and flowmetering tubes are behind schedule but are progressing satisfactorily. The Hot Air Pipe is delayed by the steel strike. The I-R Low Pressure Compressors (blowers) are being delayed by a strike at the I-R plant and have a six-months delivery after termination of the strike.

/bc